Distributed Sensors, Data Analysis, and Non-Intrusive Load Monitoring: Foundations for Reliability-Centered Maintenance on Ships

by

Jacob Daniel Skimmons

B.S., U.S. Coast Guard Academy (2020)

Submitted to the Department of Mechanical Engineering
in partial fulfillment of the requirements for the degree of

MASTER OF SCIENCE IN NAVAL ARCHITECTURE AND MARINE ENGINEERING

at the

MASSACHUSETTS INSTITUTE OF TECHNOLOGY

May 2024

Authored by:	Jacob Daniel Skimmons Department of Mechanical Engineering May 20, 2024
Certified by:	Steven B. Leeb Professor of Electrical Engineering, Thesis Supervisor
Certified by:	Erik K. Saathoff Doctoral Candidate, Thesis Supervisor
Accepted by:	Nicolas G. Hadjiconstantinou Chairman Mechanical Engineering Committee on Graduate Theses

Distributed Sensors, Data Analysis, and Non-Intrusive Load Monitoring: Foundations for Reliability-Centered Maintenance on Ships

by

Jacob Daniel Skimmons

Submitted to the Department of Mechanical Engineering
on May 20, 2024 in partial fulfillment of the requirements for the degree of

MASTER OF SCIENCE IN NAVAL ARCHITECTURE AND MARINE ENGINEERING

ABSTRACT

Advances in computing and sensing technology have brought powerful new tools within reach of shipboard engineers. With the right setup, operators can leverage statistics and digital signal processing tools to gain physical insight previously obscured by the sheer amount of work and specialized knowledge it once took to do the same. This thesis explores several applications of non-intrusive load monitoring (NILM) tools aboard a U.S. Coast Guard Fast-Response Cutter (FRC) patrol boat, novel analysis methods of the corrosion protection systems on the FRC, and practical ways of making smart data approachable. Once implemented, these methods will reduce the effort needed to safely operate a modern, high-tech ship by giving operators greater insight into how their systems perform in real-time.

Thesis supervisor: Steven B. Leeb
Title: Professor of Electrical Engineering

Thesis supervisor: Erik K. Saathoff
Title: Doctoral Candidate

Acknowledgments

I have so much to be grateful for that this brief section cannot contain it all. Truly, "my cup overflows" and these two years at MIT have put that fact in sharp relief in many different ways. In the spirit of starting with the beginning, I want to thank my parents, Kim and Brian Skimmons, for setting me on a course which led here. They have always supported me and I always had someone to call – whether it was from the cadet barracks in New London or from a satellite phone in the middle of the frozen Chukchi Sea. They also gave me two skills which have paid dividends over and over: my mother taught me how to write, and my father taught me how to be an officer.

My brother Ben also deserves a shout for helping me grow personally and for coming to visit from time to time with one of our oldest friends, Garrett Beloff. Hosting both of them in Boston was always a highlight. My sister Elise would always want to talk about computer science at home, and it was nice having someone to talk about it with. And, of course, my oldest friend Andrew Shiner has been around for everything, and I'm glad to the core that we still hang out.

I am also humbled at the thought of how many new friends I now have from MIT. Jacob Knight, Nathan Bradshaw, Jeremy Kline, Mack Cleveland, and I would have lunch in the BCS building on Tuesdays and in addition to being great company, they are truly men after God. The Graduate Chrisitan Fellowship has provided such incredible company that it feels like I have known them far longer than I actually have.

From the Coast Guard Academy, I owe a great debt to Prof. Todd Taylor, Prof. Paul Miller, Dr. Andrea Ackerman, Coach Bill Randall, Jim "Major" Groves, Rob Palmer, and Carl and Christie Crabtree for their support and mentorship while I have been back in New England.

I am also honored to have had the the Coast Guard's advanced education program and the Society of Naval Architects and Marine Engineers support me through MIT, and I hope to pay forward the investment they chose to put in me.

This work would not have been possible without the support and patience of many fine people at the Patrol Boat Product Line and on the cutters themselves, including CWO Grove, LT Montvydas, CWO Hansen, Paul Schaefer, and the crews of *USCGC William Chadwick* and *USCGC Sturgeon*.

And finally, I am eternally grateful to my advisor, Prof. Steve Leeb, for having me in his lab and for pushing to get the best out of me. Under his mentorship, I have grown and now feel I have earned the lieutenant shoulder boards I will wear at graduation. I cannot imagine a better way of spending two years in graduate school than working for him.

Biographical Sketch

Jacob D. Skimmons is a lieutenant in the U.S. Coast Guard. Originally from Gaithersburg, MD, he graduated from the U.S. Coast Guard Academy in 2020 with a bachelor's of science in naval architecture and marine engineering. Following his commissioning, he reported to *USCGC Polar Star* (WAGB 10) as an engineer officer in training. He served as the damage control assistant and deployed to the Arctic on Arctic West Winter 21 and to Antarctica on Operation Deep Freeze 22. From there, he began work as a research assistant for Professor Steve Leeb at the Massachusetts Institute of Technology's Research Laboratory of Electronics. After graduation, he will be a technical engineer in the Vessels and Cargo Branch at the U.S. Coast Guard Marine Safety Center in Washington, DC.

"I appeal to you therefore, brothers, by the mercies of God, to present your bodies as a living sacrifice, holy and acceptable to God, which is your spiritual worship."
Romans 12:1

Contents

List of Figures

List of Tables

Chapter 1

Introduction

Marine engineers face several challenges when designing and maintaining ships. Commercial and military vessels must carry all the equipment necessary to run a small town, from sewage handling to air conditioning. Unlike many small towns, however, ships must withstand harsh seas, vibration, long periods at sea, corrosion, and other features of the maritime world which make reliability challenging. Down time costs dearly, so operators are keen on planning maintenance such that a vessel can operate uninterrupted during a period long enough to make them money or complete a mission. Then, of course, there are safety concerns. If a ship catches fire at sea, they cannot call the fire department because they *are* the fire department, and they must either fight the casualty or hope for the best in a lifeboat.

Ships have more equipment on them today than ever before. This makes them more capable than ever before, but each new device adds another point of failure. Crews can cope with this by doubling down on watchstanding practices, but the watchstanders themselves are often too valuable to have them simply check on machinery all day. Computers and sensors have relieved much of this monitoring burden, but there is still work to be done in equipping crews with data-driven tools to help them do their jobs better. New tools can also monitor systems which are too inexpensive to warrant formal monitoring at the current time, but which may waste time or cause catastrophe nonetheless when they fail.

Sensor networks on ships generate volumes of data which describe how well equipment runs and how it ages, but it often takes too much work and too much specialized knowledge to extract physical meaning from it. Thankfully, methods exist that generate higher quality data than before and reveal useful information without extra effort.

1.1 Electrical Power Data for Fault Detection and Diagnostics

Engineers on Coast Guard cutters primarily engage with their machinery through the cutter's machinery control system (MCS). On the Fast-Response Cutter (FRC), a keyboard, mouse, and display screen on the bridge form the central interface. MCS takes input from all sensors in the machinery plant, groups them by type, and presents them under different tabs on the MCS display. This gives the operators easy access to everything the system monitors and lets them easily keep track of their operating parameters. If these parameters drift out of

defined limits, the system draws the operator's attention to it with an alarm.

The system saves the data for the future, but technicians can typically only export it at low resolution. One point per minute is standard, but a laptop running proprietary software from the manufacturer can record data at higher rates.

MCS is useful and it saves considerable effort to stand the watch, but this is basically an automated version of a watchstander checking if the needle on a gauge stays within the green region painted around the rim. It does a good job of drawing attention to certain types of imminent casualties, but it does little to help watchstanders plan maintenance activities or find problems with auxiliary equipment which may not have sensors at all. Additionally, cutters still have a watchstander walking around with a clipboard and pen to check equipment which does not interface with MCS as much as it should.

MCS alarms also typically do not draw attention to *soft faults*, i.e., when automatic control systems cover up deficiencies. One example of a soft fault is when an air conditioning compressor has a low refrigerant charge and only provides the right amount of cooling by running more than it should. Although it meets the operator's request and appears to work, the unit wastes energy and racks up operating hours. Typical MCS alarms would tell the operator if the temperature went out of bounds or if the compressor failed to turn on, but not if it is wasting power or on its way to a greater casualty.

1.1.1 Theories of Monitoring and Maintenance

Monitoring and maintenance go hand-in-hand. Robert Randall [1] described the main approaches as such:

- *Run-to-break.* This is the simplest approach. For some machines, it may also be the most cost-effective if the cost of monitoring or regular maintenance exceeds the value of the machine or the down time after failure.

- *Time-Based Preventative.* The Coast Guard has volumes of maintenance cards with some periodicity assigned to it. Lubricating the fuel racks on a diesel engine daily or re-coating the underwater body every four years in dry dock fall into this category. This practice may be more costly or labor-intensive than it needs to be, especially if the parts being replaced still have useful life in them at the time of replacement.

- *Condition-based.* Here, the condition determines when it is time for work. For example, a vibration monitor on a bearing may indicate it is time for replacement when vibrations exceed a certain threshold. This keeps to a minimum the resources needed to maintain certain equipment, but it may not call for maintenance at a convenient time. A good time to overhaul a prime mover would be in dry dock, not two months after dry dock when the cutter is in the middle of a patrol.

To those ends, one can monitor equipment *continuously* or *intermittently.* Critical machines with quick or hard-to-predict failure modes warrant continuous monitoring, which increases the cost of operation but reduces the chance of even more costly down time. If the failure modes develop gradually, intermittent monitoring presents a cheaper alternative.

Naturally, increasing the level of formality with respect to monitoring also increases the cost of operation. Many devices such as heaters, pumps, and certain other run-to-break auxiliary machines are too inexpensive and fail too infrequently to warrant formal, intermittent monitoring schemes. Traditionally, a watchstander's acuity has been the best tool to diagnose soft faults and developing casualties. Senior watchstanders teach new watchstanders to pay attention to their senses every time they enter the engine room so that *something will feel off* during a developing casualty.

Relying on watchstanders this way has worked in the past because there were more of them and the equipment was simpler. Today, in an age when the 418-foot National Security Cutter has but two engineers on watch at a time and some of the most complicated equipment ever put afloat, this is a mistake. LCDR Kelsey Barrion, USCG, described the problem in her essay "The Elephant in the Engine Room," which won the U.S. Naval Institute's 2023 Coast Guard Essay Contest [2] . She claimed the "elephant" was "the yawing gap between the knowledge major cutter engineers are equipped with and the complexity of the equipment they are charged with maintaining." Crews on modern cutters need modern tools to keep up, and non-intrusive load monitoring (NILM) is one of them.

1.1.2 New Perspectives from Non-Intrusive Load Monitoring (NILM)

NILM traces its origins back to the early 1990s when George W. Hart published his work on a "nonintrusive appliance load monitor" as an improvement to home electrical power meters [3]. Tracking the performance of individual appliances in a home would provide valuable information, but wiring and maintaining individual sensors on each piece of equipment presented too much of a burden for most practical settings. Whereas an intrusive approach like that requires sensors on each item *downstream* of the source, Hart recognized that different appliances produced distinct power signatures in high-resolution data taken *at the source*. With statistics, signal processing tools, and computers at hand, he developed a set of techniques which could identify those signatures and ascribe them to their respective loads – and thus was born the idea of NILM that many recognize today.

Prototype NILM systems like the MIT "all-in-on" (AIO) box take the form of a metal enclosure with a touchscreen display containing all the computing and data acquisition tools necessary to collect NILM-quality data [5]. Researchers firmly bolt the enclosure to a bulkhead or other rigid structure and run two sets of cables to a 440-V three-phase power panel. The first set contains cables which lead to current transducers around each of the three phases. The second contains voltage leads for each phase. These voltage leads are connected to the panel through a spare breaker, but are only used for sensing purposes. The AIO box is separately powered from a 120-V wall outlet. Figure 1.1 desribes the form NILM takes on some Coast Guard cutters and Figure 1.2 is an example of typical data from the system.

The AIO box samples voltage and current at 8 ksps and calculates real and reactive power for all three phases at 60 Hz. Data prepared this way is more useful to researchers, makes for smaller files, and takes less computing power to handle. A local node of a network model called Wattsworth [6] stores the data and makes it easy to handle on-site.

A shipboard engineer familiar with different types of equipment can use NILM data to inform decisions simply by examining broad patterns and features of the data, e.g., the frequency of on-off cycles for a given machine or whether only two of three phases on a

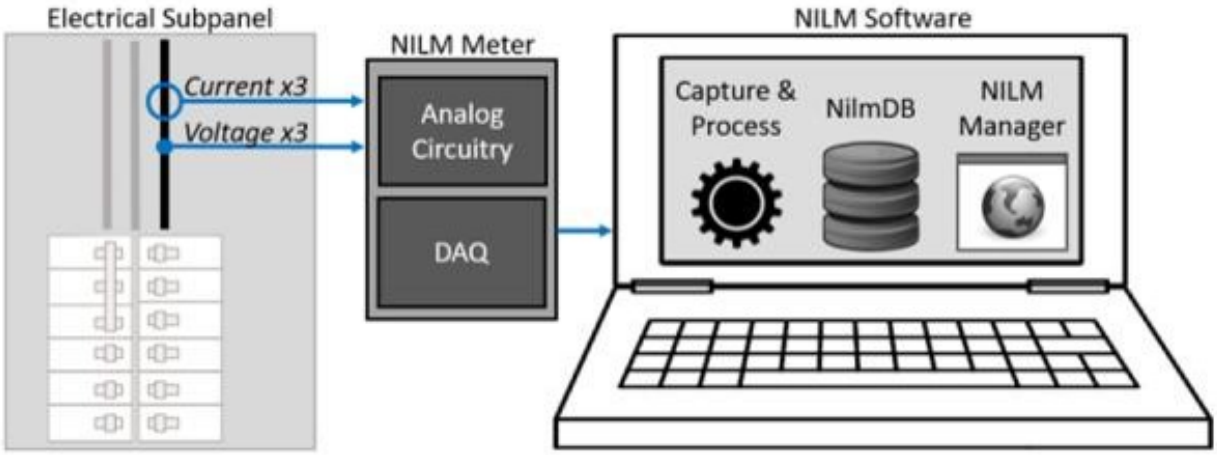

Figure 1.1: The basics of a NILM system installed on board certain Coast Guard cutters for research purposes. Adapted from [4].

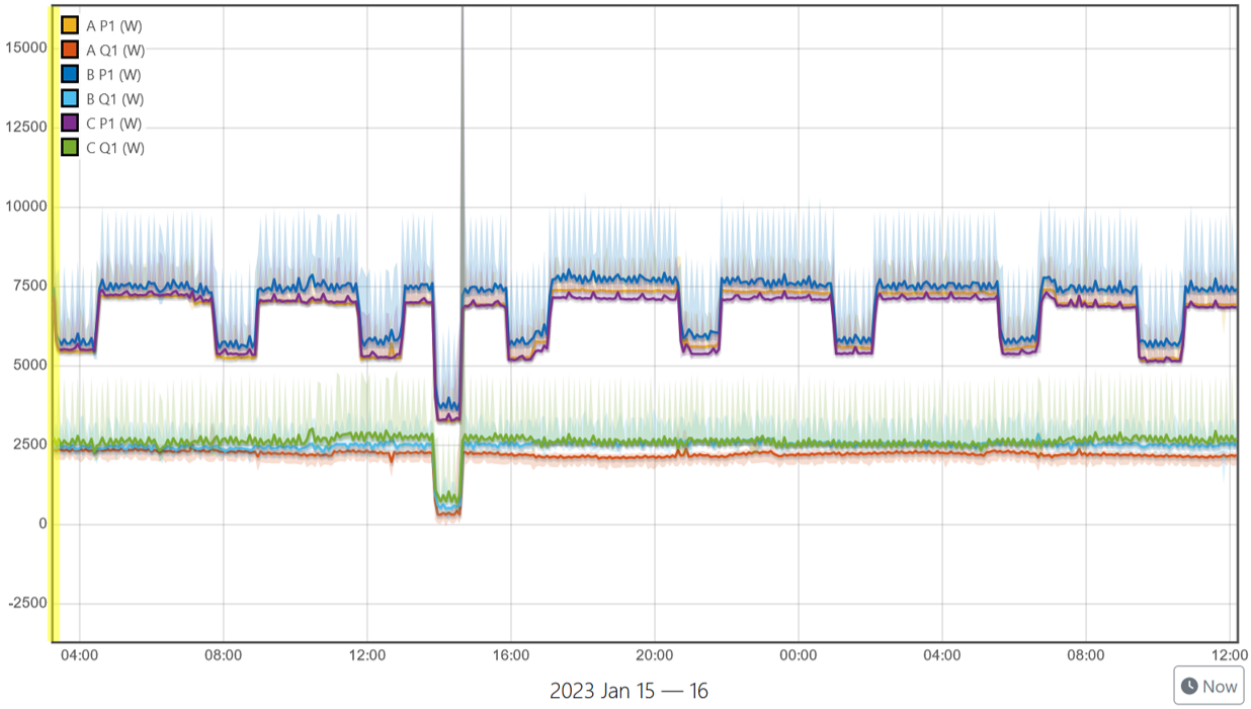

Figure 1.2: Typical NILM data taken from a Coast Guard cutter, showing different loads cycling on and off.

heater appear to draw power [7]. More nuanced analysis currently requires a trained data scientist, but these techniques are ripe for automation.

As it stands, NILM systems on Coast Guard cutters have diagnosed faults as diverse as failed motor couplings, bad sewage-system valves, faulty MCS sensors, and corroded jacket-water heaters. One particular casualty on *USCGC Spencer* (WMEC 905) involved

a jacket-water heater which showed clear signs of failure developing. By the time the crew inspected it, it had begun smoldering and threatened to start a fire [8].

Other ships are not as fortunate. After *USCGC Polar Star* (WAGB 10) left dry dock in 2023, a fire broke out on its 1A main diesel engine. The engineer officer of the watch secured the engine's pre-lube pump, but its flow switch had stuck closed. The lube oil heater did not shut off, so it overheated and ignited. A watchstander extinguished it, but the casualty proves how even a run-to-break machine "not worth monitoring" by conventional means can take out a whole ship.

The lube oil heater fire would fall right in the wheelhouse of NILM. If the NILM system sensed that the lube oil heater remained on after its pre-lube pump had shut off, it could alert watchstanders to the situation before it caused damage. There are too many types of casualties to list here which NILM can identify, but Chapter 4 discusses several practical applications on a Coast Guard Fast-Response Cutter.

1.2 Corrosion in the Marine World

Marine engineers constantly battle corrosion when designing and maintaining ships. Modern vessels usually employ one or all of the three most common corrosion-prevention tools: coatings, sacrificial-anode cathodic protection (SACP), and impressed-current cathodic protection (ICCP) [9]. Any of those tools on their own can reduce corrosion damage, but they are most effective when used in combination with each other.

1.2.1 General Overview

Corrosion occurs because of several electrochemical reactions which take place in the marine environment. When metal sits in sea water on its own, it develops a voltage with respect to a standard silver chloride (Ag/AgCl) reference electrode in the same electrolyte. Plotting the current coming out of the metal as a function of the electrolyte potential is useful for studying the corrosion behavior of a material. The voltage where the current flowing out of the metal goes to zero is the *equilibrium potential*, since there is no current flowing and the oxidation and reduction corrosion reactions occur at the same rate. Different metals behave differently at a given potential, so the Galvanic series, shown in Figure 1.3, orders them by equilibrium potential [9].

Breaking the chemical contact between metal and the electrolyte stops the corrosion reactions, and *paint coatings* have long been the simplest way to implement this [10]. The paint acts as an electrical and chemical barrier, thereby preventing ion exchange between either the anode or cathode, and the electrolyte. Thus, the most effective coatings have the highest electrical resistance.

For design purposes, it is reasonable to assume painted areas have infinite electrical resistance [11]. Others have noted that 10,000 Ω/m^2 is the practical threshold for total protection [12]. With buried pipelines, a Pearson Survey can determine how much the pipe's coating has degraded by measuring the voltage drop along the ground above the pipe [13]. Given the relatively high conductivity of seawater and the fact that ICCP systems may only read electrolyte potential from one point, a Pearson-style survey is not practical for ships.

1.2.2 Galvanic Corrosion

Galvanic corrosion describes how metals higher in the series accelerate the corrosion of those lower in the series [14]. Materials such as stainless steel and nickel-aluminum bronze (NAB) have relatively high reduction potentials compared to structural carbon steel. When different metals have electrical contact with each other and are immersed together in an electrolyte such as seawater, electrons flow from *less noble* metals like carbon steel through the metallic connection to *more noble* metals like NAB. The less noble metal (the anode) oxidizes and dissolves, and reduction takes place at the surface of the more noble metal (the cathode), usually the reduction of hydrogen ions to form gaseous hydrogen. This system forms a shorted galvanic cell, with greater differences in equilibrium potentially generally forcing the corrosion redox reaction to occur at an increased rate. Hence, less noble metals experience accelerated corrosion when in contact with more noble metals.

This phenomenon has several important uses. Introducing an even less noble metal than the one to be protected is a low-tech method of protection. Zinc, aluminum, and magnesium will all corrode before carbon steel does, so introducing them to a marine structure means they form a *sacrificial anode* which should be renewed after a certain period of time [15]. Figure 1.4 shows an example of four zinc sacrificial anodes mounted to an inspection cover which will be submerged in seawater.

1.2.3 Impressed-Current Cathodic Protection (ICCP)

Another common protection tactic is to use a direct-current power supply to oppose the current which would naturally flow between the anode and cathode. *Impressed-current cathodic protection* seeks to lower the reference potential around the anode to a point where there is a reversal in the flow of electrons out of the material [15]. For steel, this occurs when the potential of the steel hull relative to the electrolyte, measured with a Ag/AgCl reference electrode, is -850 mV. This voltage guideline does not indicate the exact potential to achieve current reversal; rather, it is a potential at which solid iron is adequately thermodynamically stable.

An ICCP system can theoretically run indefinitely, but protection current demand for an un-coated ship would be astronomical and it needs uninterrupted electrical power to work. In practice, ships receive underwater coatings as a first line of defense against corrosion. Designers place sacrificial anodes in recessed areas or places with lots of exposed cathodic metal like bow thruster tubes to give those areas extra protection. Sacrificial anodes can also make up for breakdown of the coating, or an ICCP system can serve this purpose.

When an ICCP system is used to protect areas made vulnerable by coating breakdown, parameters such as the output current and reference electrode voltage show the demand for protection. If one replaces the sacrificial anodes before they deplete, it may be reasonable to assume they provide a constant amount of protection. Therefore, the amount of coating degradation below the waterline drives the ICCP parameters.

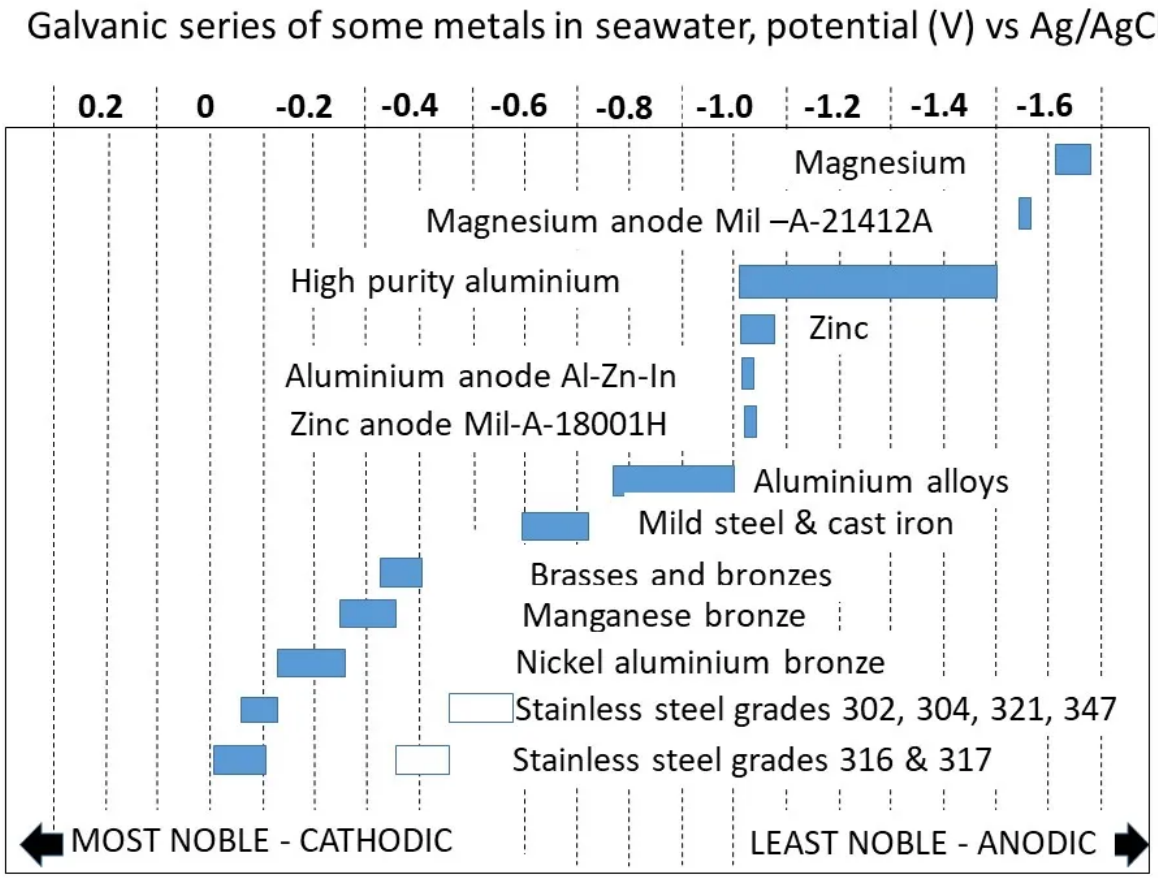

Figure 1.3: The Galvanic series [16].

Figure 1.4: New zinc sacrificial anodes.

1.3 The U.S. Coast Guard Fast-Response Cutter (FRC)

The Coast Guard commissioned the first FRC in 2012 and plans to acquire 66 in all. Built by Bollinger Shipyards in Lockport, LA, these 154-ft patrol boats conduct a wide range of missions from the Persian Gulf to Alaska. Figure 1.5 shows the *USCGC Margaret Norvell* (WPC 1105), one of the first FRCs commissioned.

1.3.1 Origins

In the early 2000s, the Coast Guard recognized an opportunity to retrofit several 110-ft *Island* class patrol boats with a stern launch so they no longer needed to use a crane to launch the small boat, among other improvements. To do so, engineers at Bollinger Shipyards chose to lengthen the vessel to 123 feet to fit all the new equipment on board. Unfortunately, they incorrectly calculated the section modulus of the converted vessels. Almost as soon as they converted ships hit the water, the hulls started buckling. After converting eight vessels, the Coast Guard scrapped the project and the Department of Justice sued Bollinger over the botched conversion [17].

Against this backdrop, the Coast Guard launched the FRC program to replace the aging 110 fleet. Instead of opting for a bespoke conversion project as with the 123s or designing its own vessel up from first principles, Bollinger drew heavily from a parent hull designed by the Dutch company Damen Group and already proven in service for South Africa [18]. With this approach, Coast Guard leadership intended to reduce both the cost of the program and the likelihood of failure.

Figure 1.5: The U.S. Coast Guard Fast-Response Cutter[19].

1.3.2 Notable Design Features

The FRC operates with a crew of 24 with an endurance up to five days. In addition to having a stern launch for a 26-ft small boat, these vessels have an advanced machinery control system (MCS) which collects sensor input from the machinery plant and allows watchstanders to control the equipment from a central location on the bridge.

FRC crews typically conduct near-coastal missions including fisheries enforcement, drug and migrant interdiction, search and rescue, and port security. These missions often entail long periods at idle or low speed punctuated by medium or high speed transits to a new operating area. A typical patrol boat mission cycle involves one or two weeks underway followed by a period at the pier in a ready recall status, followed by a time when they are down hard for maintenance and not mission-capable.

With a semi-displacement hull, the FRC can reach a top speed of 28 knots or more. Two MTU 20-cylinder diesel engines provide power to two fixed-pitch propellers, and an electric bow thruster helps with docking the vessel.

The hull is made of A106GRB carbon steel, the propellers are nickel aluminum bronze, and the propeller shafts are 316 stainless steel. To provide directional stability, two skegs come down under the stern and enclose the propeller shafts. This forms a particularly long stern tube region with two water-lubricated bearings: one in the middle, one on the aft end [20].

In terms of corrosion protection, the FRC has three protection mechanisms: an epoxy coating system, zinc sacrificial anodes, and an ICCP system made by Cathelco. Shipyard workers blast and paint the hull every four years when the vessels go to dry dock, but the zincs need more frequent attention. They need replacement once per year, so cutters contract divers to do the replacement every 12 months.

Chapter 2

FRC Stern Tube Corrosion Investigation

After several years in service, certain maintenance problems began manifesting in the FRC fleet. One of the most shocking issues relates to severe corrosion inside the stern tubes. In some cases, the damage is so great that the shipyard must cut out the stern tubes, manufacture new ones, and weld them in place. This repair work can cost the Coast Guard upwards of $250,000 every time it happens, which places unnecessary strain on the service's budget and saps time from a cutter's operational availability. It was crucial to determine the cause so the Surface Forces Logistics Center (SFLC) could prevent it from occurring in the future. This section was written in collaboration with LT Michael Bishop [21] and LT Isabelle Patnode [22], USCG.

2.1 Background

FRCs have often showed varying degrees of stern tube corrosion damage, but one particularly bad example came from Puerto Rico. On April 19, 2022, *USCGC Richard Dixon* (WPC 1113) entered dry dock at the Coast Guard Yard in Baltimore, MD. Commissioned on June 20, 2015, *Dixon* was the first cutter based in San Juan to undergo shaft removal and stern tube maintenance. After yard workers removed the shafts, they discovered that the inside of the stern tubes showed widespread coating failure and heavy rust all over. Blasting the tubes back to bare metal revealed deep pits throughout but concentrated closer to the bearing housings. The deepest pits were about 3/8 inches deep, representing almost 50% wastage in

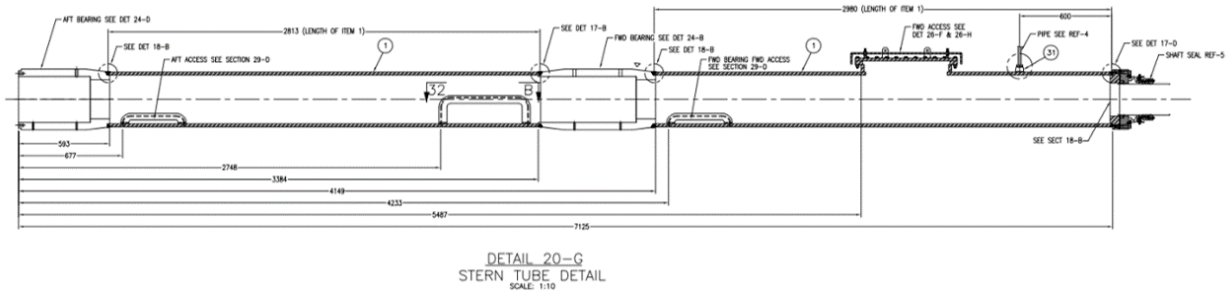

Figure 2.1: Drawing of the FRC stern tube showing the bearings and inspection covers.

Figure 2.2: Corrosion damage in the stern tube of *USCGC Richard Dixon* as discovered in dry dock.

some parts of the stern tube [23]. Figure 2.2 and Figure 2.3 show the damage.

Other cutters have also showed damage in this region. *USCGC Charles Moulthrope* (WPC 1141) was commissioned on January 21, 2021 and exhibited similar damage to the stern tube when inspected in dry dock in October 2023 [24]. Evidently, it does not take long for severe damage to befall an FRC under the right conditions.

2.1.1 Stern Tube Design and Galvanic Corrosion

Figure 2.1 is a drawing of the FRC stern tube. It is made from 14-inch schedule 80 carbon steel pipe, alloy ASTM A106GRB. It is approximately 23 feet long and has two water-lubricated polymer bearings. The propeller shaft is eight inches in diameter and made from 316 stainless steel [20].

There are three inspection covers on the underside of the stern tube, each with zinc anodes bolted to it. Starting with hull 1150, the forward and aft covers have three 2.8 lb zinc anodes each and the center cover has eight. Previously, cutters only had two zincs on the forward and aft covers and four on the middle cover. These older vessels are being upgraded

(a) (b)

Figure 2.3: Stern tube of *USCGC Richard Dixon* after sandblasting[23].

Figure 2.4: Damage to the stern tube of *USCGC Charles Moulthrope* after sandblasting[24].

Figure 2.5: Deep pitting in the stern tube of *USCGC Charles Moulthrope*[24].

to the new zinc specifications as they come in for maintenance. There is also a large 22-lb zinc anode mounted to a cover which opens to the engine room. Since the cover cannot be unbolted without flooding the engine room, workers can only replace this one in dry dock.

As with the rest of the underwater body, the inside of the stern tube receives several coats of epoxy paint to protect the surfaces. Shipyard workers renew the coating system whenever they remove the shafts according to standard SFLC specifications. Sandblasting back to near-white is a standard step in the process to remove all the old paint and rust [25].

The design of the stern tube makes it susceptible to galvanic corrosion. Stainless steel ranks higher in the galvanic series than carbon steel, and since the shaft makes electrical contact with the hull, the hull structures will preferentially corrode. The surface area ratio of cathodic metal compared to anodic metal drives the rate of galvanic corrosion. With the shaft representing almost 40% of the total surface area in the stern tube, adequate protection is critical. When designers face this situation, it is generally good practice to coat both the cathode (the shaft) and the anode (the hull structures) [26]. If only the anode has a coating, current demand from the cathode will concentrate in any coating holidays and drive deep pits into the metal, like the pitting seen in Figure 2.3.

2.2 Preliminary Findings

The logical place to begin investigating this issue was with records of the corrosion protection mechanisms. Specifically, information about what the zinc anodes and the ICCP were doing would provide insight on why the stern tube experiences under-protection. Combined with information about the vessel's maintenance history and operations, themes began to emerge.

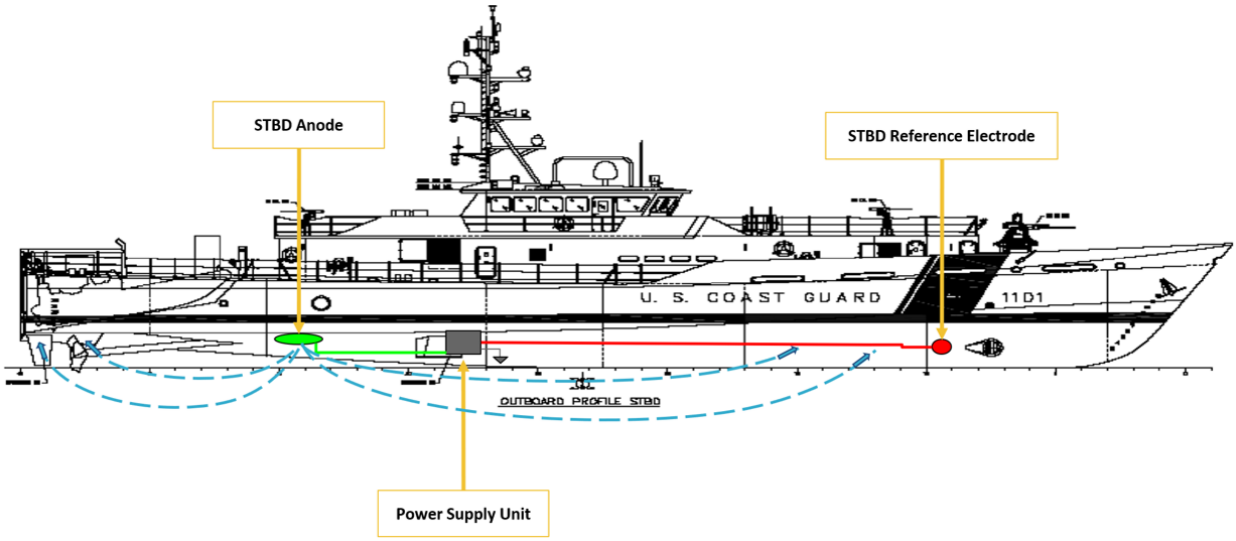

Figure 2.6: Overview of the ICCP system on the FRC.

2.2.1 Initial ICCP Log Review

Review of ICCP logs from four FRCs indicated that the ICCP systems were injecting no current for the months examined. Furthermore, readings from the reference electrodes showed that the hull remained well within the range of protection, naturally sitting at about -900 mV. Figure 2.6 shows the ICCP configuration on the FRC.

Although there is clear disparity between how protected the ICCP system thinks the cutter is and how protected certain parts actually are, it makes sense that the reference electrodes would not pick up on the bad conditions in the stern tube. Two factors working against the stern tubes are that they are enclosed spaces and they are far aft. The ICCP reference electrodes are far forward and as such are less sensitive to changes in protection status far from them. The enclosed nature of the tube means that current naturally has a more difficult time getting in, so a reference electrode even just outside the stern tube may not yield useful information regarding what is going on inside.

Another factor to consider is that the reference electrodes are only a few feet aft of the bow thruster tube which has 12 zinc anodes bolted to the inside and a *coated* thruster propeller. These anodes confer protection to the entire area and locally lower the reference potential near the electrodes, effectively blinding the ICCP system to a degree on what the state of protection is elsewhere on the cutter. Figure 2.7 demonstrates this phenomenon.

2.2.2 Stern Tube Zinc Expenditure

Figure 2.8 and Figure 2.9 show typical photographs taken during stern tube zinc replacement on various FRCs. They revealed that the zincs were often completely or almost expended, whereas common practice dictates that zincs should be replaced with no less than 20% of the original material remaining.

The cases of complete zinc expenditure are particularly troubling because they give no indication of when exactly they ran out. The stern tube may have been unprotected for a

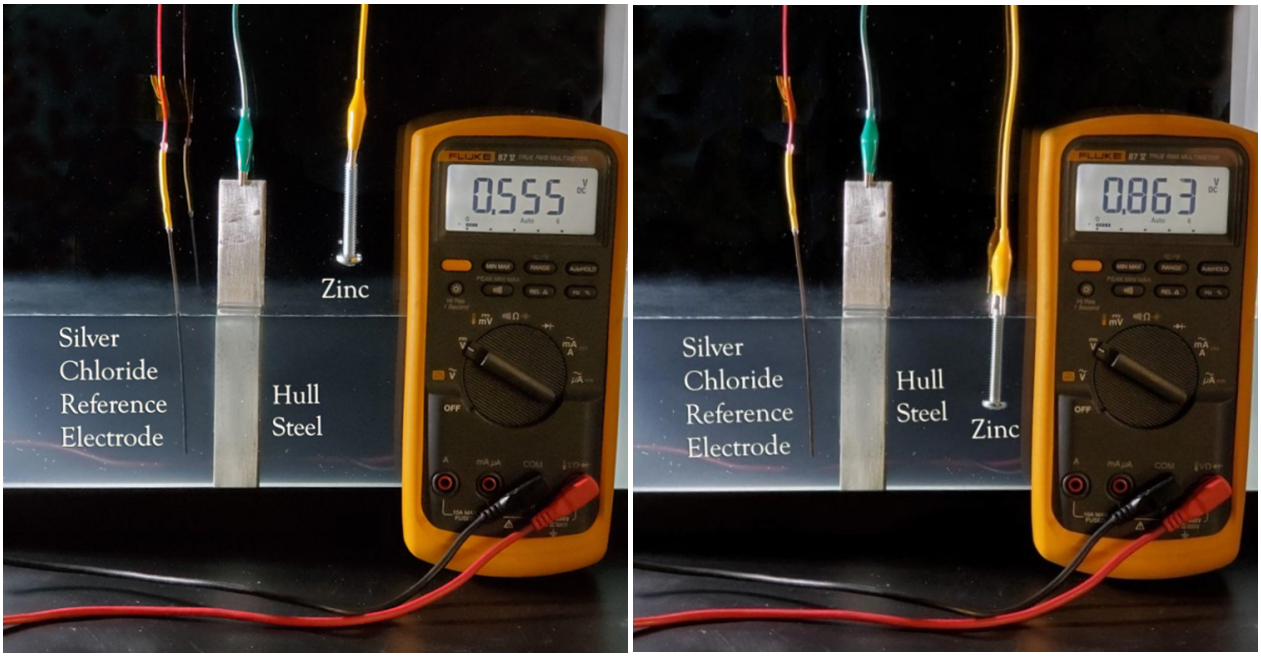

(a) Zinc out of the solution (b) Zinc in the solution

Figure 2.7: Demonstration of how a reference electrode's proximity to a zinc anode affects its readings.

week or for six months, and the zincs would look the same at replacement.

Clearly, it was necessary to estimate how zinc should be installed in the stern tube. According to ABS guidelines [27], the forward section of the stern tube needs 13.8 lbs of zinc and the aft section needs 13.2 lbs to safely last one year considering the amount of exposed stainless steel in the stern tube. The current design has a total of 27.6 lbs in the forward section and 16.8 lbs in the aft section. However, the 22 lb anode in the forward section must last four years. Only 5.6 lbs of zinc in the forward section can be renewed while the ship is in the water, meaning 11.1 lbs of zinc can be expended per year for four years based on the desired maintenance cycle.)

As it stands, the forward section of the stern tube is under-protected and the aft section is protected, but only with a safety factor of about 1.3. If environmental conditions contribute to greater zinc consumption than the ABS rules estimate, or if the zincs go longer than 12 months without replacement, the area risks under-protection.

2.3 Solutions

To summarize, the problem is that the propeller shaft demands more current than the stern tube zincs can provide for a year and the ICCP system does not contribute current to that area in its standard configuration. As a result, the zincs expend ahead of their scheduled replacement time and leave the stern tube under-protected. Because of the large cathode to anode surface area ratio, the carbon steel hull structures experience severe pitting at any coating holidays.

(a) *William Chadwick*, 18 mo. -850 mV, Boston (b) *Margaret Norvell*, 12 mo. -850 mV, Miami

Figure 2.8: Stern tube zincs at the time of replacement on two cutters.

(a) *Warren Deyampert*, 14 mo. -850 mV, Boston (b) *William Sparling*, 9 mo. -1050 mV, Boston

Figure 2.9: Stern tube zincs as removed from two Boston cutters.

(a) Hulls 1149 and earlier

(b) Hulls 1150 and newer

Figure 2.10: Zinc configuration on the center stern tube cover.

There are three things which the operators can practically do to remedy the issue:

- Increase the amount of zinc in the stern tube
- Reduce current demand by coating the propeller shaft
- Adjust the ICCP system so it injects current

The first two solutions require design changes, one more drastic than the other. An experiment aboard *USCGC Margaret Norvell* (WPC 1105) shows the extent to which the third solution can help in Section 2.4.

2.3.1 Solution 1: Additional Zinc

The Coast Guard has already implemented the first solution by adding more zinc inside the stern tube, as seen in Figure 2.10. Hulls 1150 and onward leave the shipyard with as many zinc anodes as will fit on the stern tube covers: three on the forward and aft ones, and eight on the middle one. Time will tell whether this measure is sufficient to protect the stern tube. Since hull 1150 only commissioned in 2022, its first shaft removal and stern tube inspection will be in roughly 2026.

In the meantime, recent zinc replacement on several FRCs provided an opportunity to track the wastage rate for comparison to that on other cutters. Figure 2.8 and Figure 2.9 show the difference in consumption at different service intervals and areas of operation. The vessels stationed in Boston had their zincs weighed at the most recent replacement in February 2024. In 12 months, they will be weighed again and used to draw conclusions.

2.3.2 Solution 2: Propeller Shaft Coating

Coating the shaft is the ideal solution, although it may not be easy to implement. Coatings generally do not stick well to stainless steel, and the stern tube environment is particularly

tough on coatings. Vibration, turbulent flow, and torsion of the shaft all contribute to a difficult coating situation. MIL-STD-2199 lays out guidelines for propeller shaft coatings on military vessels [28].

The bearing design also cannot readily accommodate a shaft coating 0.05 inches thick. The coating increases the diameter of the shaft, so the bearing staves must be shorter and a liner installed to form the new bearing surface on the shaft. The bearing manufacturer confirmed it could be done for the FRC, so it is still a viable option. Figure 2.23 shows the original bearing configuration, Figure 2.24 shows the proposed modification, and Figure 2.25 shows detail views of both configurations.

2.3.3 Solution 3: Increase ICCP Current

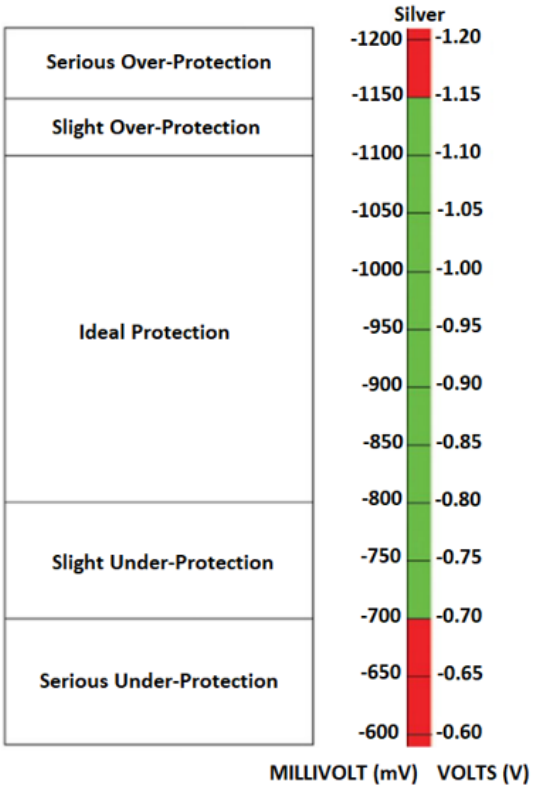

Figure 2.11: Levels of ICCP protection from [29].

Adjusting the ICCP settings is the easiest solution to implement. If the ICCP contributes current to the stern tube, it reduces the load on the zincs and makes them last longer. By changing the system's set point, an operator can force it to emit current to maintain a lower reference potential than it otherwise would. This current would reach the stern tube in theory, but data did not exist to show the extent to which it did. Thus, an experiment needed to be done on an FRC to determine this.

The main concern here is avoiding overprotection near the ICCP anodes. One source discussed the possibility of hydrogen embrittlement in similar steel alloys due to overprotection [30]. The vessel uses a special dielectric shield to protect the hull in those areas, but the present setup may not be enough at a lower reference voltage set point. The lowest acceptable set point had to be determined experimentally, and in the case of the FRC it came to -1050 mV.

2.4 Experiment on *USCGC Margaret Norvell* (WPC 1105)

Common knowledge among corrosion engineer suggests that the stern tube needed its own anodes on the inside because protection current from any source on the outside cannot

easily flow through the small gaps in the bearings or hatch covers. The increase in resistance through these areas makes it impractical to rely on the meager amount of current which can get through.

However, data did not exist to prove conclusively whether this was the case with the FRC. Since few practical solutions to the stern tube corrosion problem exist, it was worth exploring how well the ICCP system could affect that area. A field experiment was necessary to determine what the ICCP would do at different settings and how far it could be pushed before risking overprotection.

2.4.1 Objectives and Design

The experiment had to answer two questions. First, whether the ICCP current could affect the inside of the stern tube. Second, how far the system could push before risking overprotection around the anodes.

To that end, it made the most sense to do the experiment during zinc replacement on an FRC. Three conditions of stern tube zinc could be tested: zinc at the end of its service life, no zinc, and brand new zinc. Stepping the ICCP system to different levels of output current would provide discrete points for future reference.

The standard method of assessing the state of corrosion protection is with an Ag/AgCl reference electrode. Measuring the voltage of the hull with respect to the electrode yields an indicator of how close steel is to its equilibrium potential. Figure 2.11 shows the standard chart from Cathelco identifying regions of protection. Above -800 mV, steel is underprotected and liable to corrode. Below -1150 mV, the symptoms of overprotection show. The hull produces excess hydrogen in this state, which can lead to a phenomenon called *cathodic disbondment* of the paint coating in which the paint no longer adheres to the substrate and flakes off [31]. Some sources indicate hydrogen embrittlement can occur in certain types of steel [30].

Since the stern tube was not designed with reference electrodes in mind, special electrodes had to be made which could fit inside the tube. To investigate overprotection, another set of electrodes was created to attach to the hull near the ICCP anodes.

2.4.2 Custom Ag/AgCl Reference Electrodes

Since the hatch covers were bolted in place with 3/8-16 countersunk machine screws, modeling the custom reference electrodes after this form factor was a logical choice. The sensor element itself is just a silver strip coated with an AgCl coating, so it can be as small as the screws. The trade-off here is that a smaller sensor surface is less reliable in the long run since damage to the coating has a proportionately greater effect than with a larger surface area. The sensors for this experiment only had to last a short period of time, so long-term reliability was not a concern.

Figure 2.12 shows a screw-type electrode. In essence, these custom screw electrodes were just that: 3/8-16 screws which protruded about 1.25 inches into the stern tube, and which had a silver strip epoxied into a hole bored down the middle. The strip did not extend beyond the end of the threaded section, but about one inch of its length was exposed to seawater which flooded the inside of the screw. The head was enlarged and a three-inch

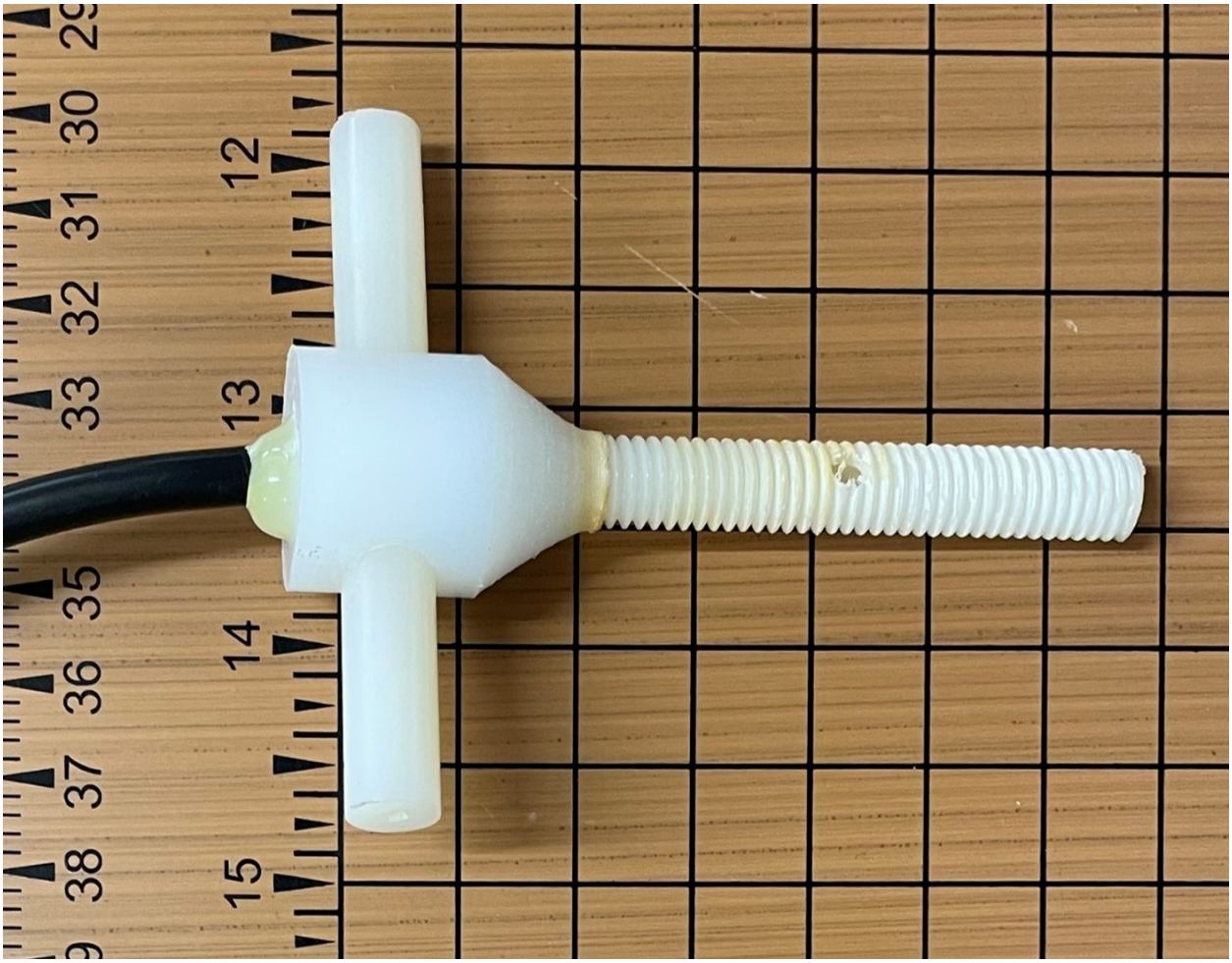

Figure 2.12: Custom screw-type reference electrodes for the stern tube.

dowel inserted through it so a diver could easily screw it in without special tools. The silver strip was soldered to a barrel jack connector on the end of a 10-inch wire. The connector was waterproof, but connecting it when flooded underwater would not matter since the gasket in the connector only kept the rest of the water around the boat from interfering with the signal. The diver could connect the barrel jack to its corresponding connector which took the signal back to the data logger on the deck of the cutter. Figure 2.13 shows a simpler stick-type electrode used on the outside of the hull and Figure 2.14 shows an electrode in place. Figure 2.15 shows the data logger, electrodes, and cables used in the experiment.

2.4.3 Results

Figure 2.16 shows how data was collected from the ICCP unit. Figures 2.17 through 2.19 show the effective change in stern tube electrolyte potential as the ICCP transitions from its regular set point of -850mV to -1110mV. Figures 2.20 through 2.22 show the electrolyte potential in the stern tube as a function of ICCP current for different zinc conditions. In every case, the potential decreased as the ICCP emitted more current.

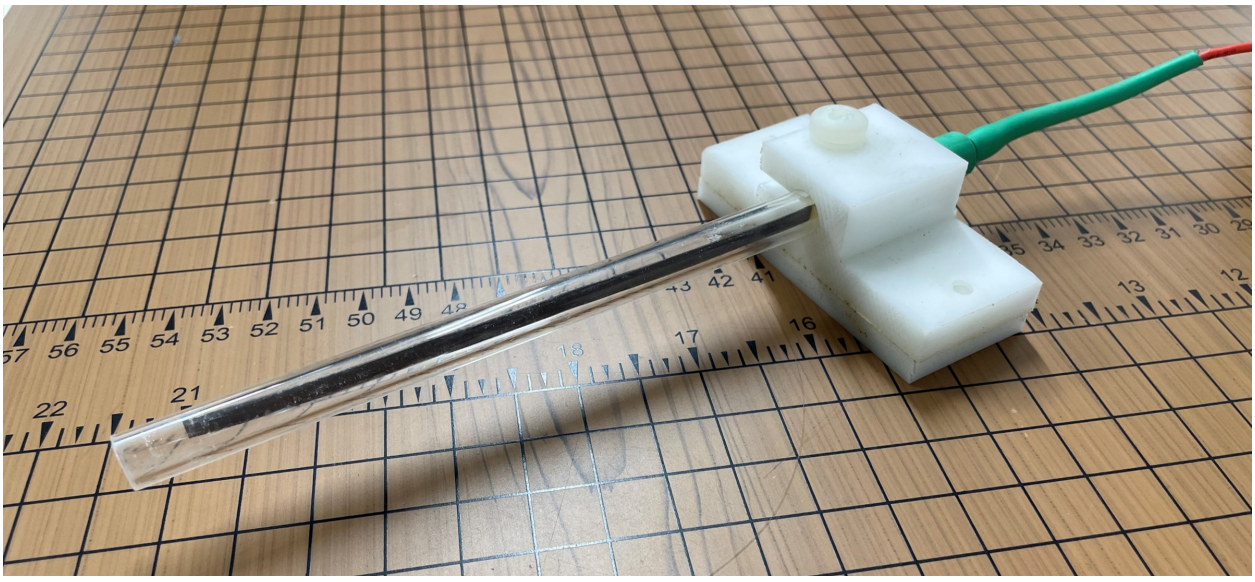

Figure 2.13: Custom stick-type reference electrodes used near the anodes.

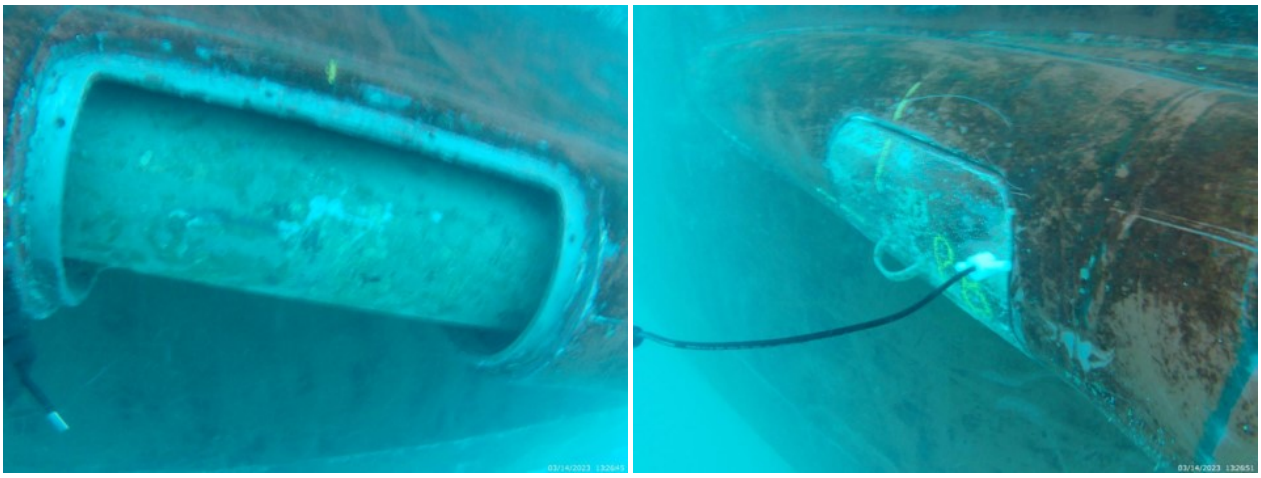

(a) Cover removed, showing exposed shaft (b) Cover in place, with screw electrode

Figure 2.14: Underwater stern tube photographs taken during the *Margaret Norvell* experiment.

Figure 2.15: The data acquisition kit used in the *Margaret Norvell* experiment.

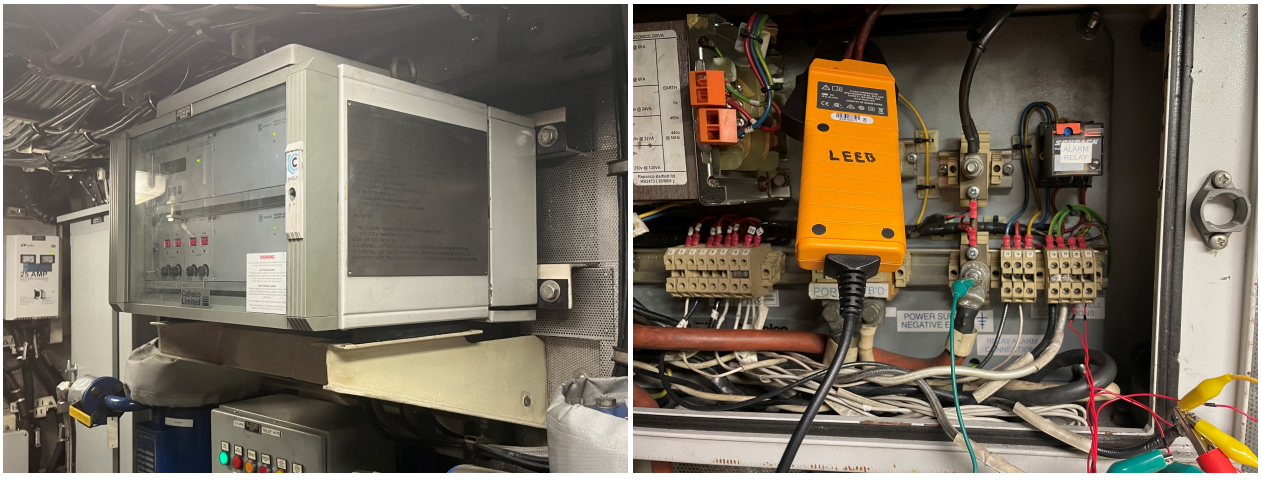

(a) The ICCP power supply (b) Data collection points inside the ICCP

Figure 2.16: The Cathelco ICCP unit in the FRC engine room.

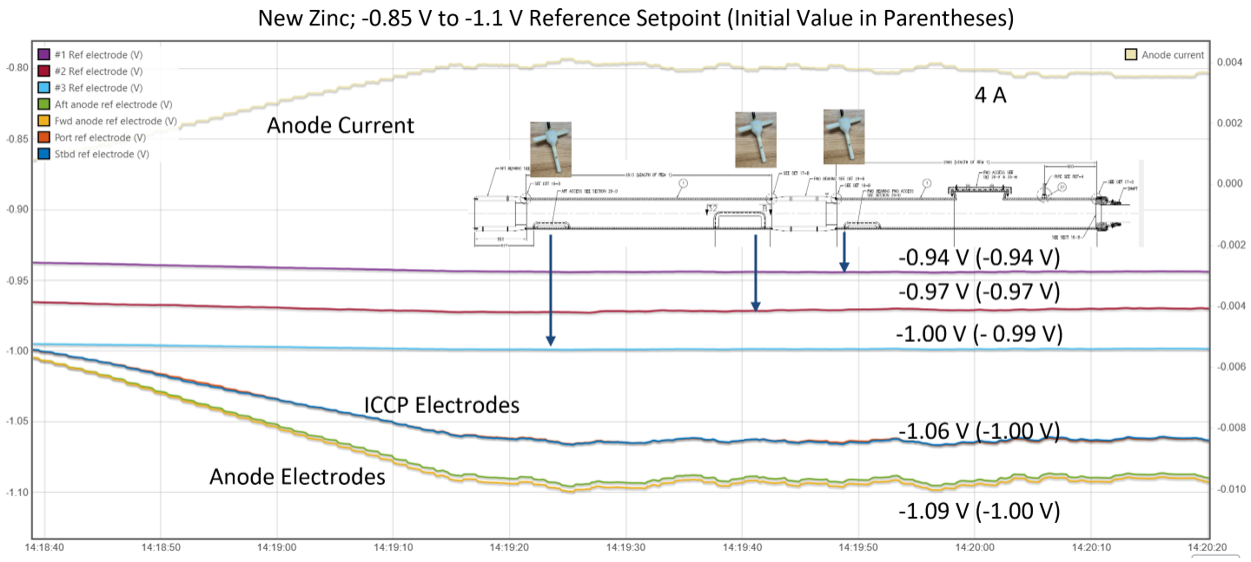

Figure 2.17: Change in potential inside the stern tube from ICCP setting of -850 mV to -1100 mV, new zinc anodes in place.

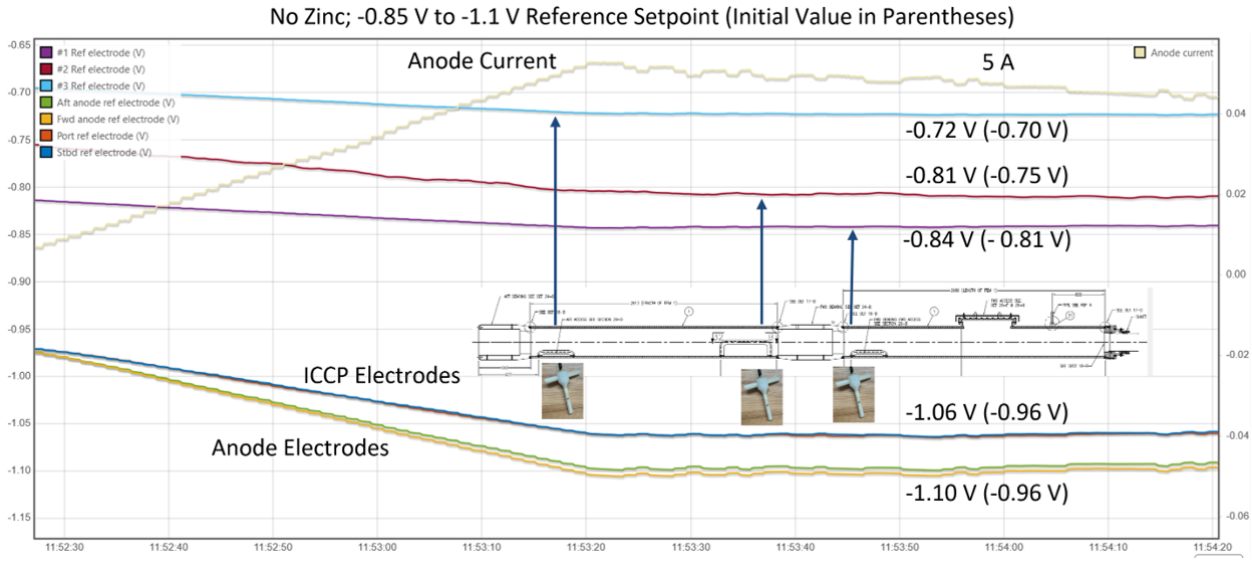

Figure 2.18: Change in potential inside the stern tube from ICCP setting of -850 mV to -1100 mV, no zinc anodes in place.

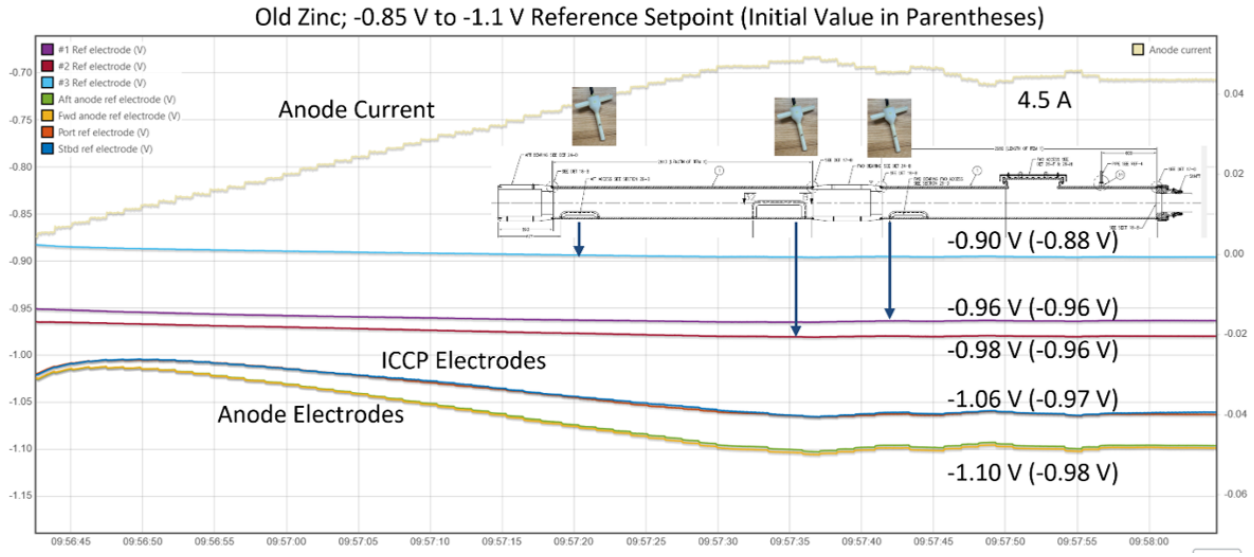

Figure 2.19: Change in potential inside the stern tube from ICCP setting of -850 mV to -1100 mV, old zinc anodes in place.

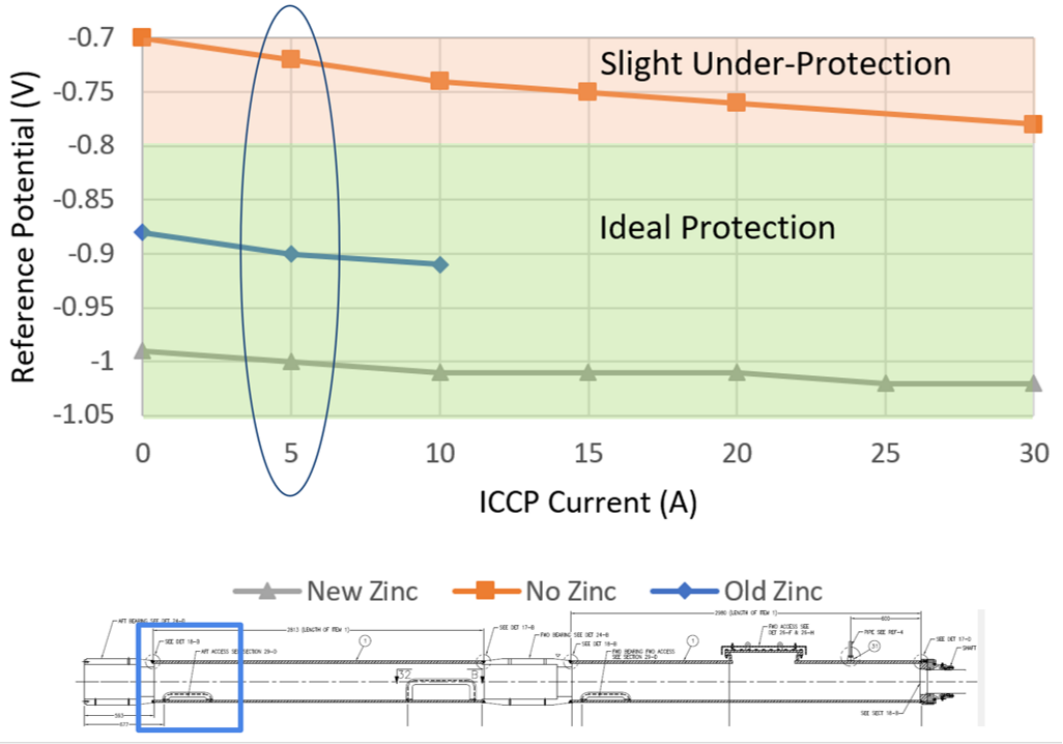

Figure 2.20: Potential in the stern tube as a function of ICCP output current, aft stern tube cover.

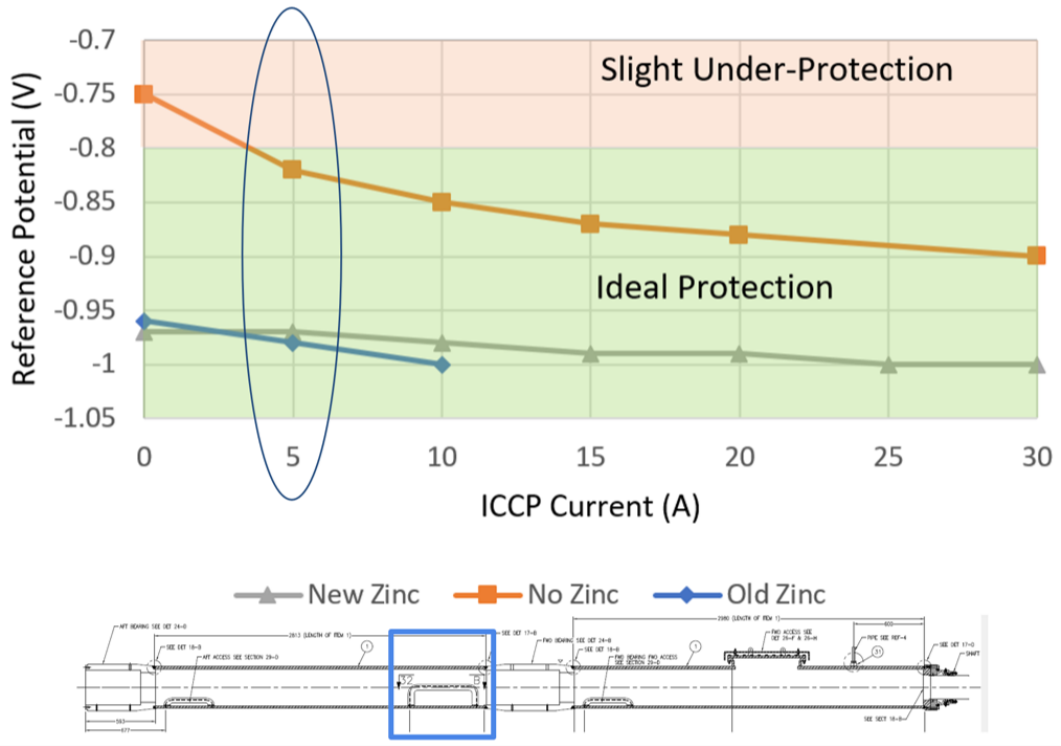

Figure 2.21: Potential in the stern tube as a function of ICCP output current, middle stern tube cover.

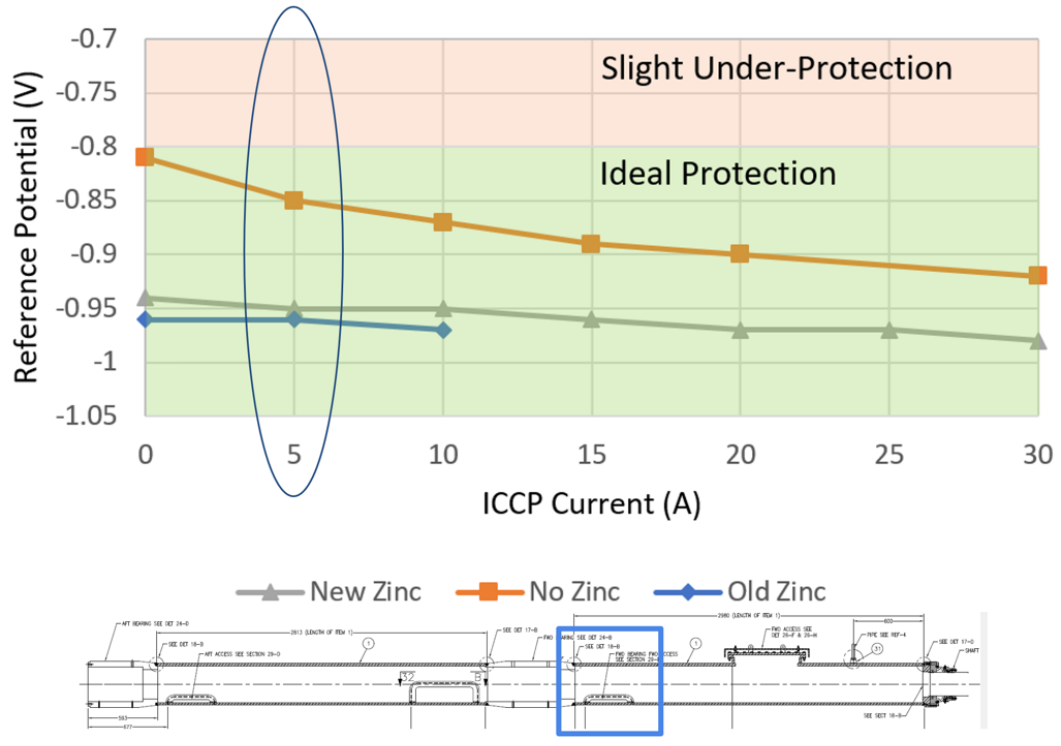

Figure 2.22: Potential in the stern tube as a function of ICCP output current, forward stern tube cover.

2.5 Conclusions

The stern tube corrosion problems in the FRC class stem from design choices which created an environment prone to galvanic corrosion. Although the designers recognized the need for corrosion protection measures back there, the original setup did not protect the area enough. The original quantity of zinc would expend well ahead of its scheduled replacement date in some cases, and aggravating factors like delayed maintenance only made matters worse.

Even through coating the propeller shaft would address the cause of the galvanic corrosion, it is the most difficult solution of the three discussed here to effect. The Coast Guard has also reached the practical limit to the number of zinc anodes which can fit in the stern tube without significant design alteration. As for the ICCP, changing the settings from standard would provide a degree of protection to the stern tube. It would not be enough to protect the stern tube without other measures, but it may give the operators enough extra purchase out of the zincs to keep disastrous galvanic corrosion problems from destroying the hull structures before the vessels receive maintenance on an economical schedule.

The Coast Guard has started a fleet trial with five cutters around the country set to -1050 mV: *USCGC Raymond Evans* (WPC 1110) in Key West, FL; *USCGC John McCormick* (WPC 1121) in Ketchikan, AK; *USCGC Oliver Berry* (WPC 1124) in Honolulu, HI; *USCGC Joseph Doyle* (WPC 1133) in Key West, FL; and *USCGC William Sparling* (WPC 1154) in Boston, MA. The results of this experiment will determine whether to configure the rest of the fleet in the same way.

One way of checking the efficacy of changing the ICCP set point is to examine the zincs at replacement. If the theory is sound, there should be considerably more zinc left in the stern tubes on the -1.05-V ships. Several Boston FRCs had their zincs replaced in February 2024, including *Sparling*, and some preliminary results suggested that the new setting may work as intended. Figure 2.9a shows the zincs from *USCGC Warren Deyampert* (WPC 1151) after 14 months at -850 mV whereas figure 2.9b shows the zincs from *Sparling* after 9 months at -1050 mV. It is not right to conjecture too far here given the difference in service time, but the zinc condition in February 2025 when all would have seen roughly the same time in the water will enable further conclusions on this subject.

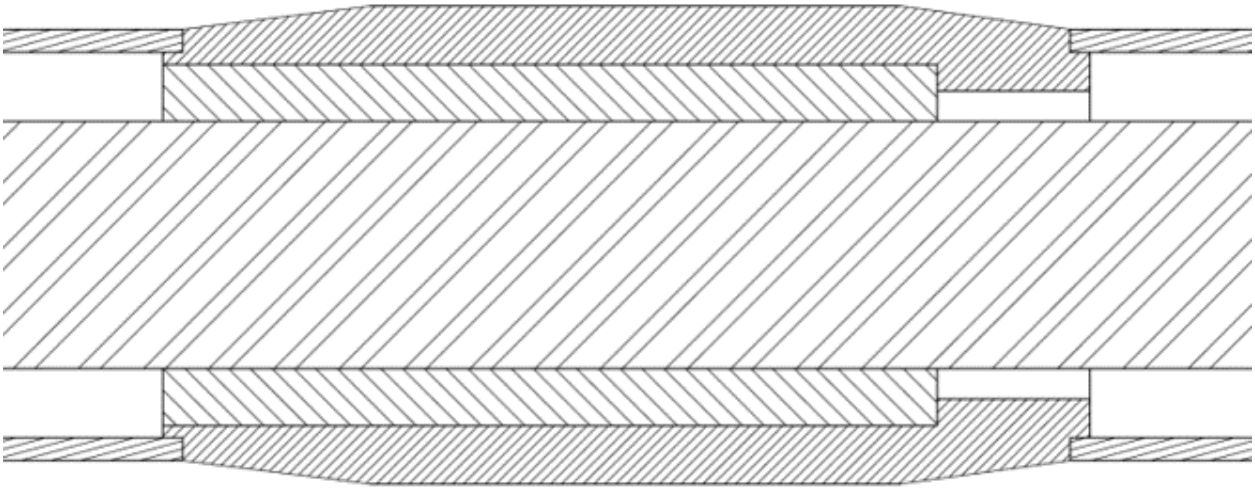

Figure 2.23: Original FRC bearing configuration.

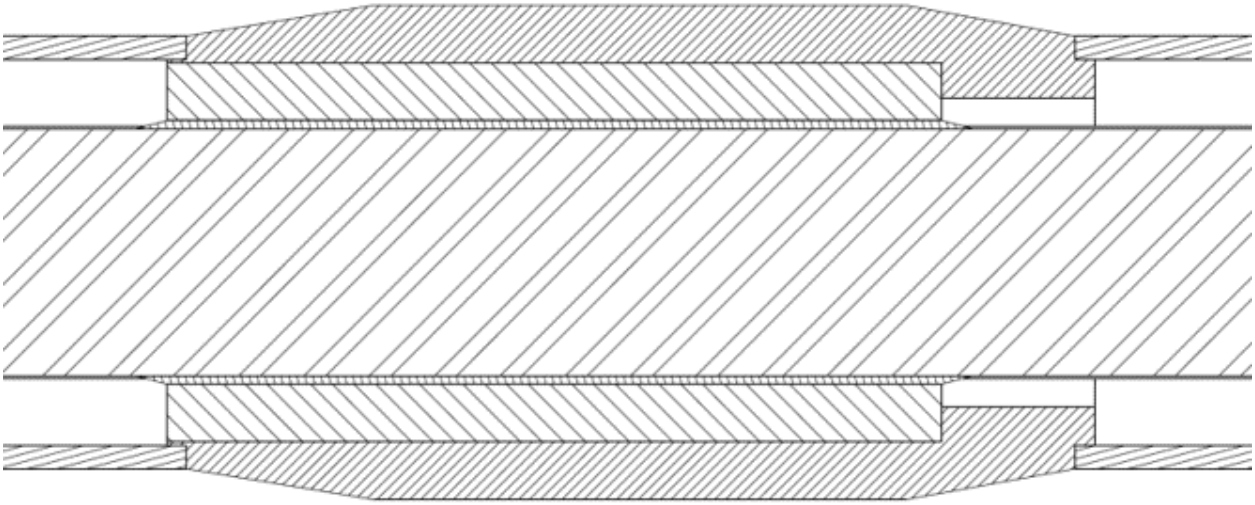

Figure 2.24: Modified FRC bearing configuration to accommodate a liner and coating.

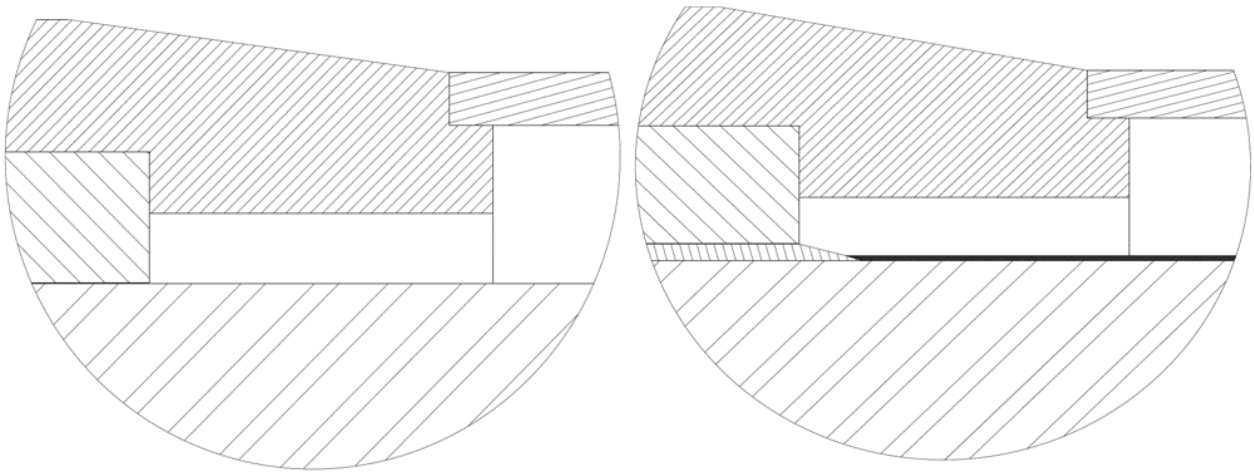

(a) Original

(b) Proposed

Figure 2.25: Detail views of the current and proposed FRC bearing configurations.

Chapter 3

Impressed-Current Cathodic Protection (ICCP) Data Analysis

After investigating the stern tube corrosion problem, it became apparent that the ICCP logs may contain important information which can go overlooked. The standard log sheet states that crews must send them to Cathelco (the system manufacturer) and the support staff at SFLC so these groups can also have visibility on how the system performs, mostly to check basic functionality.

The analysis efforts here go a step further. Since the crews spend considerable time preparing and organizing ICCP logs, it is important to ensure the collection method is valid and that the data truly contains useful information. After all, there is no point in spending the time to collect the data if it is not useful. In addition to determining what the present data set offers, analysis of experimental data taken underway on *Chadwick* showed what becomes available with enhanced data collection efforts.

As it currently stands, the ICCP logs give the operators decent insight on whether the system works and shows a few phenomena related to corrosion. However, the logs are not as useful as they could be if the Coast Guard were to invest in automatic logging and analysis.

3.1 Data Collection Method

The ICCP system is a stand-alone unit and does not interface with MCS in many ways. It can activate an MCS alarm on the bridge through a singular alarm state relay, but operating parameters and controls only appear on the system itself in the engine room.

Figure 3.1 shows part of a typical ICCP round sheet. Once per day, a watchstander goes up to the display and writes down several parameters: geographic location, water temperature, anode output current and voltage, port and starboard reference electrode voltage, and mode (typically automatic).

Cutter crews often take ICCP readings at the start of each day on the midnight round. This is important because patrol boats often anchor at night or simply go back to the pier to reduce crew fatigue instead of remaining underway. Although the round sheets do not account for vessel speed at the time of measurement, it is reasonable to assume that the vessels were stationary when the watchstanders made most of the log entries.

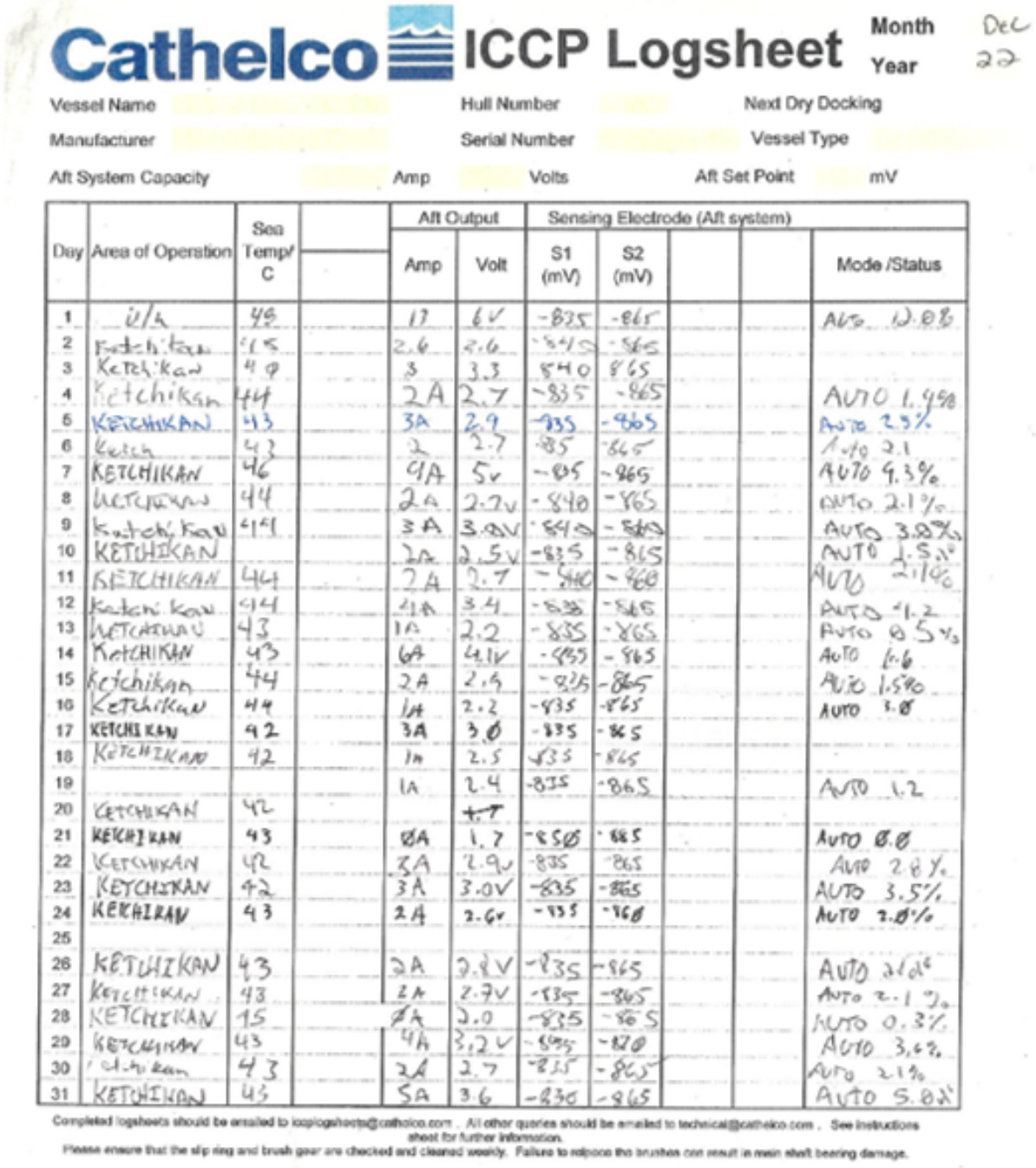

Cathelco ICCP Logsheet

Month DEC
Year 22

Vessel Name | Hull Number | Next Dry Docking
Manufacturer | Serial Number | Vessel Type
Aft System Capacity | Amp | Volts | Aft Set Point | mV

Day	Area of Operation	Sea Temp/ C		Aft Output Amp	Aft Output Volt	Sensing Electrode (Aft system) S1 (mV)	S2 (mV)			Mode /Status
1	u/a	45		17	6V	-835	-865			AUTO 12.0%
2	Ketchikan	45		2.6	2.6	-845	-865			
3	Ketchikan	49		3	3.3	840	865			
4	Ketchikan	44		2A	2.7	-835	-865			AUTO 1.4%
5	KETCHIKAN	43		3A	2.9	-835	-865			AUTO 2.3%
6	Ketch	43		2	2.7	-835	-865			AUTO 2.1
7	KETCHIKAN	46		9A	5v	-805	-865			AUTO 9.3%
8	KETCHIKAN	44		2A	2.7v	-840	-865			AUTO 2.1%
9	Ketchikan	44		3A	3.0V	-840	-865			AUTO 3.0%
10	KETCHIKAN			2A	2.5V	-835	-865			AUTO 1.5%
11	KETCHIKAN	44		2A	2.7	-840	-860			AUTO 2.1%
12	Ketchikan	44		1A	3.4	-835	-865			AUTO 1.2
13	KETCHIKAN	43		1A	2.2	-835	-865			AUTO 0.5%
14	KETCHIKAN	43		6A	4.1V	-835	-865			AUTO 6.6
15	Ketchikan	44		2A	2.9	-825	-865			AUTO 1.5%
16	Ketchikan	44		1A	2.2	-835	-865			AUTO 3.0
17	KETCHIKAN	42		3A	3.0	-835	-865			
18	KETCHIKAN	42		1A	2.5	-835	-865			
19				1A	2.4	-835	-865			AUTO 1.2
20	KETCHIKAN	42								
21	KETCHIKAN	43		0A	1.7	-850	-865			AUTO 0.0
22	KETCHIKAN	42		3A	2.9v	-835	-865			AUTO 2.8%
23	KETCHIKAN	42		3A	3.0V	-835	-865			AUTO 3.5%
24	KETCHIKAN	43		2A	2.6v	-835	-860			AUTO 2.0%
25										
26	KETCHIKAN	43		2A	2.8V	-835	-865			AUTO 2.0%
27	KETCHIKAN	43		2A	2.7V	-835	-865			AUTO 2.1%
28	KETCHIKAN	15		0A	3.0	-835	-865			AUTO 0.3%
29	KETCHIKAN	43		4A	3.2V	-835	-870			AUTO 3.6%
30	Ketchikan	43		2A	2.7	-835	-865			AUTO 2.1%
31	KETCHIKAN	43		5A	3.6	-830	-865			AUTO 5.8%

Completed logsheets should be emailed to icpplogsheets@cathelco.com . All other queries should be emailed to technical@cathelco.com . See instructions sheet for further information.
Please ensure that the slip ring and brush gear are checked and cleaned weekly. Failure to replace the brushes can result in main shaft bearing damage.

Figure 3.1: Typical ICCP logsheet from an FRC.

Logs are organized by month and sent to SFLC and Cathelco. Approximately 270 logs from 24 different cutters contributed to this study. Seven vessels had more than one year of continuous data available. Dry dock photographs and hull cleaning reports provided information on the condition of the underwater body when available. As a vessel comes out of dry dock or first enters service after being painted, it is fair to assume that the coating on the underwater body is totally intact.

3.1.1 Factors Affecting Protection Current Demand

Outside of problems with the power supply itself, there are four main factors influencing what appears in the ICCP logs: the hull condition, the state of polarization, the environment, and the functionality of the reference electrodes. Each one affects the electrolyte potential and consequently the amount of current allegedly required to maintain protection. Speed played an outsize role in determining the protection current requirement, and this phenomenon will be explored in Section 3.4.

Variation in the underwater body condition is the primary reason ships carry ICCP systems with greater current capacity than they typically need at a given time. Since corrosion is an electrochemical process, one way of inhibiting it is by adding an electrical and chemical barrier between the electrode surfaces and the electrolyte. Since ancient times, coatings have been the primary means to do this [26]. Not just any coating will work, however. In order to effectively prevent corrosion, the coating must have high electrical resistance and remain stable when submerged in water for long periods of time. Corrosion engineers typically consider 10,000 Ω/m^2 as the threshold resistance value for protection [12].

Polarization describes whether the vessel has reached a steady-state corrosion rate. When a ship first enters the water, there are many surfaces which have not yet corroded or built up passive films. The resistance properties of the paint film may also change in response to contact with seawater. As such, corrosion occurs rapidly right as the vessel enters the water. Over time, the rate of corrosion typically slows down [32]. As this happens, the protection current demand decreases.

Environmental factors such as water temperature and the state of hull fouling also affect ICCP current demand. Warm water conducts electricity better than cold water and speeds up chemical reactions, so corrosion occurs faster. Marine organisms also grow faster in warm water, which can have corrosive effects [32]. However, certain types of fouling can reduce corrosion by functionally acting as a coating [26].

Sensors are particularly sensitive to fouling [33]. Marine growth around a silver chloride reference electrode affects how well it can sense the electrolyte potential by degrading the coating, insulating parts of the sensor, shorting it to the hull, or chemical byproducts interfering with the readings. Since fouling and environmental factors are not typically constant, the effect may drift between certain limits over time.

Since the ICCP system relies on the reference electrodes for output current feedback control, the system will blindly inject protection current if the sensors do not have a clear reading of the hull potential. If the reference electrodes fail hard from breakdown of the AgCl coating or something broken inside, the effect on the system performance may be drastic.

3.1.2 ICCP Log Content and Discussion

The ICCP logs capture most of the salient details on how the system functions. Geographic location can provide insight on seawater chemistry and biological factors. Temperature translates to electrical conductivity and therefore the relationship between output current and voltage. The reference electrode voltages obviously give indications of the state of protection and whether those readings are reliable. Output current and voltage relate what the system is doing in a given situation.

Cathelco technicians can use this information to determine if the system is responding to different input parameters as it should since it is useful for helping operators troubleshoot the system in the field. The biggest piece of missing information is the vessel's speed, since that parameter has a huge effect on current demand [34]. Since the corrosion reactions depend on delivery of dissolved oxygen, speed through the water speeds up the reaction by effectively increasing the rate of oxygen delivery through increased agitation. This is one of the most essential bits of information used when describing a corrosion environment.

3.2 Findings

The charts presented here only represent a section of the collected data. Of all the logs in the study, the overwhelming majority indicated the ICCP system put out 0A at the -850 mV set point and the reference voltage readings naturally fell between -900 mV and -1000 mV. Seven out of 24 ships displayed signs of electrode failure at some point in time, indicated by a substantial and unphysical deviation between port and starboard reference electrodes readings. The state of polarization heavily influences the ICCP system at certain times, and the noise in the data precluded efforts to confidently determine the condition of the underwater body coating.

3.2.1 Typical ICCP Behavior

Figure 3.5 shows typical ICCP data from *USCGC Oliver Berry* (WPC 1124), homeported in Honolulu, HI. The record begins January 2021 and goes through March 2024. The large gap in the summer of 2023 represents when the vessel went to dry dock for maintenance. Following dry dock, the crew set the ICCP system to -1050 mV. At -850 mV, the ICCP consistently injected 0 A of anode current. Following the reference voltage change, it injected roughly 2 A consistently. Pictures from dry dock indicated that even at the end of the vessel's maintenance cycle, there was less than one percent bare metal on the underwater body.

The behavior here represents what the majority of ICCP systems do in the FRC class. Watchstanders write down "0 A" every day, the unit works, and the ship does not experience widespread premature coating failure. After dry dock at the four-year mark, the coating is reset and the cycle starts over again.

3.2.2 Hull Polarization

Figure 3.10 shows ICCP data from *USCGC William Sparling* (WPC 1154) starting when it first entered the water at the shipyard in Louisiana through its first few months of operation

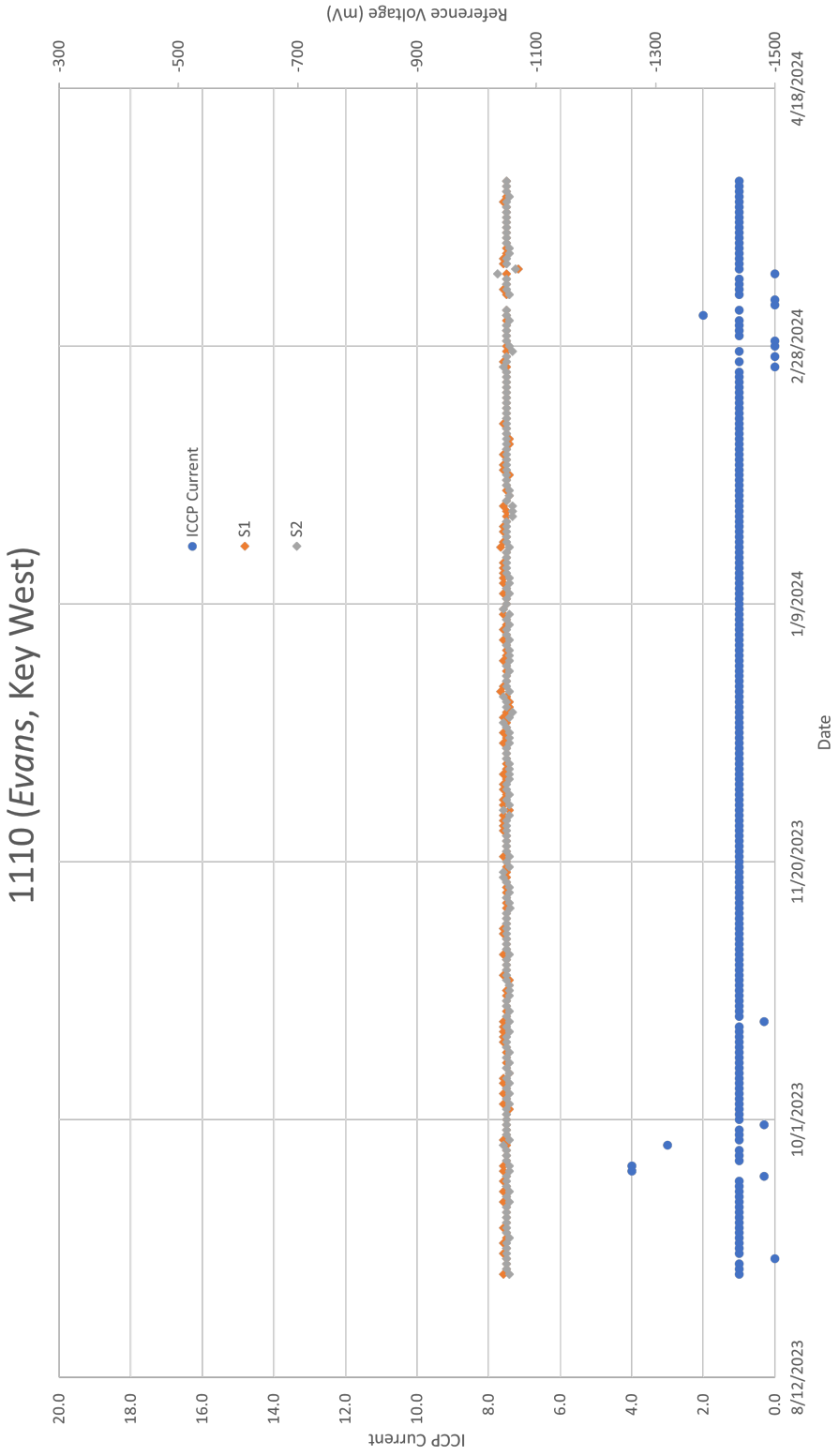

Figure 3.2: ICCP data from *USCGC Raymond Evans* (WPC 1110).

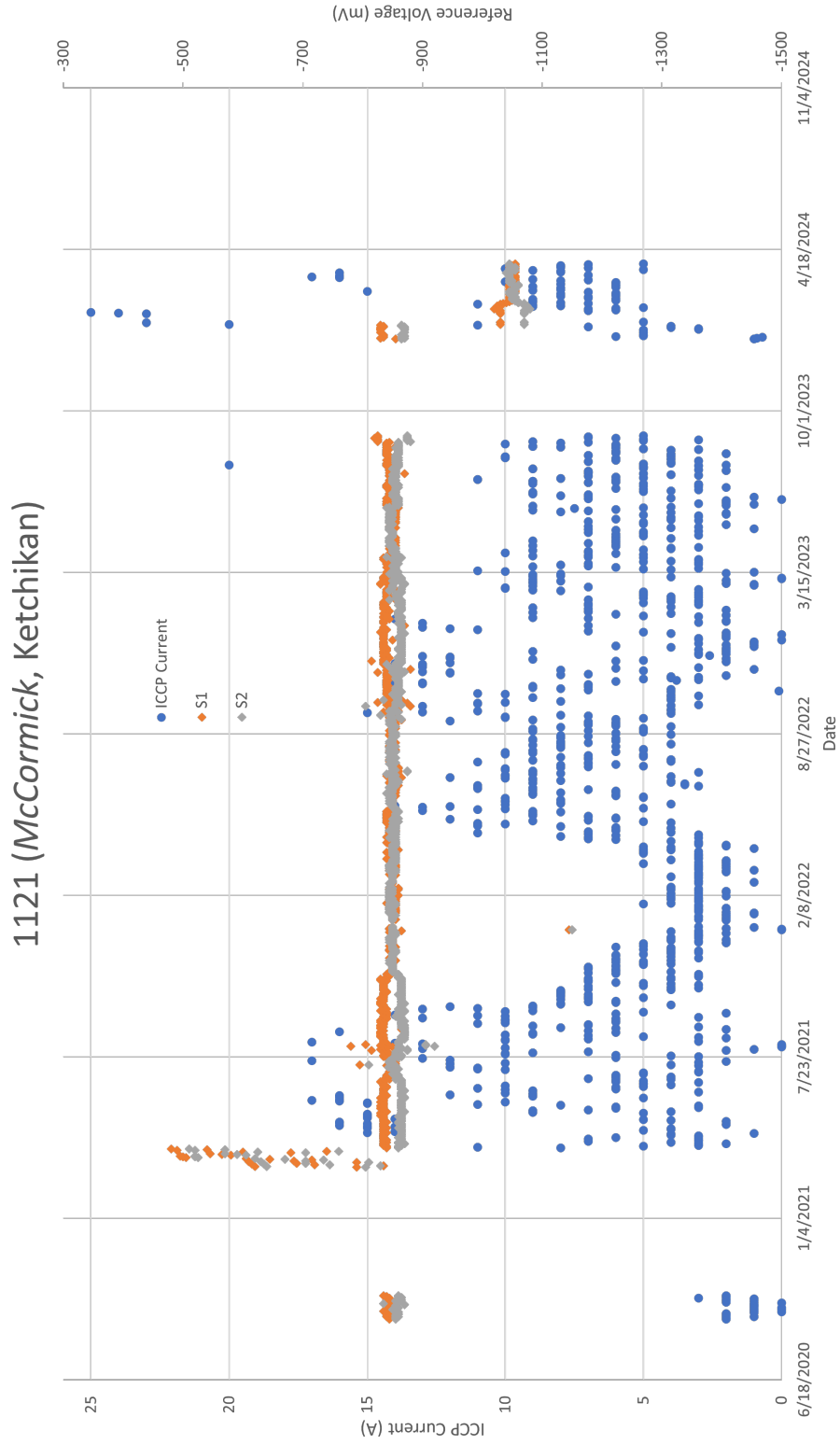

Figure 3.3: ICCP data from *USCGC John McCormick* (WPC 1121).

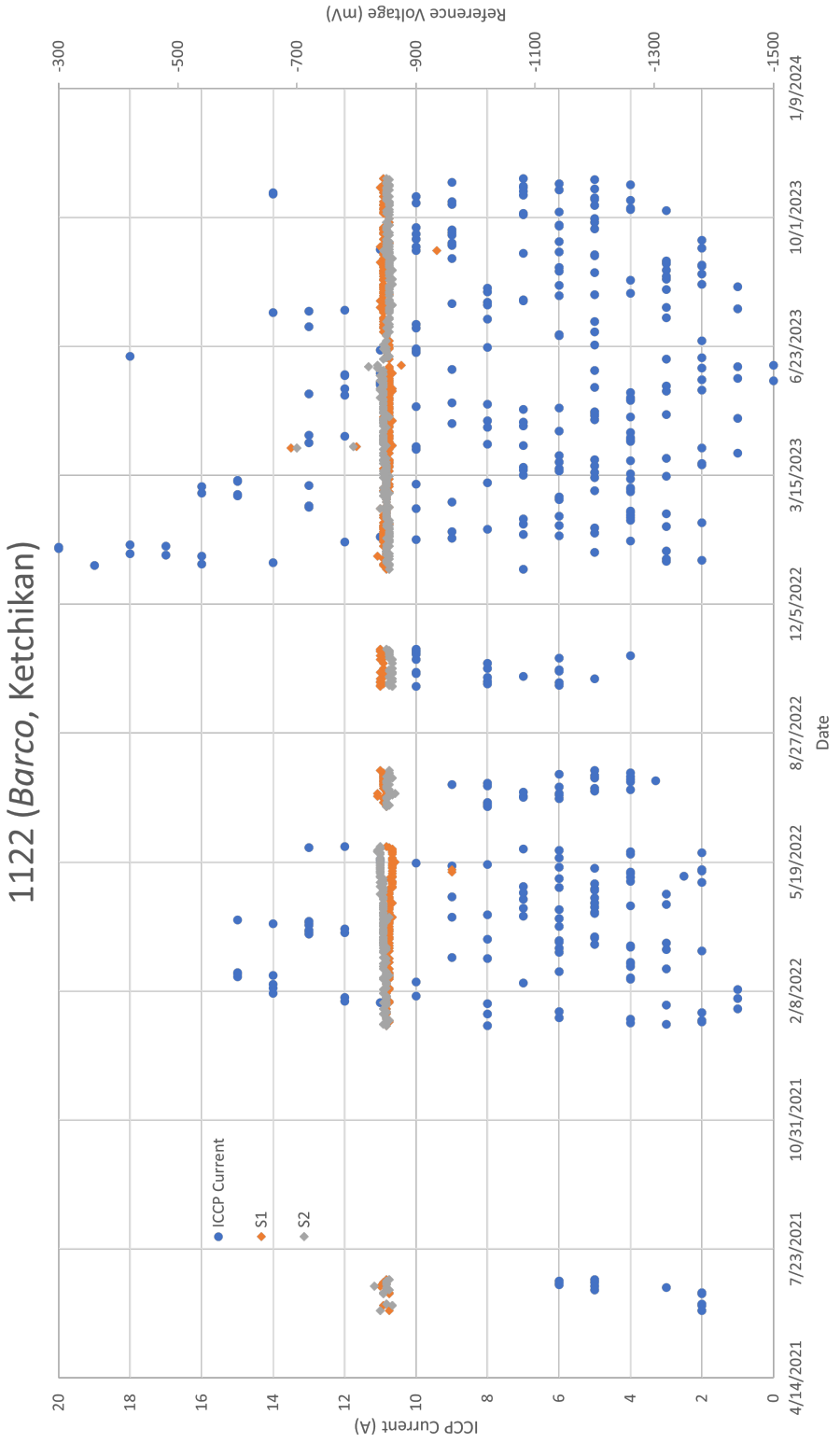

Figure 3.4: ICCP data from *USCGC Bailey Barco* (WPC 1122).

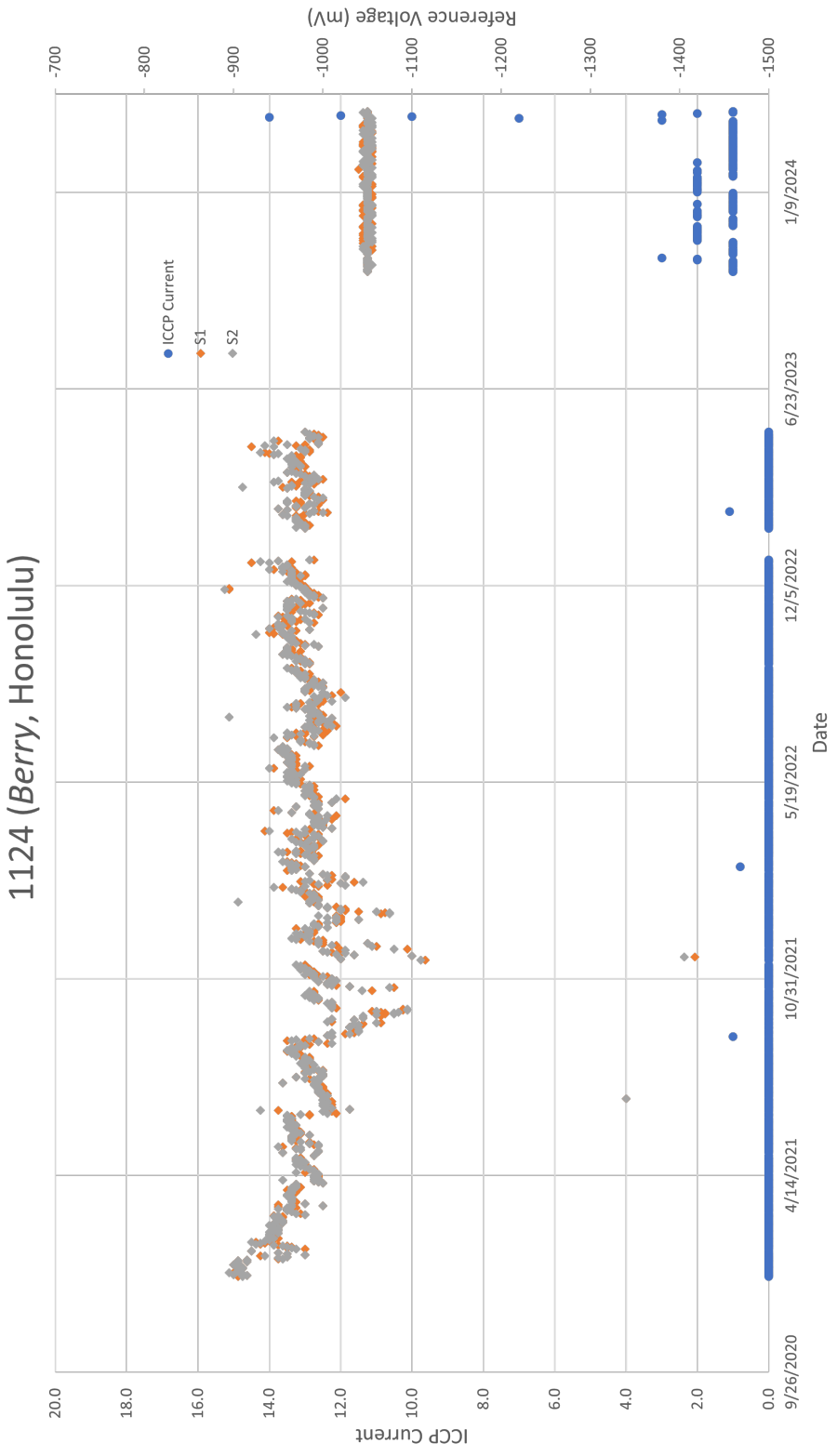

Figure 3.5: ICCP data from *USCGC Oliver Berry* (WPC 1124).

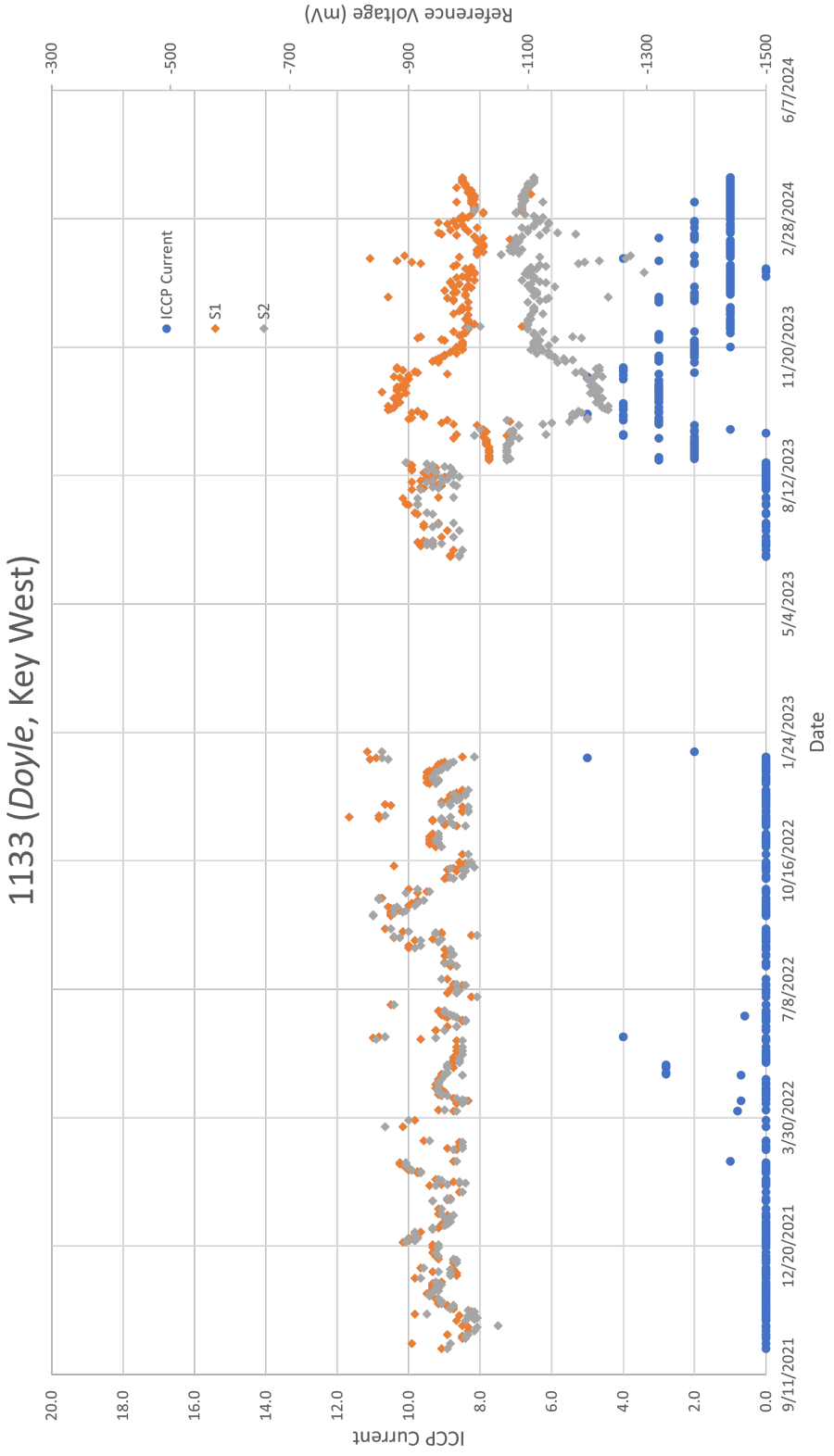

Figure 3.6: ICCP data from *USCGC Joseph Doyle* (WPC 1133).

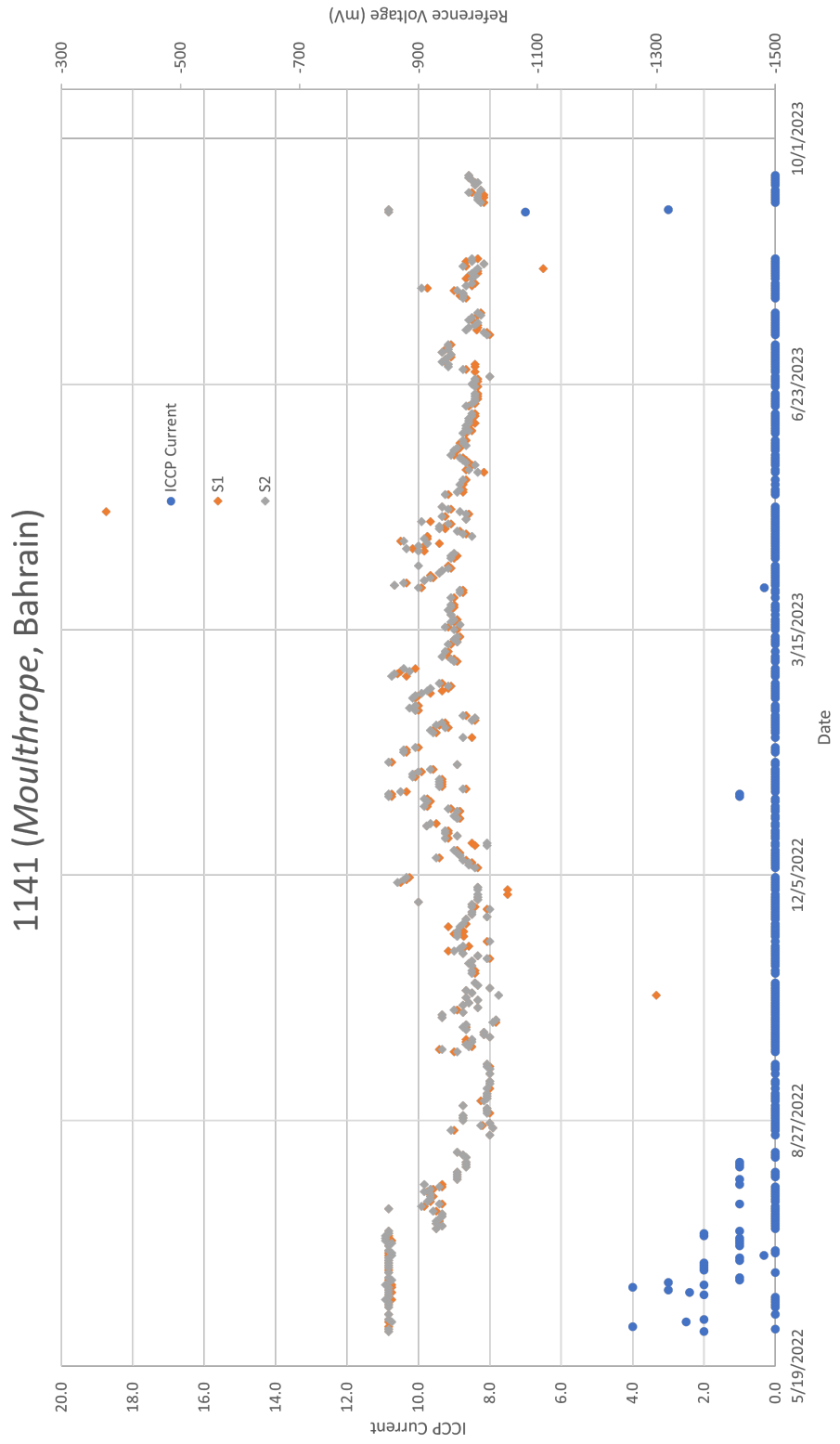

Figure 3.7: ICCP data from *USCGC Charles Moulthrope* (WPC 1141).

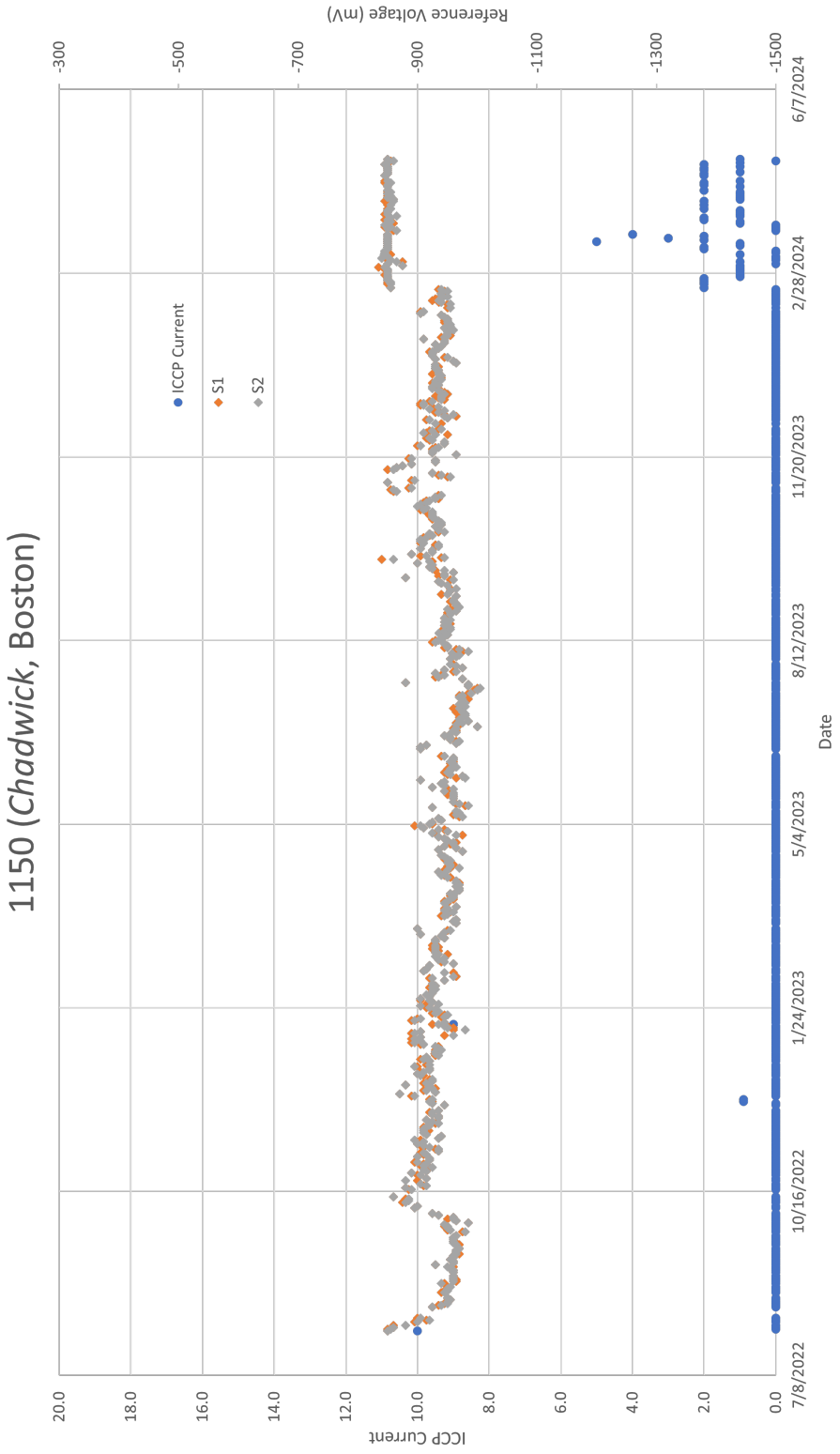

Figure 3.8: ICCP data from *USCGC William Chadwick* (WPC 1150).

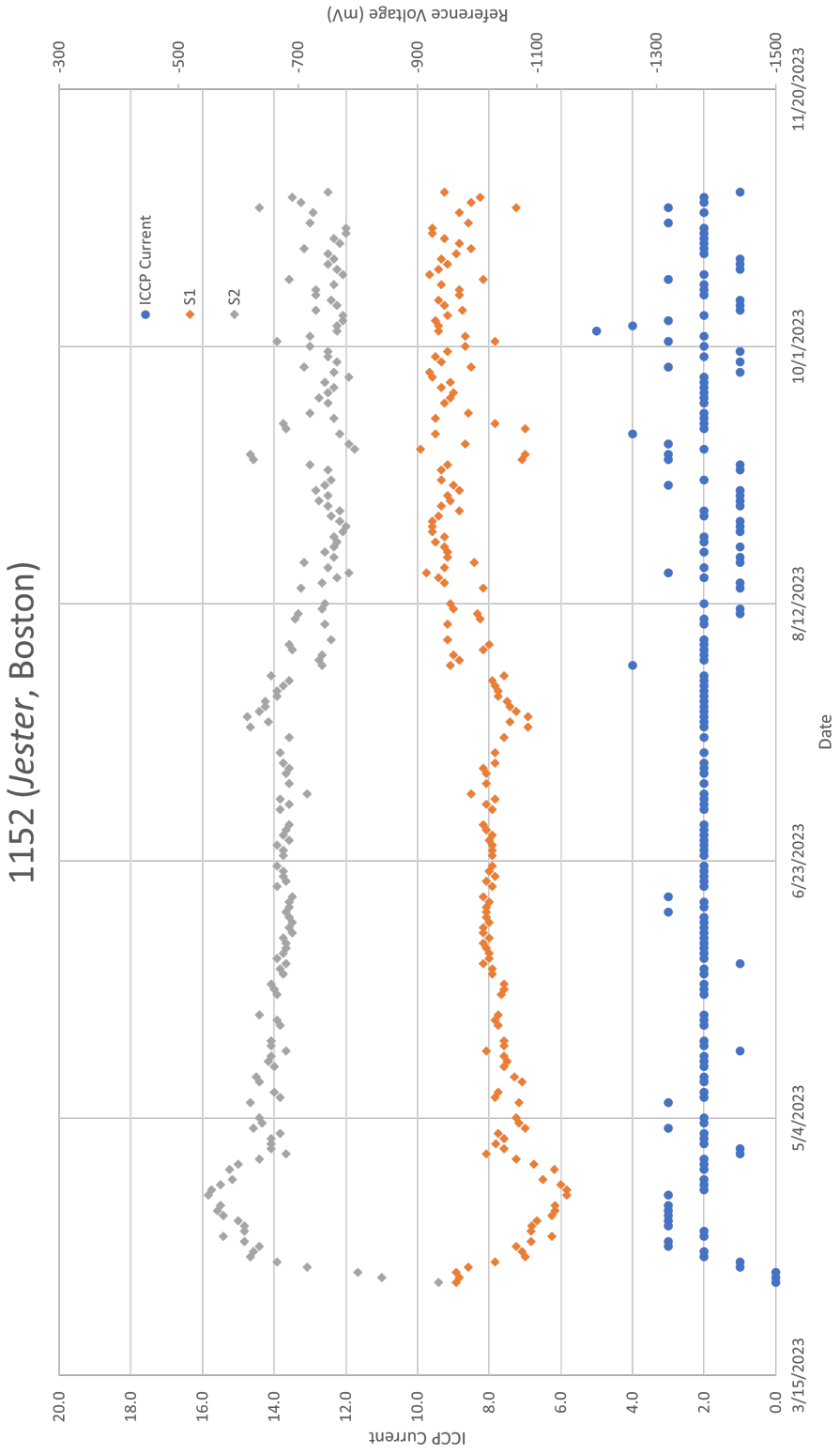

Figure 3.9: ICCP data from *USCGC Maurice Jester* (WPC 1152).

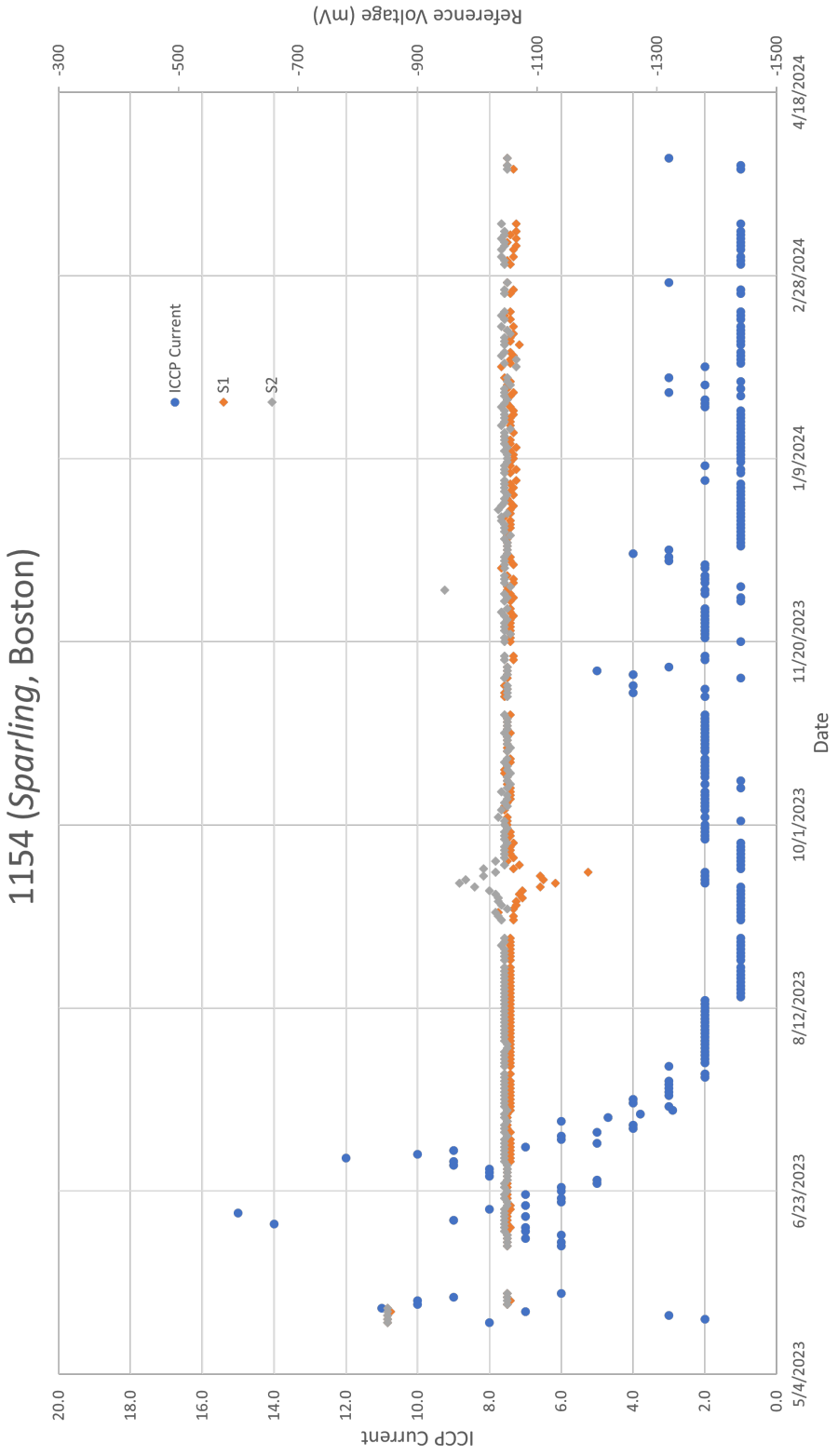

Figure 3.10: ICCP data from *USCGC William Sparling* (WPC 1154).

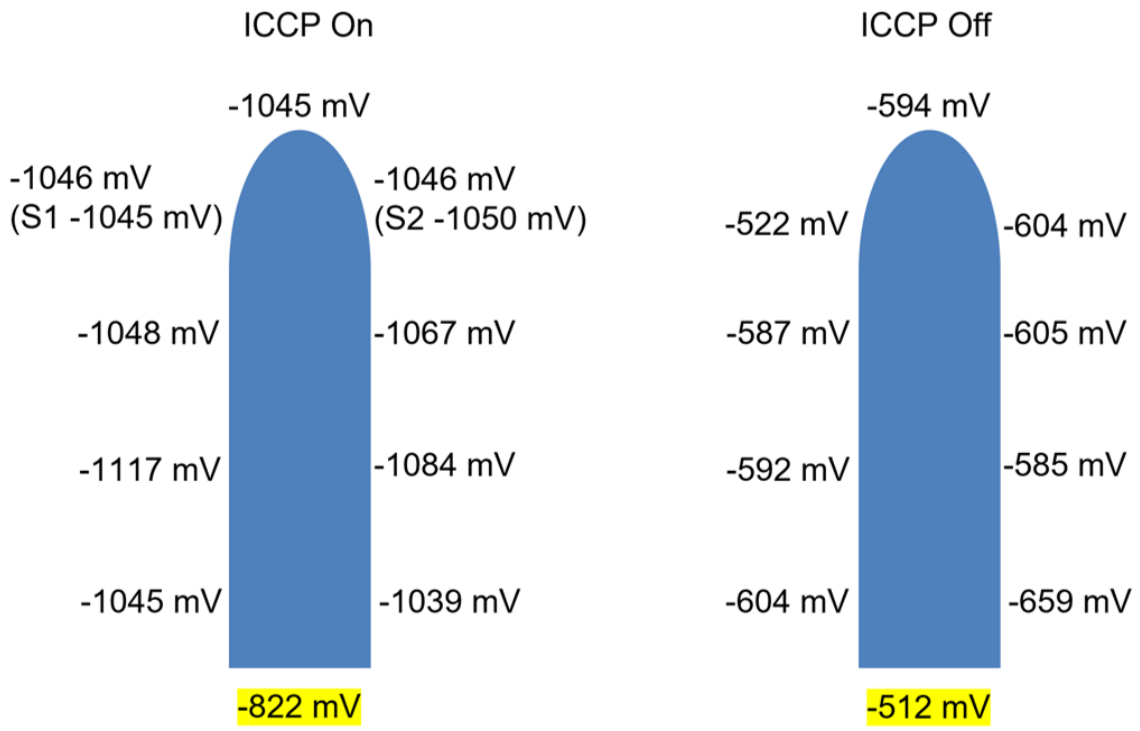

Figure 3.11: Hull potential survey for *USCGC John McCormick* (WPC 1121).

homeported in Boston. Despite having a nearly perfect coating from the shipyard at the start, the ICCP initially put out up to 10 A to maintain -1050 mV. Over time, the current demand decreased until the vessel more or less reached steady state. The period of decrease in current demand lasted roughly three months following entry to the water. Other vessels in the study followed similar patterns, such as in Figure 3.7 for hull 1141.

Figure 3.8 shows data from *USCGC William Chadwick* (WPC 1150), another typical Boston FRC. The first available log was August 2022 and the most recent is April 2024. The ICCP system injected 0 A for about a year and a half and the reference voltages remained mostly constant. On February 20, 2024, divers cleaned the hull and polished the propellers. Immediately after that, the ICCP began injecting 2 A to maintain protection at -850 mV.

The ICCP contributes current when the zincs reach saturation and cannot output any more current. This is simply a property of how much anode surface area is available. As the hull begins to polarize and those corrosion reactions slow down, the zincs are no longer saturated and can meet the current demand, the reference potential falls below the protection threshold, and the ICCP system returns to generating 0 A. This is the typical pattern for how polarization effects manifest in ICCP logs.

The state of polarization is relatively easy to identify. The first feature is its proximity to a dry docking or a hull cleaning, both of which reset the state of polarization to a degree on various ships. The second feature is its tendency to decay over time, whereas coating damage would increase ICCP current demand over time. According to FRC data, polarization often takes about three months but may take longer in cold water.

During polarization, the logs do not show steadily high current demand. Instead, the

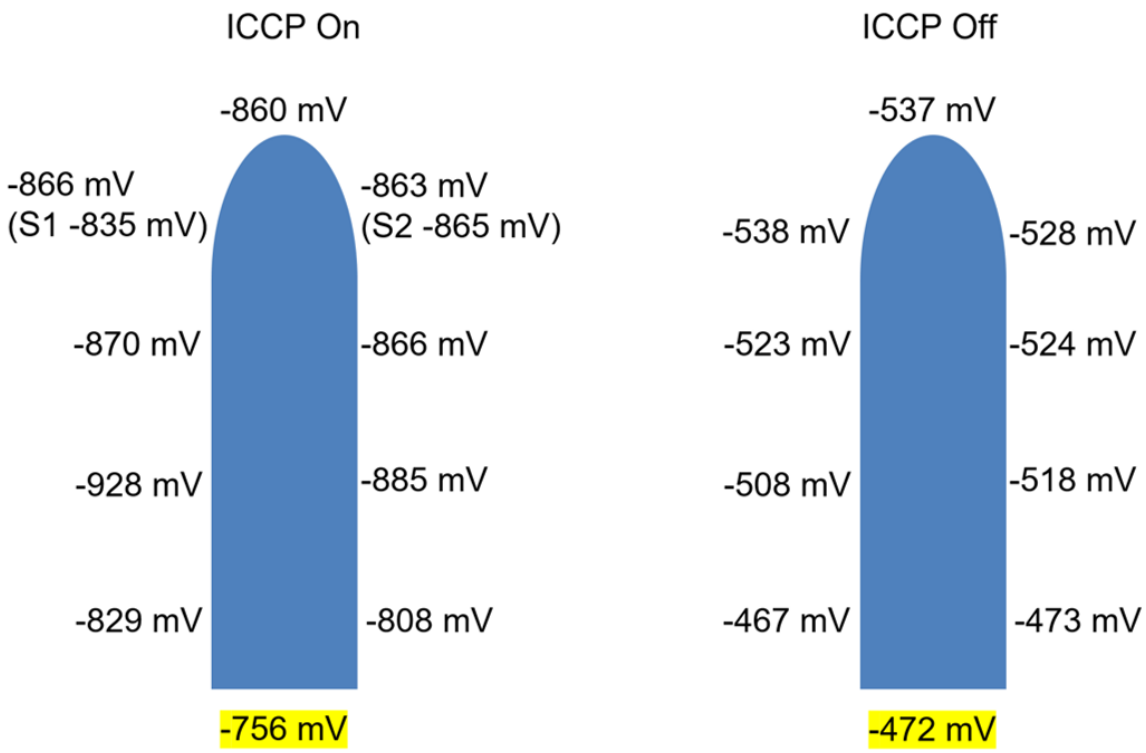

Figure 3.12: Hull potential survey for *USCGC Bailey Barco* (WPC 1122).

system appears to output every value between an upper and a lower bound, and it is the upper bound which decreases over time. The variation is likely due to the effects of day-to-day changes in hull fouling and currents around the vessel.

There are notable exceptions, however. Figure 3.3 and Figure 3.4 show data from *USCGC John McCormick* (WPC 1121) and *USCGC Bailey Barco* (WPC 1122) in Ketchikan, AK. These are the only two vessels in the study group that showed consistently high current demand at an ICCP set point of -850 mV, which did not fit the conventional understanding of how the ICCP systems worked.

These vessels received hull potential surveys with an independent AgCl reference electrode to check system functionality, the results of which are in Figure 3.11 and Figure 3.12. According to dry dock and hull cleaning reports, both vessels had no more than 1% bare metal at any point during the study period.

In this case, environmental factors in Alaska likely inhibited the polarization process from happening on the same time scale as in other parts of the world. Passive films that form on nickel-aluminum bronze propellers, for example, are themselves corrosion products. Since corrosion happens slower in cold water, it takes longer for those passive films to form and the propellers demand more current. This finding is supported by the hull potential surveys, which indicate a highly localized protection-current sink at the rear of the vessel. Further work is needed to determine the extent of biological factors based on the flora native to Ketchikan's waters.

3.2.3 Reference Electrode Failure

Figure 3.9 shows data from *USCGC Maurice Jester* (WPC 1153) in Boston from the first available record in April 2023 through November 2023. The ICCP was set to -850 mV. Note the relatively large discrepancy between the port and starboard reference electrode readings and the output current of about 2 A.

(a) Fouling on and inside the electrode

(b) The separated rubber boot

Figure 3.14: The broken S2 reference electrode from *USCGC Maurice Jester* (WPC 1152).

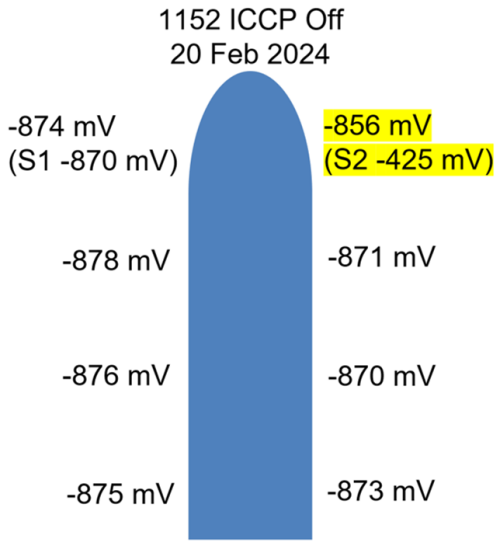

Figure 3.13: Hull potential survey of *USCGC Maurice Jester* (WPC 1152).

This suggests that something is wrong because a new vessel like *Jester* should not consistently require current from the ICCP system after the polarization period ends. This vessel received a hull potential survey with an independent Ag/AgCl reference electrode, and Figure 3.13 shows the outcome. Whereas the survey indicated the reference potential near the S2 electrode was about -856 mV, the ICCP system read -425 mV. This means the reference electrode was misleading the system with bad readings.

The clear indications of reference electrode failure in both the voltage streams and the output current stream make it possible to analytically suspect this may be the case. The electrode readings first diverge – one stays put and the other rises. When the average between the two readings rises above the ICCP set point, then the system puts out current to bring the average down to the desired level of protection. As a result, the

reference electrode readings appear to be mirrored about the set point, which is simply a feature of how the system uses the average between the two electrodes to determine what level of current to inject.

The FRC system often outputs 1 A to 2 A during electrode failure. When all these factors are observed at the same time, an operator can reasonably suspect failure of one of the reference electrodes. Seven of 24 vessels in this study exhibited these signs concurrently at some point in their ICCP records, meaning this issue may be relatively common.

Jester had its reference electrode replaced on April 29, 2024 after the Coast Guard became aware of the issue. Cathelco technicians are studying the failed electrode to determine what went wrong, but initial observations on the day of replacement showed two things out of the ordinary. First, marine fouling had built up inside the electrode. Second, the rubber boot around the outside of the electrode had separated from the metal electrode body for about 1/4 of its circumference. These are seen in Figure 3.14. Further investigation is necessary to determine the precise effect both of these had on the failure.

3.2.4 Relation to Stern Tube Corrosion

Figure 3.7 shows the logs from *USCGC Charles Moulthrope* (WPC 1141) based in Manama, Bahrain. This vessel commissioned on January 21, 2021 and had suffered severe corrosion in the stern tube region by its first dry docking in October 2023. It showed high initial current demand related to polarization which decayed over time and considerable variation in the reference electrode voltage readings.

As expected, *Moulthrope's* ICCP logs did not give indications of under-protection in the stern tube. The reference electrode and output current readings are fairly typical, similar to those from other vessels which have not had corrosion problems this bad.

The quality of *Moulthrope's* logs provided an opportunity to explore ways of filtering out noise and accounting for seasonal variation in the reference electrode readings. Temperature only had an R^2 value of 0.11 when plotted against reference voltage, shown in Figure 3.15. Using a median filter of various widths did not significantly help. Tides and currents also did not significantly correlate with the data. According to experts at Cathelco, fouling around the electrode would have a greater effect on the voltage readings than any of those other factors. Since it is practically impossible to quantify the amount of fouling with the tools presently available, this may be the subject of another study.

3.2.5 Coating Condition Estimation

Santana-Diaz and Adey [35] discussed a method of determining coating condition from ICCP data. However, their technique relies on an idealized ICCP system with 12 reference electrodes evenly spaced along both sides of the vessel. Many vessels do not have systems that complicated; ICCP systems have as few reference electrodes as possible to keep maintenance costs down, and one on either side often works adequately.

According to the "perfect paint" assumption, corrosion models often assume that intact underwater coatings have infinite electrical resistance [11]. As the coating deteriorates, the effective resistance decreases and more current must flow to maintain -850 mV. The data

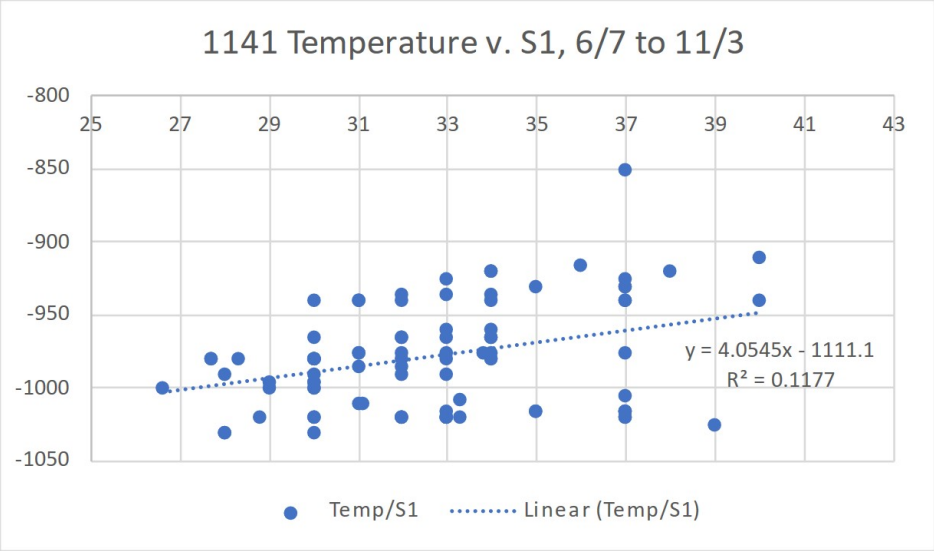

Figure 3.15: ICCP reference voltage versus water temperature for *USCGC Charles Moulthrope* (WPC 1141).

suggests that 1% bare metal on an FRC only raises the reference potential from about -920 mV with perfect paint to about -850 mV with the damage. This assumes that fouling, calcareous deposits, or other environmental factors do not also confer some degree of corrosion protection, which would alter electrolyte potential.

The logs from the vessels in this study did not represent a wide enough range of coating damage to reveal how any more than 1% bare metal would affect the data. This is good news for the vessel's maintainers since it appears that the epoxy coating system lasts as long as they need it to.

Looking at this feature through the lens of reliability-centered maintenance, this may be as optimal as the maintenance cycle will allow. If the owners would tolerate more coating failure before recoating, they could get more life out of each coating application and spend less money on paint over the lifecycle of the vessel. Other systems may still need dry dock maintenance at the four-year mark, so the ideal coating lifecycle may not align neatly with the other systems. Since the operators would not tolerate taking the vessel out of service for dry dock at some intermediate time when the coating finally reaches their standard for "failure," simply recoating at four years with approximately 1% bare metal would favor reliability the most.

3.3 COMSOL Model

The COMSOL Multiphisics corrosion module uses finite-element numerical methods to solve the Laplace equation for current, voltage, dissolved species transport, electrode kinetics, and other properties related to electrochemistry [36]. It can divide 3D models into various boundary elements, assign material properties, and calculate the results according to different sets of assumptions. The purpose behind creating a COMSOL model was to validate findings in the field by matching different situations to common parameters. In this case, the model

here accurately described FRCs in both the pre- and post-polarization states.

3.3.1 Design and Materials

A half-hull model of the FRC forms the defining feature of the COMSOL model here. Although the model hull form matches the actual hull form almost perfectly, certain features were omitted or simplified to manage element size and increase computational speed. For example, the sea chests were ignored altogether and the zinc anodes simplified to flat, rectangular regions on the hull with roughly the same surface area as the actual anodes. The propellers were also modeled as short cylinders with the same diameter and roughly the same surface area as the real ones. According to DeGiorgi [37], this is a valid simplification which does not cause the model's behavior to differ too greatly from that of the real vessel.

Material selection is important when defining properties for the boundary elements. The equilibrium potential is arguably the most important since it determines which areas form the cathode and which form the anode in this situation. There are three materials at play: structural steel, nickel-aluminum bronze (NAB), and zinc. The structural steel and NAB boundaries had a film resistance applied according to the coating condition whereas the zinc anodes were assigned no film resistance.

Paint systems fail when they show a certain density of scrapes and holidays which go down to the base material. These scrapes are discrete, individual features, but it is not practical to model the resistance to the hull in parallel with the resistance of thousands of little scrapes. Choosing a bare patch of a particular size in a corrosion model can produce the desired effect, but it is equally useful to use a continuous, lumped model of hull resistance. Based on the equation for resistors in parallel, (3.1) shows the model input for paint film resistance as a function of percent failure, d.

$$R_{hull} = (R_{intact}^{-1}(1-d) + R_{damaged}^{-1}(d))^{-1} \tag{3.1}$$

As in reality, the model was sensitive to even small changes in the film resistance on the propeller and of damaged paint areas. The field data gave insight on what these values should be, and the model was calibrated around a few discrete situations identified in the data where the propeller condition and hull coating condition were both known. Table 3.1 summarizes the identified values and Figure 3.16 through Figure 3.18 show the simulations. The color of the hull in those figures represents the reference voltage as read from the scale on the right hand side of the figures.

Item	Resistance (Ω/m^2)
Propeller, un-polarized	0
Propeller, polarized	10-12
Paint, intact	10,000
Paint, damaged	2

Table 3.1: COMSOL Model Parameters

Limiting current density is another important parameter. Since anode reactions can only happen so quickly in real life, the size of an anode surface determines how much current

it can handle. Thus, limiting current density describes generally when those reactions hit saturation and will not naturally accommodate more electron flow. The model uses 5 A/m^2 as the overall limiting current density.

3.4 Accounting for Vessel Speed

Since speed greatly affects the demand for ICCP current but the logs do not contain information about the vessel's speed through water, a separate experiment on an FRC provided high-resolution data for speed through water and every ICCP parameter.

The results showed a clear relationship between current demand and vessel speed. Additionally, data points were more tightly clustered at high speeds, which removes much of the noise seen in the data at low speeds. Evidently, this is important to consider if one's goal is to determine the condition of the coating on the underwater body.

3.4.1 Objectives and Design

Taking measurements aboard an FRC while underway was the only way of mapping ICCP parameters to vessel speed with any kind of certainty. To that end, several parameters needed to be recorded closely: speed through the water, port and starboard reference voltage, ICCP output current and voltage, propeller shaft speed, and time alignment data for all the above. Ideally, the vessel would cover the full range of operating speeds to adequately fill out the domain.

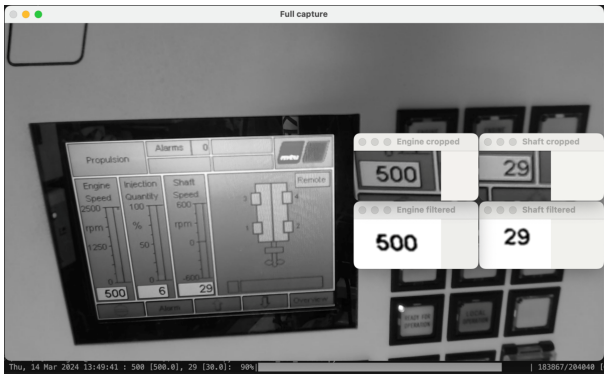

Figure 3.19: Screenshot of the OCR script transcribing values from the engine control unit.

Consulting with the crew yielded the plan, which they carried out on March 14, 2024. *Chadwick* first transited out of Boston harbor to a fishing fleet with the ICCP set to maintain -850 mV. There, the crew conducted two fisheries enforcement boardings, then returned to Boston with the ICCP set to -1050 mV. On both the outbound and inbound transits, the vessel reached its top speed in excess of 28 knots whereas it would mostly remain stationary during the boardings.

One key assumption was that the hull and zinc condition would not change during the test. Since *Chadwick* had just had its hull cleaned and zincs replaced on February 20, the zincs were providing as much protection as they ever would. The divers who cleaned the hull reported 5% bare metal below the waterline, although this claim is dubious given the poor visibility in Boston Harbor and that they reached this figure simply by eye.

The MIT team used a Hioki data logger to record each ICCP parameter. This required opening the ICCP power supply, attaching voltage leads from the data logger to various

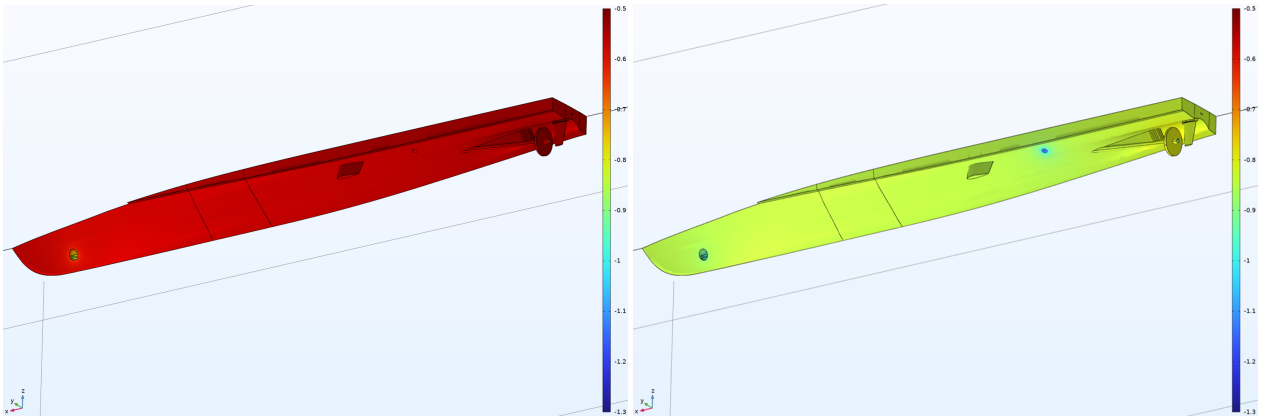

(a) 0 A ICCP, 100% paint, intact zincs (b) 1.5 A ICCP, 100% paint, intact zincs

Figure 3.16: Un-polarized FRC models, -850 mV set point.

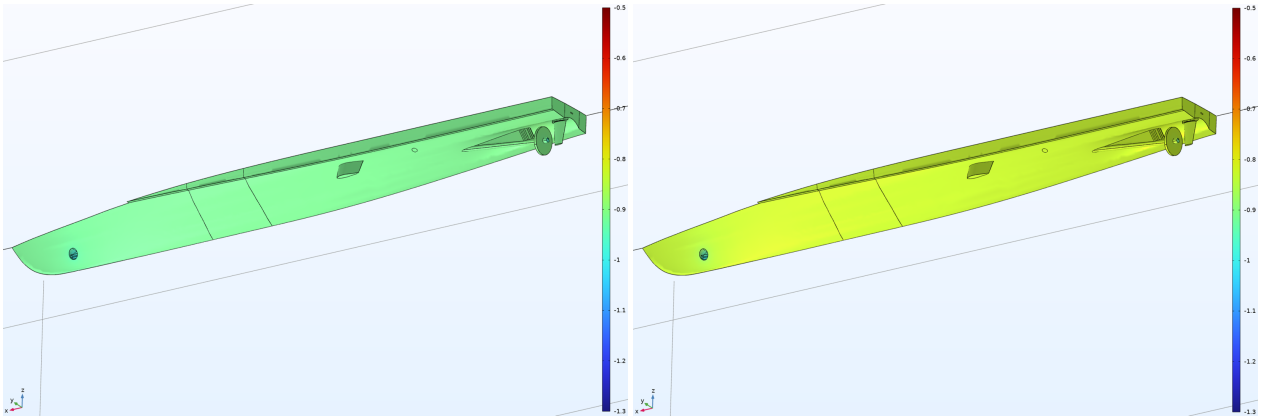

(a) 0 A ICCP, 100% paint, intact zincs (b) 0 A ICCP, 99% paint, intact zincs

Figure 3.17: Polarized FRC models, -850 mV set point.

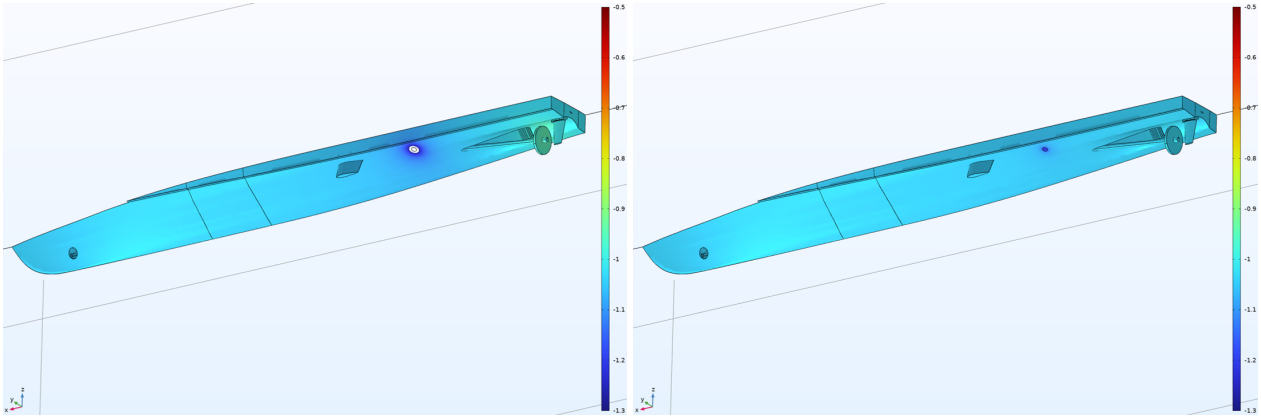

(a) 4.1 A ICCP, 100% paint, intact zincs (b) 1.6 A ICCP, 100% paint, intact zincs

Figure 3.18: Un-polarized and polarized FRC models, -1050 mV set point.

Figure 3.20: Setting up the camera to record for OCR.

terminals inside the unit, then securing the partially-opened unit with a ratchet strap to ensure it would not move at sea.

The MTU laptop designed to interface with MCS could allow a technician to sample data at 1 Hz or more. This would have yielded data on propulsion engine parameters and shaft speed. Instead of taking this route, the team explored data collection techniques with optical character recognition (OCR) packages in Python. Cameras pointed at the local engine control screens recorded various parameters including shaft speed (Figure 3.20), and the movie files were post-processed with a Python script to extract the numbers on the screen and the timestamp (Figure 3.19).

Recording speed through the water was more challenging. Due to security concerns, personal electronic devices were not allowed in certain parts of the vessel and the team was not allowed to record the navigation display as with the engines. The navigation system logged its data every two minutes, but this would not accurately resolve changes in speed. This left one option: record speed manually every 15 seconds in a notebook and transcribe the numbers the following day.

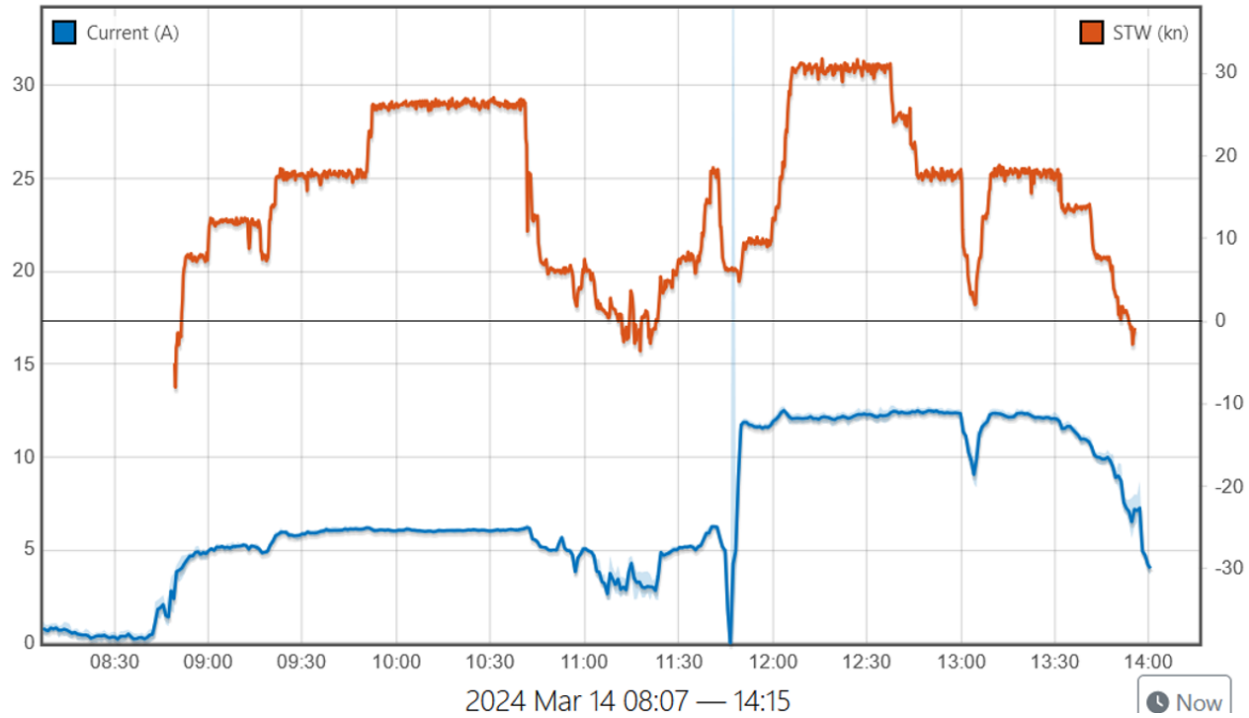

Figure 3.21: ICCP current (blue, left axis) and speed through water (red, right axis) for the *Chadwick* experiment.

3.4.2 Results

The whole mission lasted about six hours and the data provided adequate coverage of all speeds. Figure 3.21 shows the experimental data in the time domain. Figure 3.22 shows the ICCP current plotted against the log of speed through water.

There are two obvious clusters: one for when the ICCP was set to -850 mV, and another for when it was set to -1050 mV. Above approximately 12 knots, the system appears to have hit a saturation point beyond which the protection current demand does not increase as speed increases. Within these clusters, there is a linear relationship between current demand and logarithmic speed before forming a shoulder region at the saturation point.

At the time of the experiment, *Chadwick* had damage to the coating on the underwater body and the ICCP had to put out roughly 1 A at the pier. On vessels with a more intact underwater coating than *Chadwick*, there would be a toe region in the current versus log speed graph since the ICCP puts out 0 A at the pier and would continue to do so until the vessel was moving fast enough to raise the potential to -850 mV.

There is a clear decrease in the standard deviation of the output current data as speed increases. Therefore, it follows that the amount of current at saturation would make a better estimator of the vessel's paint condition. More work is needed on vessels of various coating conditions to confirm this theory.

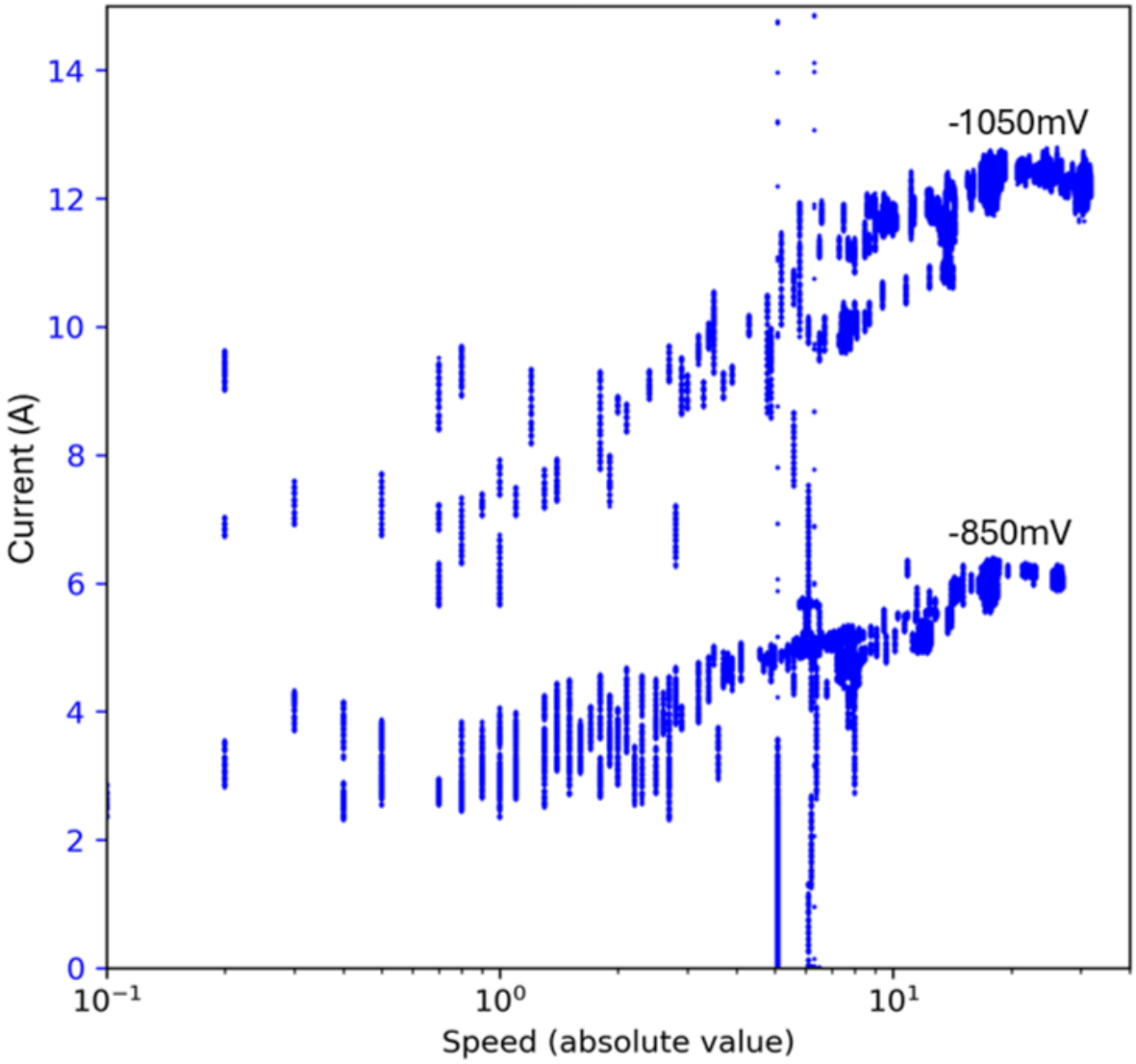

Figure 3.22: The data from figure 3.21 plotted as ICCP current versus speed through water.

3.5 Conclusions

The present data collection scheme does not tell the whole story because of the low sample rate and the lack of speed data. The data is also inherently biased by collecting ICCP parameters at one time of day, rather than at a random time. The underway experiment showed how the ICCP system on a ship with logs consistently reading "0 A" puts out several amps when at speed and that the data points are much more tightly clustered at high speeds than at slower speeds. Since vessel speed mainly affects the diffusion of dissolved oxygen and the agitation around each electrode surface, there comes a point where the corrosion process has enough of both and will not proceed faster as it reaches its saturation point. Environmental factors have a proportionately greater effect below saturation, but not as much beyond it. Since the -850 mV and -1050 mV settings formed such distinct clusters, it follows that the current demand at saturation is a much better indicator of coating condition than current demand at rest – especially since moving water would have removed loose material on the hull which could affect its state of protection. A future experiment would be useful to investigate this claim.

The quality of the data and the sample rate hindered the efforts to draw meaningful conclusions from the data. As it stands, the crew manually records the parameters just once per day on a clipboard. Location information is typically not specific (e.g. "Gulf of Alaska") and many entries are missing for no apparent reason or borderline illegible.

Focusing the crew's attention on record keeping would take their attention away from more important matters, so this is not the ideal solution. Automatic logging is a well-established practice in most other areas of shipboard engineering, so implementing it for the ICCP system should be straight-forward. It would eliminate measurement bias, give a more detailed picture of what is going on, allow analysts to confidently draw conclusions, and free the crewmember with the clipboard to do more productive work. Computing power and electronic storage are cheap. The Coast Guard would do well to fully embrace their capability.

Computers can also relieve the burden of data analysis. Automatically identifying reference electrode failure based on the conditions described here would help the crew maintain the cutter better by drawing their attention to problems and the resources to address them. Any investment here will pay for itself in reduced maintenance costs.

Chapter 4

USCGC William Chadwick (WPC 1150) NILM Installation

Prototype NILM systems have been installed on several Coast Guard Cutters over the past few years, but *Chadwick* is the first FRC to have one. Unlike older vessels such as *Thunder Bay* and *Spencer*, the FRC uses modern control systems and other technological updates. Since all the FRCs sent to Boston were brand-new from Bollinger Shipyards, there was a great opportunity to develop forward-looking fault detection and diagnostic (FDD) techniques rooted in NILM for the new generation of cutters.

After planning the installation and putting it into place, both AIO boxes have been collecting power data from two 440-V power panels in *Chadwick's* engine room. In certain cases, the portable AIO box (Porta-NILM) provided data from systems not within the purview of the fixed system. This chapter describes the installation process, the equipment visible on the engine room power panels, and a few special cases of FDD work. Given how diverse the equipment is, there will be plenty more opportunities for future work.

4.1 Installation Overview

Figure 4.1 shows the front of *Chadwick's* AIO boxes, Figure 4.2 shows the back, and Figure 4.3 shows the power panels being monitored. Power panels 3-27-1 and 3-27-2 cover a range of equipment throughout the FRC. They lie on either side of the forward bulkhead of the engine room and draw power directly from the main 440-V distribution panel. Of all the panels on board, these two provided the most interesting NILM opportunities because of the particular equipment on them. The 440-V system on the FRC is delta-connected, and these two panels are rated for 125 A at 450 VAC.

The AIO boxes themselves are located on a platform above the engine room main level, where the propulsion engine jacket water expansion tanks are. This was a discrete, convenient place between the panels where both boxes could be located right next to each other. Special brackets made from stainless steel mount the boxes to the railings on either side of the platform. The voltage and current cables run from each box to its respective power panel along the established cable ways in the overhead of the engine room. At the power panels, the voltage leads go to a spare breaker and the current cables go to LEM current transducers

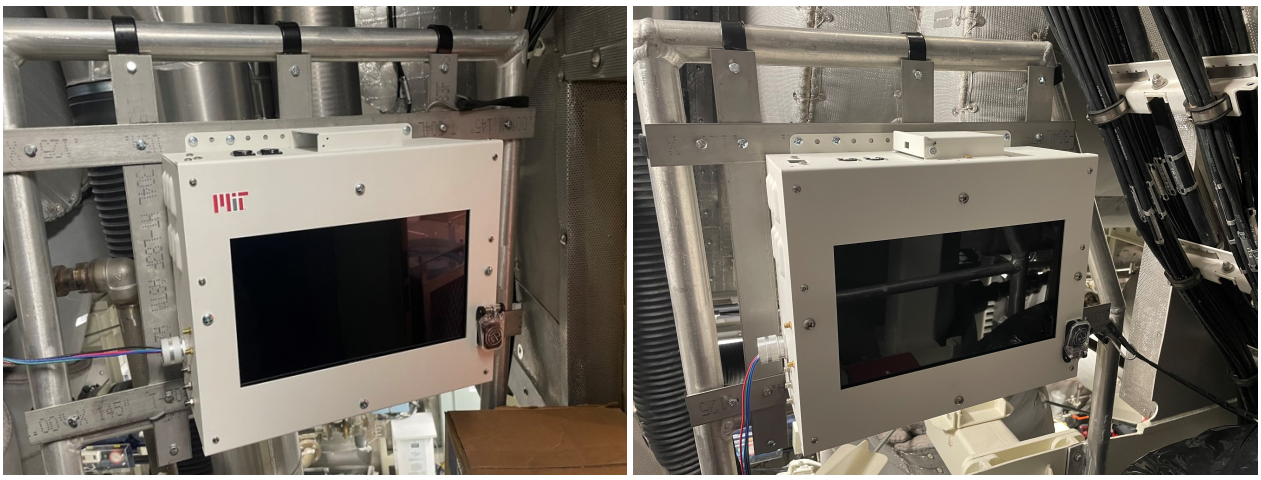

(a) Port (b) Starboard

Figure 4.1: Front views of the AIO box installations on *William Chadwick*.

(a) Port (b) Starboard

Figure 4.2: Back views of the AIO boxes on *Chadwick*, showing the bracket construction.

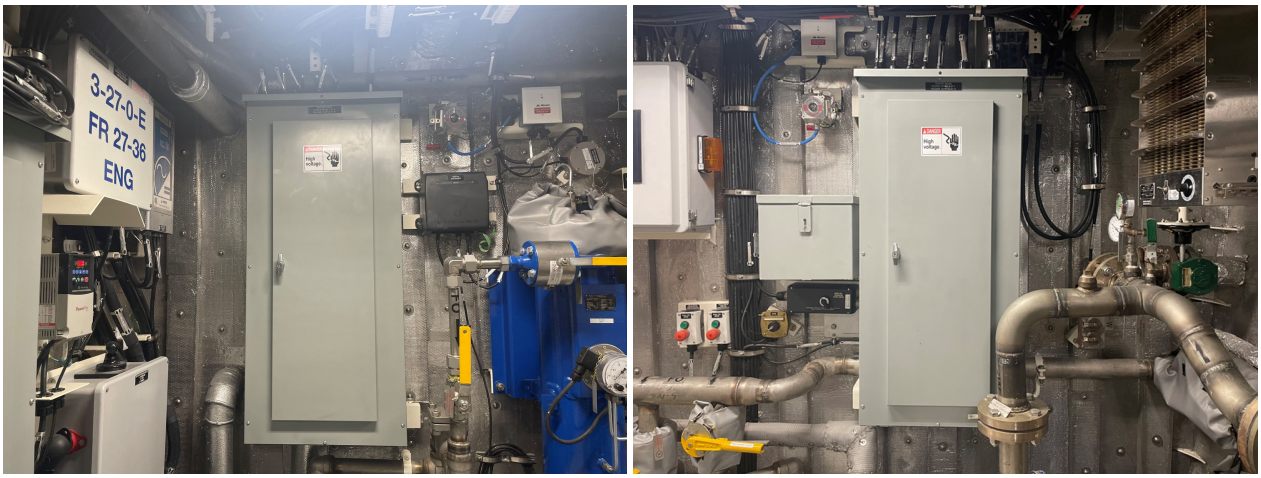

(a) Panel 3-27-2 (Port) (b) Panel 3-27-1 (Starboard)

Figure 4.3: The two engine room power panels being monitored.

Figure 4.4: Porta-NILM

around each phase.

Porta-NILM essentially works the same way. Instead of having the AIO box mounted permanently, it is mounted to the inside of a wooden case so an operator can deploy it wherever needed. The voltage leads can go to a power receptacle or to any set of exposed 440-V terminals. Figure 4.4 shows Porta-NILM itself.

Load	Amperage
HVAC Main Control Panel, C1	60 AT
Steam Humidifier	15 AT
SCBA Recepticle	15 AT
Watermaker - Reverse Osmosis Unit	25 AT
Exhaust Fan, Forward Aux	15 AT
Steering Gear Room Heater, Stbd	15 AT
Cathodic Protection System	15 AT
Generator Room Heater No. 1, Stbd	15 AT
Steering Gear Room Exhaust Fan, Stbd	15 AT
Emergency Generator Room Heater	15 AT
450/120 Transformer Bank, C1 Panel	60 AT

Table 4.1: Panel 3-27-1 (Starboard)

Load	Amperage
Steering Gear Room Heater, Port	15 AT
Oily Water Separator	15 AT
Sewage System	30 AT
Steering Gear Room Exhaust Fan, Port	15 AT
Engine Room Heater No. 1, Stbd	15 AT
Tankless Water Heater No. 2	40 AT
Engine Room Heater No. 2, Port	15 AT
Generator Room Heater No. 2, Port	15 AT
Forward Aux Space Heater	15 AT

Table 4.2: Panel 3-27-2 (Port)

4.2 Panel 3-27-1 Loads

What follows is a brief description of each load in Table 4.1 and some basic information about the loads.

4.2.1 HVAC Main Control Panel, C1

This breaker serves the C1 air conditioning compressor shown in Figure 4.5, model HGX5/1240-4 S made by GEA in Frickenhausen, Germany. Like most shipboard air conditioning units,

Figure 4.5: Air conditioning compressor C1

this one uses the refrigeration cycle to cool water for use in chiller units around the ship. It has a heat exchanger to cool the refrigerant with seawater and is rated for 44.5 kW at peak performance. The unit is thermostatically controlled, the thermostat itself being located on the main deck near the galley entrance. It will cycle on or off automatically at any time to maintain the proper temperature within the living spaces. The other compressor, C2, cools the bridge and the IT space. Figure 4.6 shows the system starting, Figure 4.7 shows the system's signature during heavy loading with the compressor in "low", and Figure 4.8 shows a typical compressor run.

4.2.2 Steam Humidifier

This is a heater within the HVAC system which vaporizes water to maintain a minimum relative humidity during cool weather when the electric heat is on. It draws 8.22 kW at peak performance.

4.2.3 SCBA Recepticle

Every Coast Guard cutter carries a breathing air compressor to refill air cylinders for the self-contained breathing apparatus (SCBA) used in shipboard damage control efforts. It is driven with an induction motor and is rated for 5 HP (3.7 kW). Given that the crew only refills SCBA cylinders periodically, this load only appears infrequently.

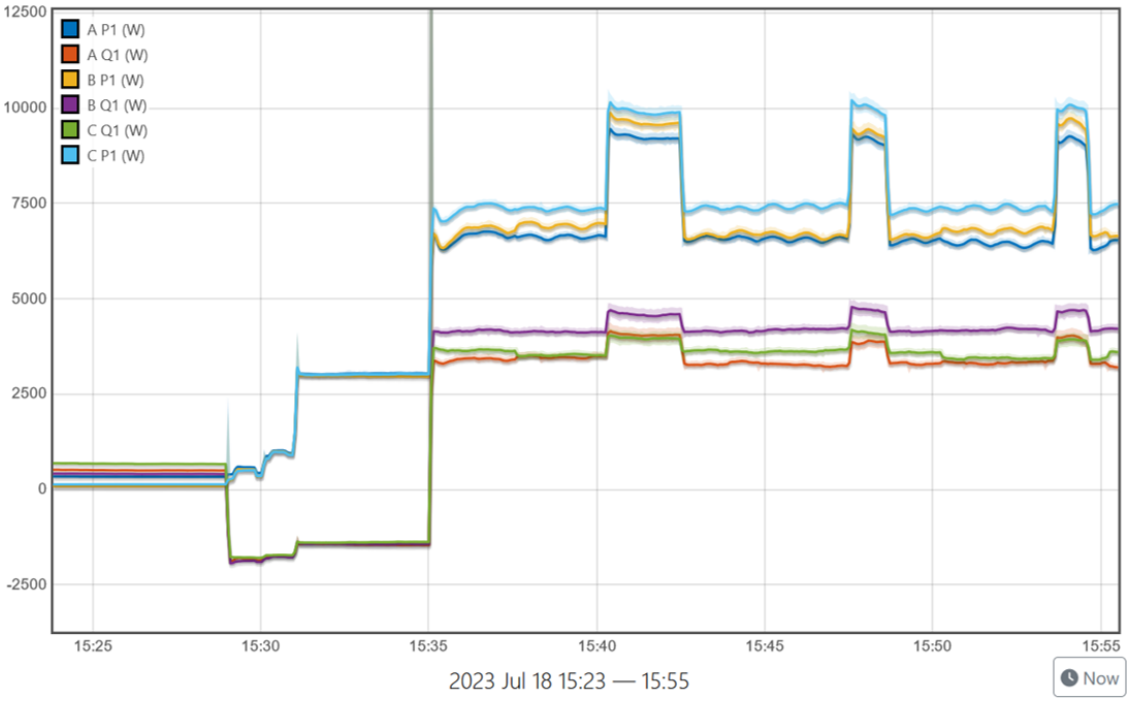

Figure 4.6: Restart of the C1 HVAC system.

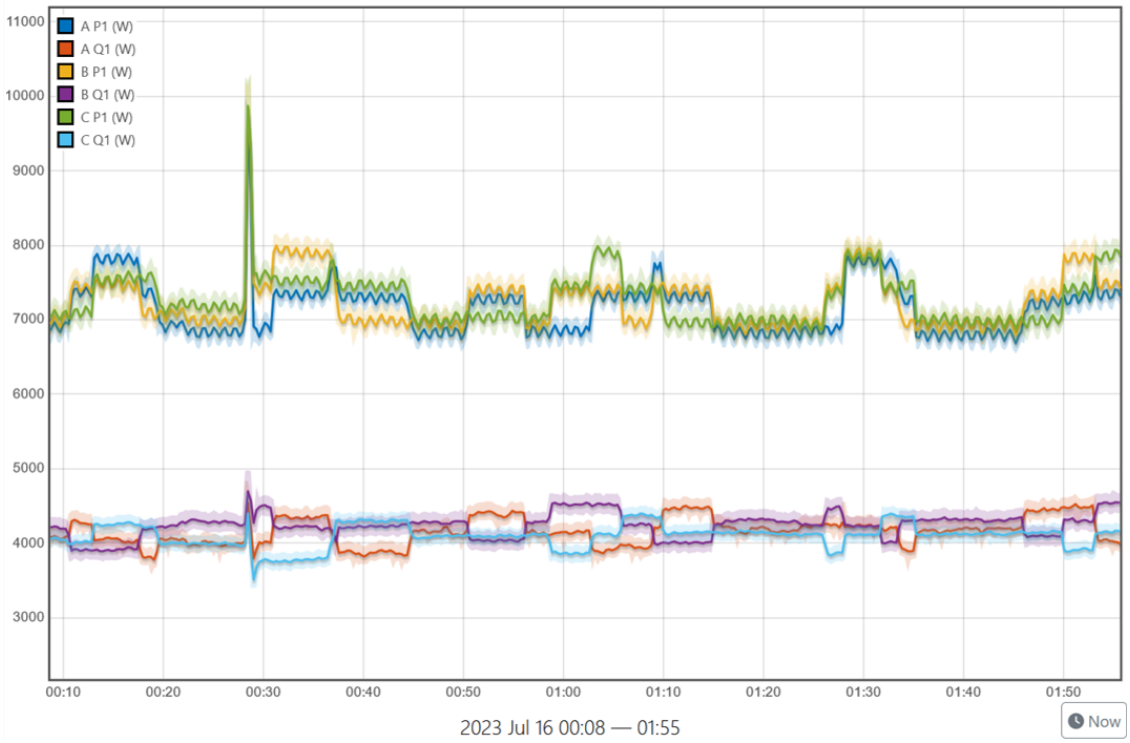

Figure 4.7: Signature from the HVAC main control panel, showing miscellaneous equipment and harmonic distortion from the HVAC control systems.

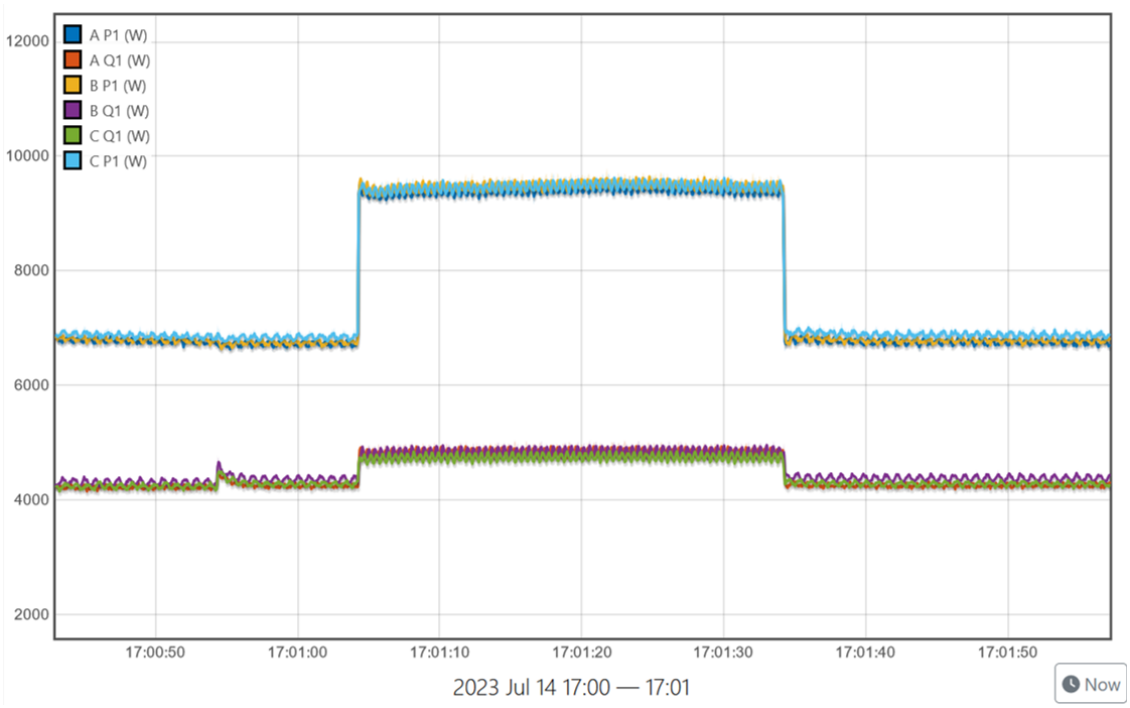

Figure 4.8: Signature from the C1 compressor transiting to "high" during heavy loading.

4.2.4 Watermaker - Reverse Osmosis Unit

The FRC uses reverse osmosis to make fresh water underway. In reverse osmosis, a pump pressurizes water and forces it through a semi-permeable membrane which allows water to pass through but stops dissolved material from doing so. Operators maintain the unit by paying attention to the differential pressure across the membrane and the dissolved solids on the discharge side. If either are unsatisfactory, the filters may need to be changed. This load draws 2 kW. Given the short duration of most underway trips, crews can often take enough water with them to last a day or more and can refill the water tanks at the pier. This saves wear on the reverse osmosis unit and, consequently, it also runs infrequently.

4.2.5 Exhaust Fan, Forward Aux

This is a standard ventilation exhaust fan for a machinery space with "high" and "low" settings for different flow rates. Here, an induction motor drives a fan blower which vents to the ship's exterior. The motor is rated for 0.5 HP (∼0.4 kW). See Figure 4.14 for signature.

4.2.6 Steering Gear Room Heater, Stbd

The steering gear room is relatively small, hence the small size of this heater. When the space reaches the proper temperature, it shuts off on its own and cycles on again as needed. It draws 1.5 kW in operation and appears as a 3-phase resistive load, an example of which is shown in Figure 4.9.

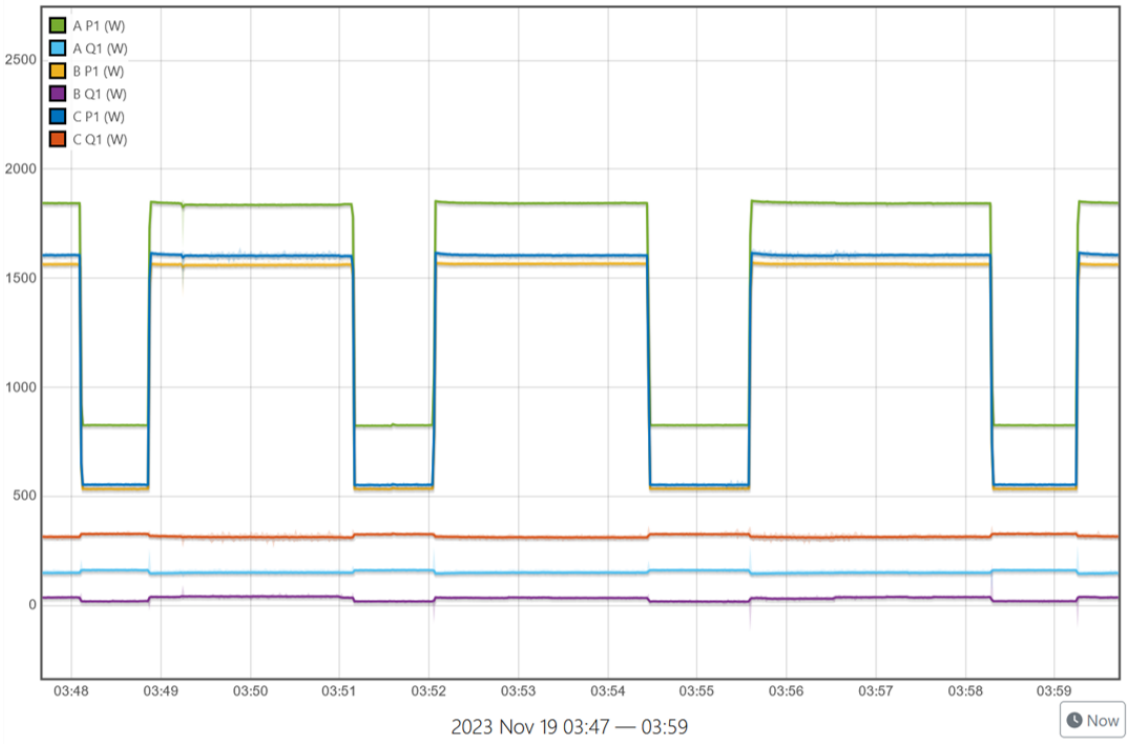

Figure 4.9: Typical 3-phase heater NILM signature.

4.2.7 Cathodic Protection System

The exact operation of the Cathelco ICCP system is discussed in-depth elsewhere in this document. However, this breaker also serves the anti-fouling system incorporated into the same unit. Several copper anodes located in the large seawater intake pipes emit DC current to discourage marine growth from clogging the pipes. Typically, this is only about 0.3 A per anode. The ICCP system itself is a transformer and DC power supply, and as such generates various harmonics. It only draws the necessary amount of power to meet demand, but it is rated up to 1.68 kW.

This load is difficult to distinguish. Figure 4.10 shows the distinct self-test function on startup, where the system puts out up to 50 A for a brief moment. Generally speaking, the ICCP system never puts out more than 15-20 A in operation. Even at this elevated output level, it is practically impossible to see its effect in the first harmonic power stream because it is so small.

4.2.8 Generator Room Heater No. 1, Stbd

This is another typical 3-phase electric heater. It is rated for 2.25 kW. See Figure 4.9 for signature.

4.2.9 Steering Gear Room Exhaust Fan, Stbd

This is another typical exhaust fan, rated for 0.25 HP (0.2 kW). See Figure 4.14 for signature.

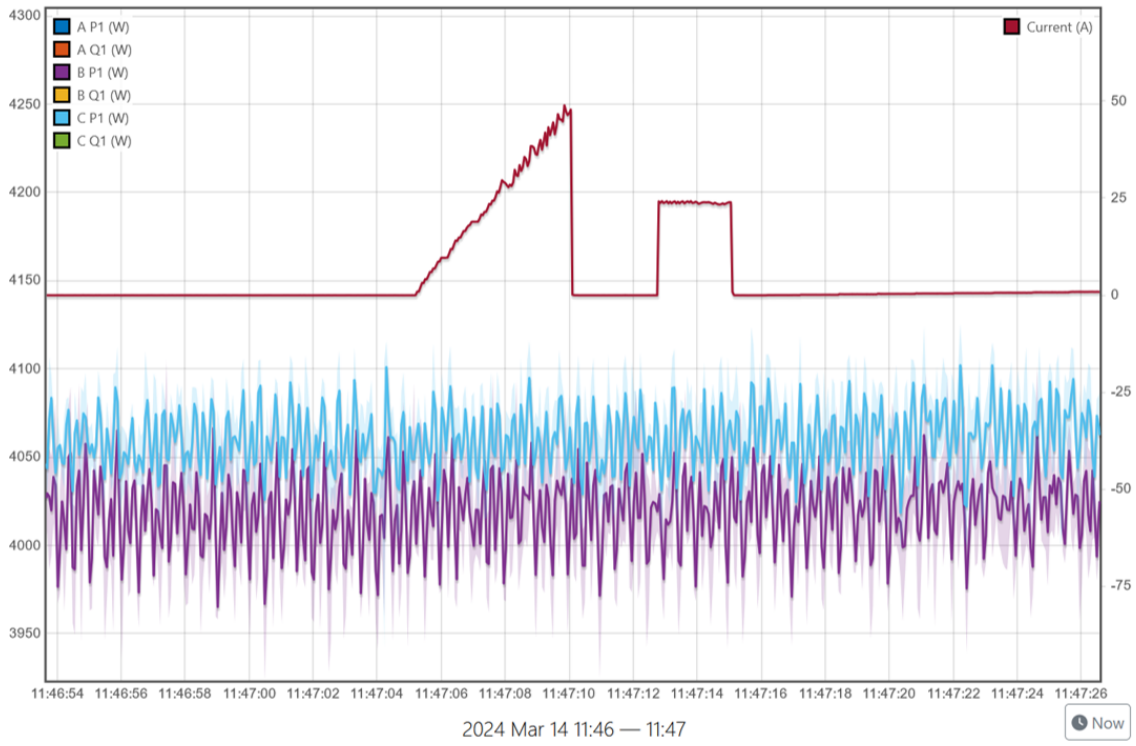

Figure 4.10: ICCP self-test current (red, right axis) plotted alongside real power (left axis). Even up to 50 A output, any effect on power is lost in the noise floor.

4.2.10 Emergency Generator Room Heater

This is another typical 3-phase electric heater, rated for 2.5 kW. See Figure 4.9 for signature.

4.2.11 450/120 Transformer Bank, C1 Panel

This breaker serves a transformer bank for all the miscellaneous heaters and fans on the C1 HVAC system. These loads are all 2 kW or less and include small heaters and fans for heads and the pilothouse. A run from one of the heaters is shown in Figure 4.11.

4.3 Panel 3-27-2 Loads

What follows is a brief description of each load in Table 4.2 and some basic information about the loads.

4.3.1 Steering Gear Room Heater, Port

This is the counterpart to the starboard heater on the other panel. It is rated for 1.5 kW. See Figure 4.12 for signature.

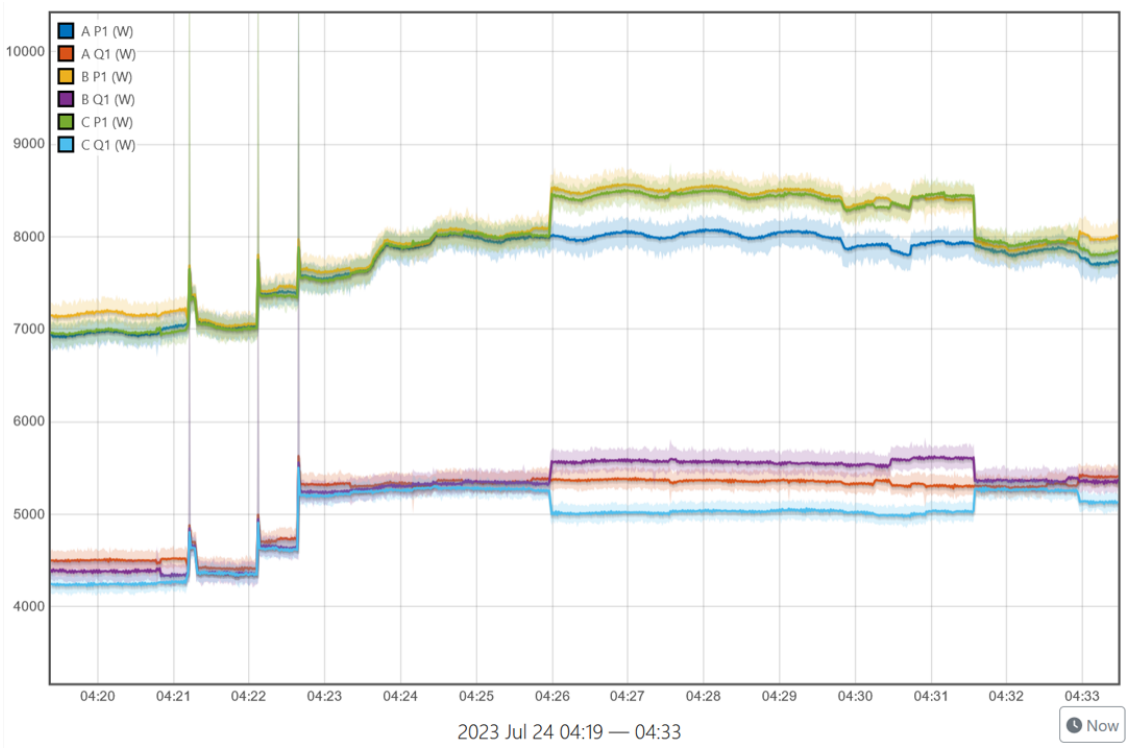

Figure 4.11: Single-phase heater from the C1 transformer bank, turn-on event at 0426. Note the distortion to the power streams due to the HVAC control systems.

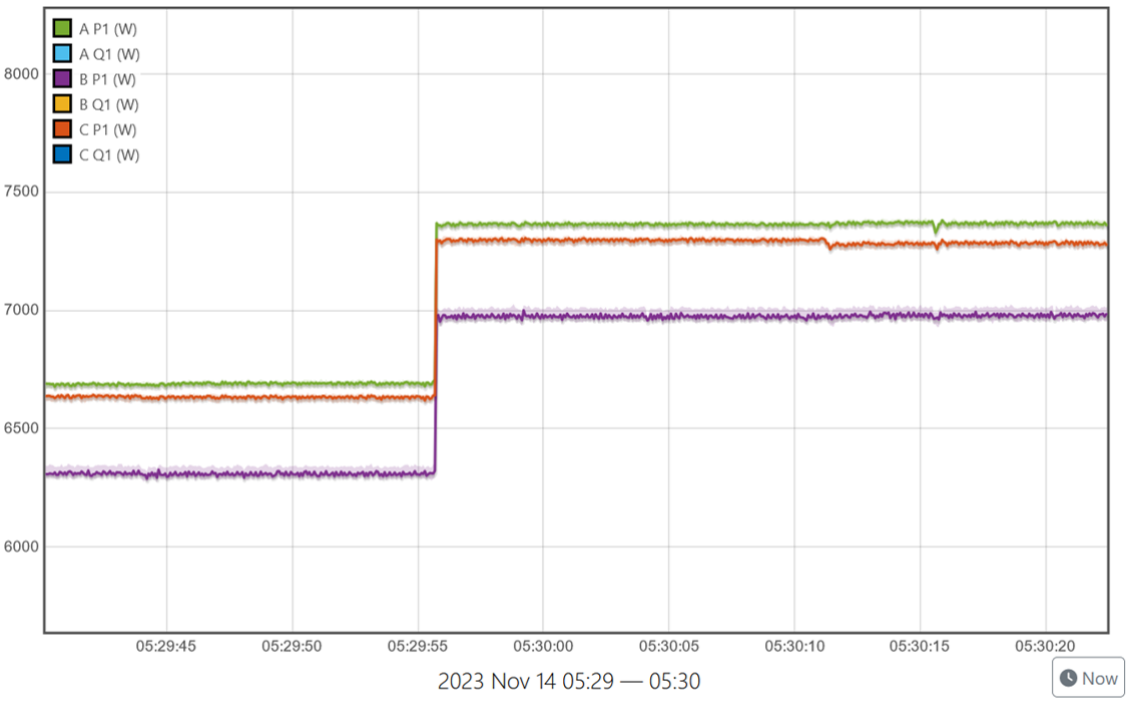

Figure 4.12: 1.5 kW space heater.

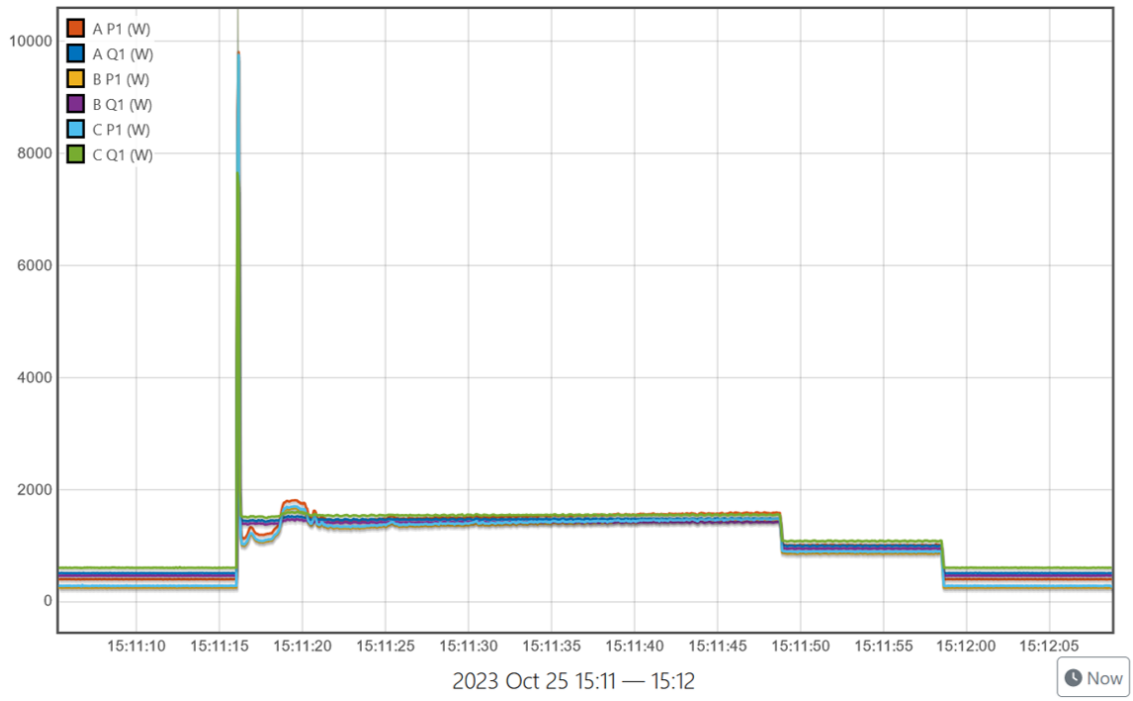

Figure 4.13: Typical run of both Vacuumarator pumps.

4.3.2 Oily Water Separator

Ships have oily water separators to treat contaminated bilge water so that the bulk of the liquid can be safely discharged. The units use pumps and motors to separate the liquids with centrifugal force so the remaining oily material can be stored at greatly reduced volume, or it can be processed further so that the oily material can be burned in an incinerator. Since FRCs do not carry incinerators, the oily material is stored and unloaded in port. FRCs do not generate large amounts of oily water and there are many convenient times to unload it, so this machine only runs occasionally. It is rated for 0.79 kW.

4.3.3 Sewage System

The FRC uses a vacuum collection, holding, and transfer (CHT) system for handling sewage. There are four machines which draw power from here: two Jets Vacuumarator pumps, one transfer pump, and a blower. When a crewmember flushes a toilet, a vacuum tank in the forward aux space sucks the waste through the pipe and into itself. When pressure sensors detect a rise in pressure in the tank, the controller automatically turns on one or both Vacuumarator pumps to remove air and sewage and lower the pressure again. These pumps can both macerate sewage and pull a vacuum, simplifying the system's design and maintenance needs. The Vacuumarator pumps discharge to a holding tank, where the blower bubbles air through the contents to aid in breakdown and prevent the buildup of toxic gas. The transfer pump can then pump the sewage overboard or to a shoretie. The Jets pumps are model 15MBD and use 2.55 kW each when running. The transfer pump is rated for 2 HP (1.5 kW). The blower is rated for 0.94 kW.

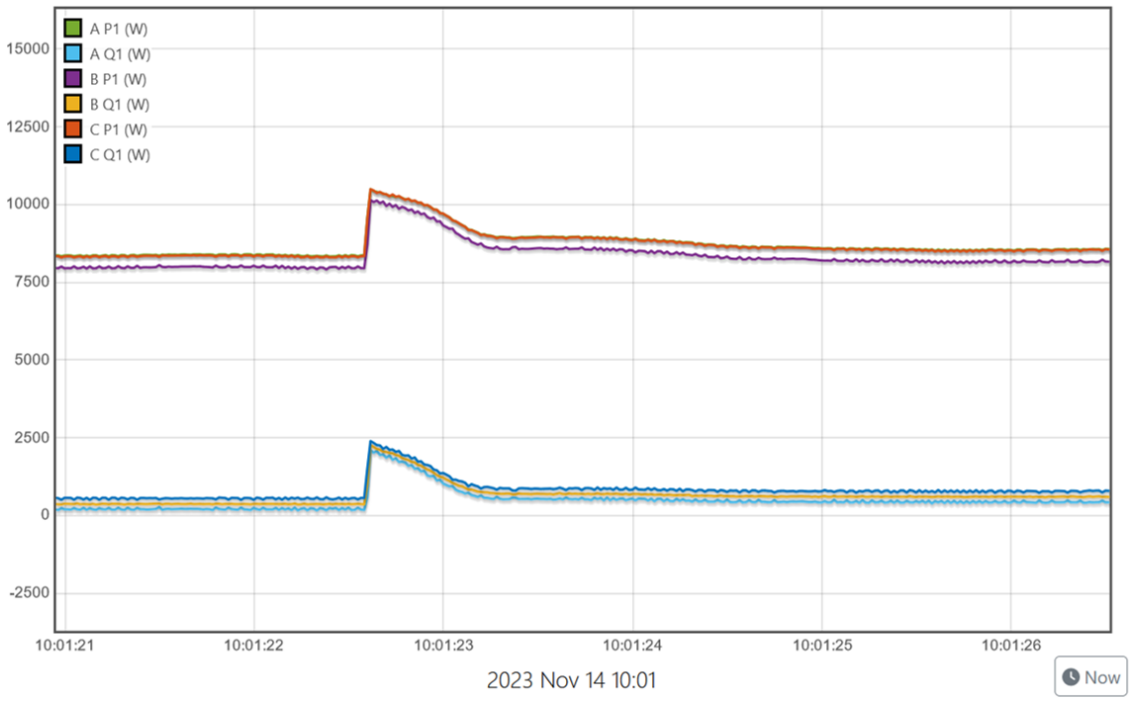

Figure 4.14: Steering gear room exhaust fan.

The Vacuumarator pumps cycle on and off regularly according to how much the sewage system is being used; both are typically set to "auto" and cycle at roughly the same time. Figure 4.13 shows a typical run of both Vacuumarator pumps.

The blower motor runs constantly, and the transfer pump is only used periodically since it can take several days or weeks during slow times to fill the sewage tank.

4.3.4 Steering Gear Room Exhaust Fan, Port

This is another typical exhaust ventilation fan, rated for 0.25 HP (∼0.2 kW). See Figure 4.14 for signature.

4.3.5 Engine Room Heater No. 1/2

These are large space heaters mounted to the bulkheads in the engine room. They are rated for 8 kW each and have a built-in fan to circulate air through the elements. Like other heaters, they can cycle on and off as needed to maintain the proper engine room temperature. See Figure 4.15 for signature.

4.3.6 Tankless Water Heater No. 2

Rather than maintain a large hot water tank, the crew's heads have tankless water heaters installed to serve the sinks and showers. Unlike simple resistive water heaters, these ones use power electronics to rapidly cycle the heating element on and off to provide the right amount of heating power according to the flow rate through the heater. Thus, they produce

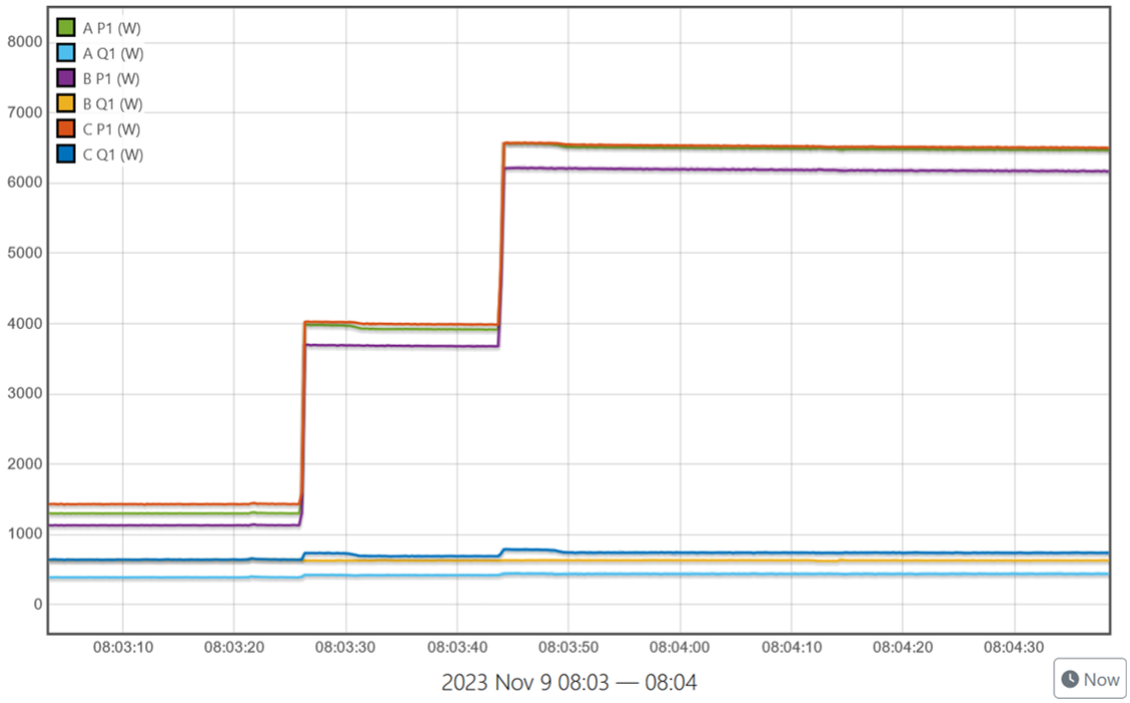

Figure 4.15: Both engine room heaters turning on roughly 20 seconds apart.

peculiar NILM signatures shown in Figure 4.16 and Figure 4.17. Although they are easy to identify, analysis is more challenging because of the rapid succession of on-off events. It is rated for 24 kW.

4.3.7 Generator Room Heater No. 2, Port

This is another typical electric space heater, rated for 2.25 kW. See Figure 4.9 for signature.

4.3.8 Forward Aux Space Heater

This is another of the same heater type used in the engine room, rated for 8 kW. See Figure 4.15 for signature.

4.4 Applications

The challenge when developing FDD techniques is that appliances in the field need to break so the researchers can examine the data for leading indicators. To be fair, machines break all the time in the Coast Guard. But on a brand-new ship, most appliances work as well as they ever will, and the occasional break-down must happen "in the right place and at the right time" for the NILM system to record it. Nevertheless, the brief few months on *Chadwick* have provided some FDD opportunities and allowed the researchers to test the limits of the measuring equipment.

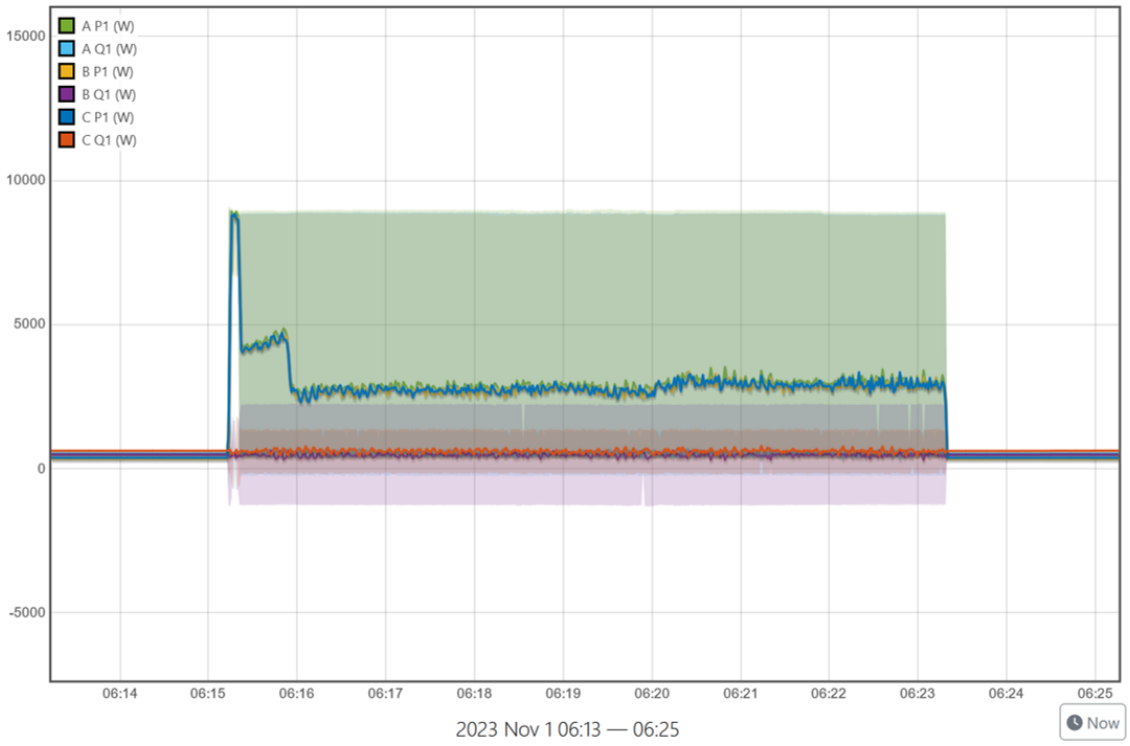

Figure 4.16: Tankless water heater NILM signature. The shaded region represents the envelope of the power trace. See Figure 4.17 for details on how the inside of the envelope looks.

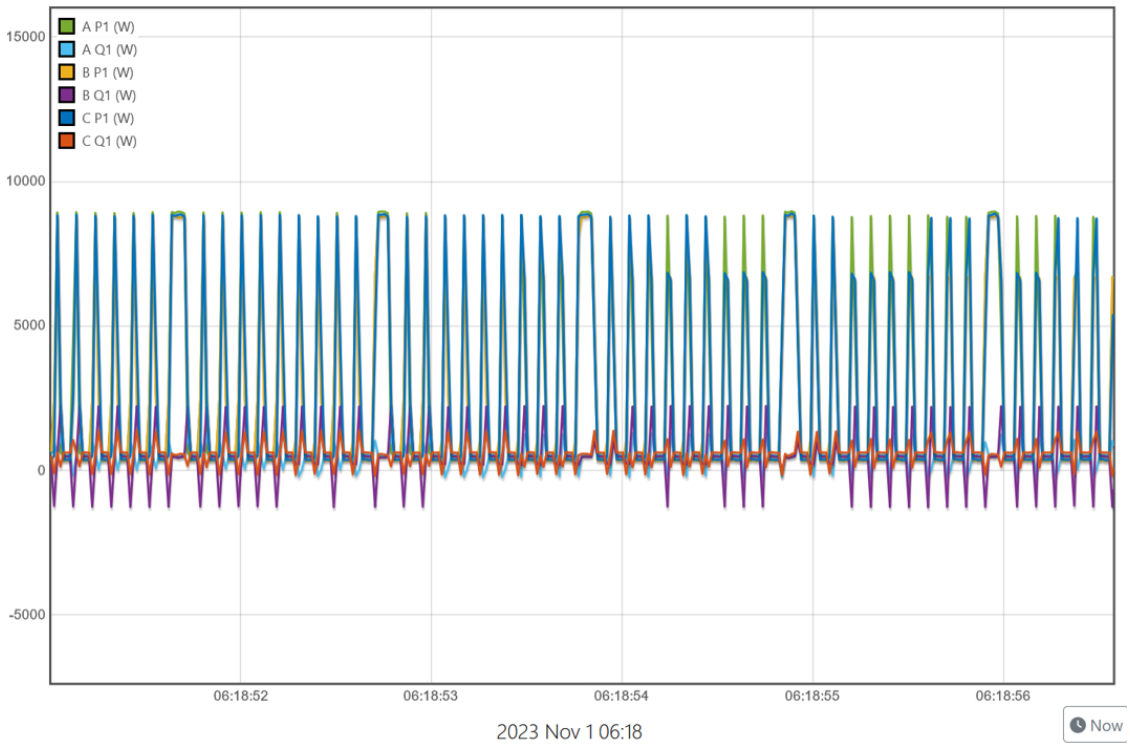

Figure 4.17: Close-up view of the water heater NILM signature.

4.4.1 Dishwasher Heater Ground Fault

Although the galley is not visible from the fixed NILM system, the crew drew attention to a ground fault with one of the dishwasher's boost heaters, shown in Figure 4.18. Identifying the problem with traditional techniques proved time-consuming and difficult, but the fault showed clearly in data collected with Porta-NILM.

Watchstanders first became aware of a ground fault alarm on MCS which seemed to trigger and clear at random. It typically only lasted a minute or two before going away. Traditionally, an electrician's mate would begin troubleshooting by turning off breakers one by one and re-testing for the ground fault. If the fault went away after flipping one breaker, then the fault would be somewhere on that circuit. When the ground fault clears in less than two minutes, this tactic becomes impractical since it would go away before a technician could even reach a panel to start flipping breakers. Since the dishwasher is not monitored by MCS, electrical power provides the only source of data about its operation.

The crew eventually found the ground after several weeks of searching and a stroke of intuition on part of the electrician's mate chief. NILM, however, provides a more scientific way of finding ground faults.

Dishwashers are typically complex finite-state machines with several heaters and pumps which turn on at different parts of the washing cycle. A boost heater is necessary here to bring up the hot water temperature from however hot it is in the galley to above 170 °F to sanitize the dishes. This makes its power signature distinct from every other appliance on the ship and easy to identify. By identifying what turns on and when, one can pick out the offending equipment by plotting the MCS ground fault alarms and the ground current against the electrical power data.

Since the ship's 440-V system is delta-connected, the sum of the current from all phases should equal zero. If it does not, some must be leaking to ground. With this simple math, it becomes possible to find when the ground fault occurs and what turned on at the same time. Since the NILM system in the engine room cannot see the galley power panel, the researchers connected Porta-NILM directly to the galley power panel instead. Figure 4.19 displays data from the galley power panel, showing the dishwasher turn on twice, the ground current, and the MCS ground fault alarms.

When the dishwasher's boost heater turns on, the MCS ground fault alarm triggers almost simultaneously due to the rise in ground current. Once the dishwasher finishes its cycle and the heater turns off, the alarm clears just as quickly. Naturally, this method of finding grounds applies to any machine identifiable with NILM techniques and could save technicians large amounts of time as they maintain various systems, on ships and on shore installations.

4.4.2 Impressed-Current Cathodic Protection System Identification

NILM has traditionally been most useful with finite state machines for several reasons. First, the transient events which appear in the power stream when a machine turns on and off usually have sharp characteristics which make them easy to identify. Second, it may be reasonable in many cases to assume that the steady-state power consumption remains mostly constant while the machine is on. This means that the "off" event will be more or less

Figure 4.18: Boost heater from the dishwasher. Note the filament wires sticking out. Corrosion did the damage to the heater – according to the technicians, removal did virtually no damage to it.

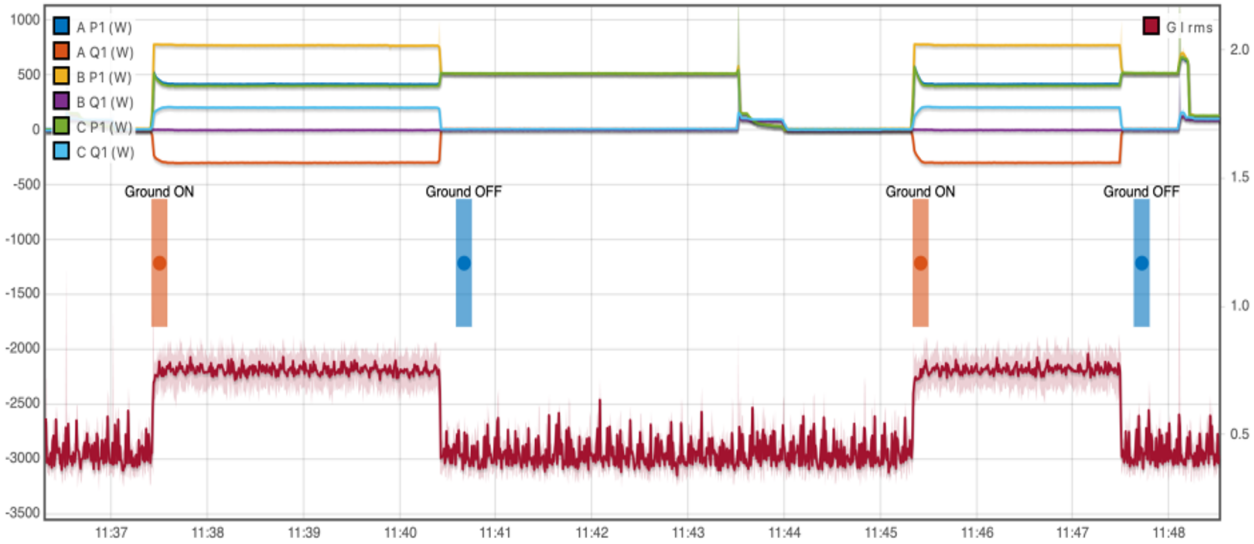

Figure 4.19: NILM signature of the dishwasher alongside ground current and the MCS ground fault alarm.

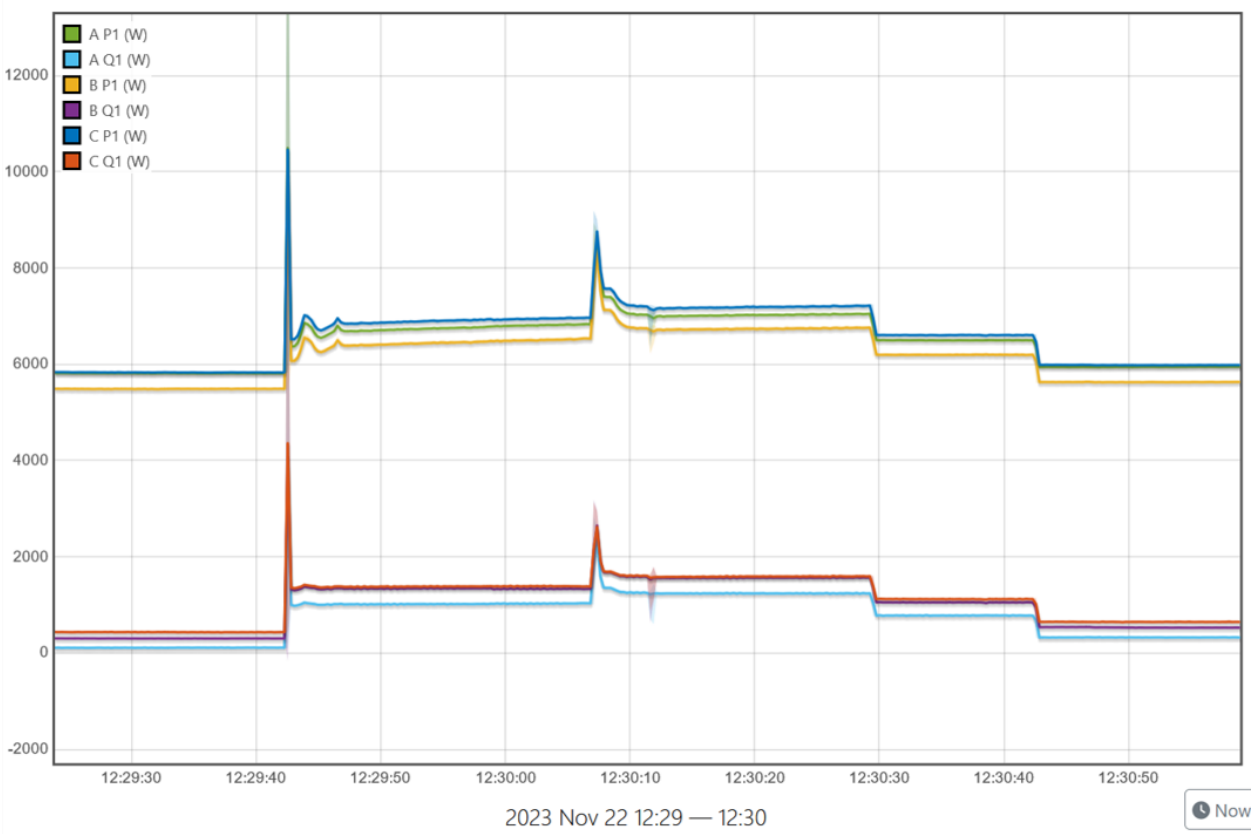

Figure 4.20: Sewage pump runs where one pump started well after the other. It is difficult to tell whether the first pump ran for a long time and the second pump a much shorter time on top of it, or whether the first pump turned off first and the second pump turned off second.

the same size as the "on" event, or at least consistent enough to accurately assign it to its cause. Third, it is often unlikely that two such transient events will align so perfectly that a computer interprets two distinct events as one. That little bit of misalignment is critical for accurately identifying loads.

Assigning the cause of changes in steady-state power is a more difficult problem. For example, if there are four identical heaters online at a given time and one of them reduces its power consumption for whatever reason, a NILM system has trouble determining which heater (or heaters) experienced the reduction because the individual steady-state signatures are so similar. There must be something distinct about the character of the steady-state power for the NILM system to latch on to when tracking power usage. Figure 4.20 illustrates this problem.

Harmonics are one useful tool for telling power signatures apart. Since not all machines produce harmonics on all levels, knowing the distribution can narrow the field when looking for causes of a change in power.

Such is the case with the ICCP system. It can adjust the amount of power it draws according to the corrosion protection current demand or the anti-fouling system. When it does so, it does not change as a step but as a continuous adjustment. Initially, Porta-Nilm was connected directly to the system's power cables as in Figure 4.21 to gain clear insight on

Figure 4.21: Porta-NILM being used to assess the ICCP system.

how its power signature looks. Then data from the fixed system provided a view in context.

When the ICCP system turns on, it conducts a self-test in which it steadily ramps up its output power and then suddenly drops to zero. It is easy to spot in the fundamental line frequency, and it also appeared in the seventh harmonic of the line frequency. Since nothing else on the panel produced strong effects in the seventh harmonic, changes to the power stream in the first harmonic proportional to a change in the seventh are because of the ICCP system.

This revelation opens the door for several FDD opportunities. Not only can the NILM system assess the functionality of the ICCP system itself, but it can keep track of its power consumption and, by extension, the condition of the hull or the zinc anodes. In the absence of automatic logging of the ICCP parameters, examining the power consumption may be the next best approach to continuously tracking its performance as well.

4.4.3 NILM Equipment Limitations

During the first few weeks of the NILM system installation, a strange phenomenon became apparent in the voltage waveform whenever the C1 air conditioning compressor turned on as in Figure 4.22. During the initial inrush of power as the motor was getting up to speed, the voltage on one of the phases appeared to spike for two line cycles before returning to normal as in Figure 4.23. After discussing possible causes with the crew, it became apparent that the compressor functioned perfectly and this was not a symptom of arc pitting or another electrical fault.

Porta-NILM showed the same spike when it was connected to the starboard power panel.

When the current sensor cables were disconnected from the fixed AIO box, the phenomenon did not appear. This artefact in the voltage waveform did not occur in reality, but it was a symptom of the current sensors drawing more power than the AIO box could supply. The C1 compressor draws such a great inrush of power on startup that the sensors cannot keep up. As a result, the system could not calculate the voltage correctly.

It is worth considering equipment limitations when otherwise inexplicable features appear in the power stream. Before dedicating time to serious troubleshooting, it may be that the measurement technique is at fault.

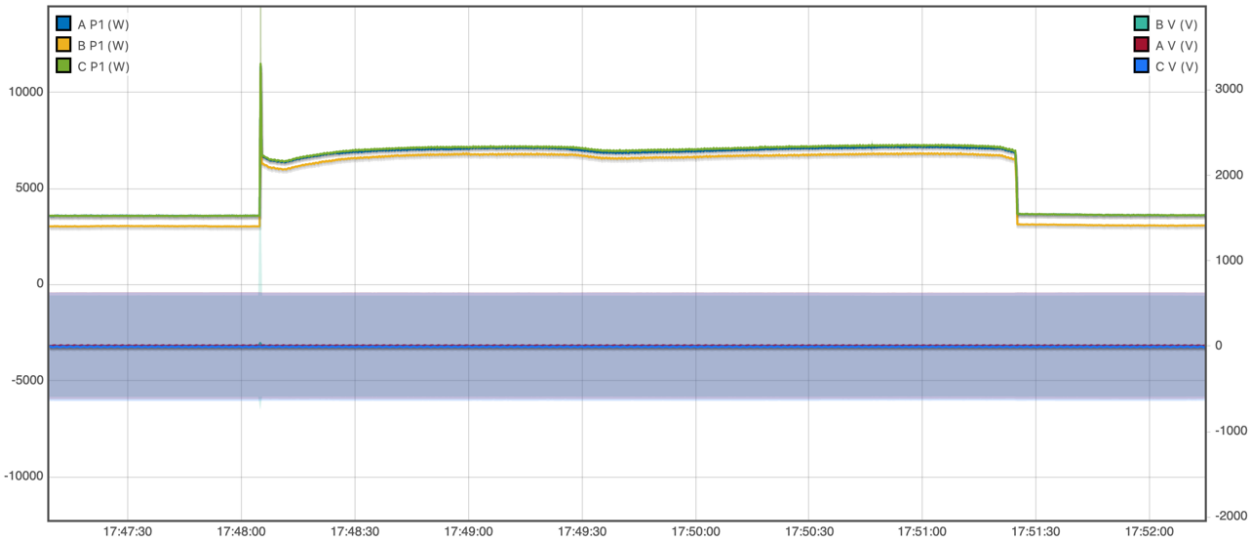

Figure 4.22: Run of C1. Note the lack of distortion from the HVAC control systems.

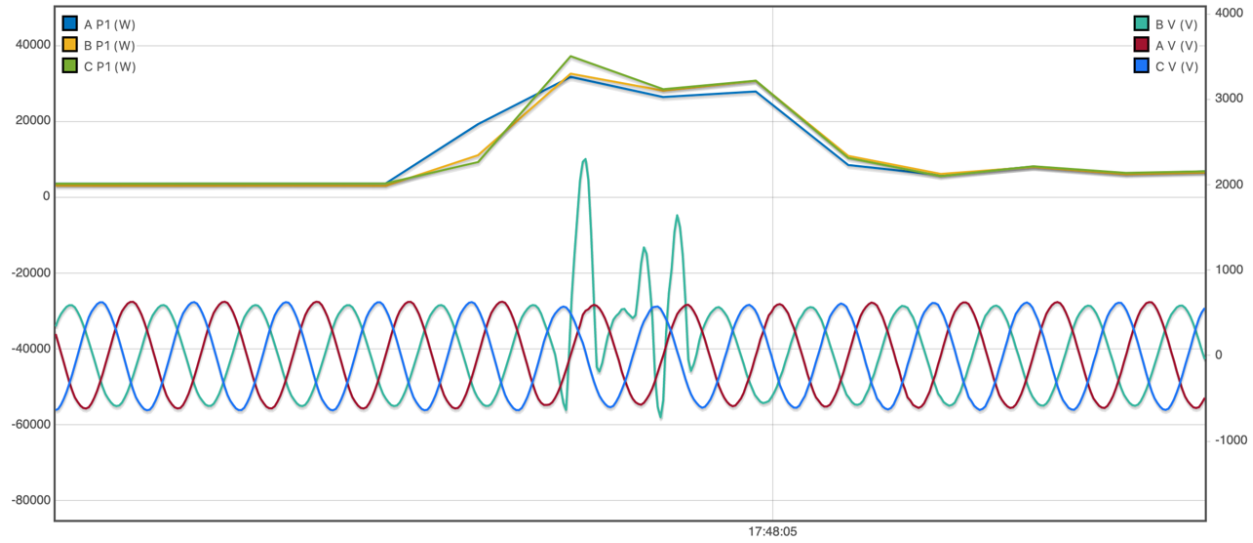

Figure 4.23: Voltage anomaly which coincided with the start of C1.

Chapter 5

Conclusions and Future Work

The work described here is not an end in itself, but a way of approaching shipboard maintenance and fault detection challenges with modern, data-driven tools. The methods should make life easier for all concerned by making it easier to gain physical insight from the volumes of data generated on Coast Guard cutters. More high-quality data opens more opportunities for analysis, but the crew cannot be burdened with tedious collection and processing techniques — they can contribute too much to be bothered with writing down numbers by hand on a clipboard. And, since they're typically not trained in statistics and computer science, a properly designed set of tools should make the benefits of those fields both accessible and useful to petty officers in the engine room.

The stern tube corrosion investigation gave the experts at SFLC information on how the state of corrosion protection in the FRC stern tubes changes and why the hull structures there are so prone to damage. It also drew attention to an unconventional solution which may remediate the situation enough that it no longer poses a maintenance nightmare. Furthermore, the ICCP log analysis sought to add value to the FRC maintenance efforts. Since every crew spends time generating and maintaining logs, it was worth verifying that the data could be scientifically useful in the first place. In the spirit of innovation, it was also worth exploring how one could process the data for other uses and what good it would do to enhance the collection regime.

Similarly, NILM explores fault detection and diagnostics with a previously under-used source of data. Several challenges remain in automating the analysis efforts and making them reliable as power data becomes more convoluted with advanced systems, but the FRC makes an excellent proving ground for this technology. With more data at hand and more variation in equipment performance, the data set will grow to a size where it becomes productive to develop an algorithm with one part of the set and test it on another. Machine learning algorithms can also be well-suited for filtering out noise and extracting features.

Watchstanding and shipboard maintenance practices must change as technology advances. The need for innovation is the only constant here, and hopefully the efforts in this thesis help the Coast Guard keep pace with the state of the maritime industry.

Appendix A

Hull Potential Survey Instructions

Contact | LTJG Maxwell Buchanan
mcb25@mit.edu
(206) 430-4567

1 HULL POTENTIAL SURVEY AND REFERENCE ELECTRODE ACCURACY TEST

Rev 1.4 20 March 2024

MIT Research Laboratory of Electronics

Tools/Test Equipment:

Silver-Chloride stick electrode and cable. (1 ea)

Ground clamp and cable. (1 ea)

Alligator clip to banana-plug connector. (2 ea)

Double-sided alligator clip cable. (1 ea)

Fluke 87 Multimeter (or equivalent). (1 ea)

Multimeter probes. (2 ea)

Zinc bar or bolt (1 ea)

Steel bar/rod (1 ea)

Beaker or Plastic cup (1 ea)

Waterproof carrying case. (1 ea)

References:

United States Coast Guard Maintenance Procedure Card (MPC) WPC-154 B10010.0

Procedure:

Initial Steps

1. Ensure the ICCP system is energized, set to auto, and functioning. (starboard machinery panel 3-27-1)
2. Record the ICCP output current and output voltage in the appropriate section of table 1.
3. Record the S1 and S2 reference voltages from the ICCP panel in the appropriate section of table 1.

Calibration

4. Fill beaker/plastic cup with seawater.
5. Using the double-sided alligator clip cable, connect one end to the zinc bar and the other end to the steel rod.
6. Using an alligator clip to banana-plug connector, connect the clip side to the steel rod and the plug side to the positive terminal of the multimeter.
7. Using the other alligator clip to banana plug connector, connect the clip side to the exposed wire end of the electrode cable and connect the banana plug to the negative terminal of the multimeter. Refer to figure 2 for the proper configuration.
8. Place the steel and zinc in the beaker filled with seawater.
9. Measure the voltage in the beaker by submerging the stick electrode in the seawater. The voltage should read roughly 0.92 V DC (920 mV). Record the calibration voltage in the corresponding results section.
10. Remove the zinc from the beaker and measure the voltage again with only steel and the electrode in the beaker. The voltage should read roughly 0.65 to 0.67 V DC.

11. Remove the steel and the electrode from the beaker and disconnect all cables.
12. Attach ground cable to the nearest grounding strap, hatch, or bare metal fitting.
13. Using one alligator clip to banana plug connector, connect the clip side to the exposed wire end of the ground cable and connect the banana plug to the positive terminal of the multimeter.
14. Insert a regular test probe to the negative terminal on the multimeter. Test the ground connection by setting the multimeter to measure resistance and connecting the probe to another nearby piece of bare metal. Confirm less than 1 Ω ground-to-ground resistance.
15. Remove the test probe from the negative terminal on the multimeter.
16. Using the other alligator clip to banana plug connector, connect the clip side to the exposed wire end of the electrode cable and connect the banana plug to the negative terminal of the multimeter.
17. Ensure the multimeter is set to the V DC mode.

Test Hull Potential with Power Energized

18. Standing at the rail at centerline bow, lower the electrode into the water until the 6 ft mark on the electrode cable (white tape) is at the waterline. Make sure to lower the electrode as close to the hull as possible without touching it.
19. Wait until the voltage reading is stable and then record the voltage in the “Power Energized” results section to 3 decimal places.
20. Take voltage measurements as above at the following locations (shown in figure 1) :
    - Frame 10 port
    - Frame 10 stbd
    - Frame 20 port
    - Frame 20 stbd
    - Frame 30 port
    - Frame 30 stbd
    - Frame 40 port
    - Frame 40 stbd
    - Stern centerline

Test Hull Potential with Power Secured:

21. Secure the ICCP system. (starboard machinery panel 3-27-1).
22. Repeat steps 18 through 20 with the ICCP secured, recording results in the corresponding “Power Secured” results section to 3 decimal places.

Final Steps:

23. Rinse the stick electrode with potable water.
24. Calculate the difference between the S1/S2 voltages recorded in step 2 and the port/starboard voltage readings at frame 10. Record the difference in the appropriate section of the results table.
25. Energize the ICCP system and return to normal operation (starboard machinery panel 3-27-1).
26. Return all equipment to the waterproof carrying case, ensuring everything is dry prior to storage.

Cutter Name & Hull #:__USCGC BAILEY BARCO #1122_____

Date:__08APR2024_____

Table 1: Hull Potential Survey and Reference Electrode Accuracy Results

Calibration	
Voltage (mV)	**1.036VDC**

ICCP Power Energized			
Reference Electrodes and ICCP Status			
Output Current (A)	8A	Output Voltage (V)	**4.4V**
S2 (mV)	-835	S1 (mV)	**-865**
Difference (S2 – Frame 10 PORT) (mV)	31	Difference (S1 – Frame 10 STBD) (mV)	**2**

PORT		**STBD**	
Location	**Reading (mV)**	**Location**	**Reading (mV)**
Frame 10	-866	Frame 10	-863
Frame 20	-870	Frame 20	-866
Frame 30	-928	Frame 30	-885
Frame 40	-829	Frame 40	-808
Bow Centerline	-860	Stern Centerline	-756
Notes:			

ICCP Power Secured			
PORT		**STBD**	
Location	**Reading (mV)**	**Location**	**Reading (mV)**
Frame 10	-538	Frame 10	-528
Frame 20	-523	Frame 20	-524
Frame 30	-508	Frame 30	-518
Frame 40	-467	Frame 40	-473
Bow Centerline	-537	Stern Centerline	-472
Notes:			

PORT SIDE MEASUREMENT LOCATIONS

Figure 1

STBD SIDE MEASUREMENT LOCATIONS

Figure 1: Frame Locations from MPC 10010.0

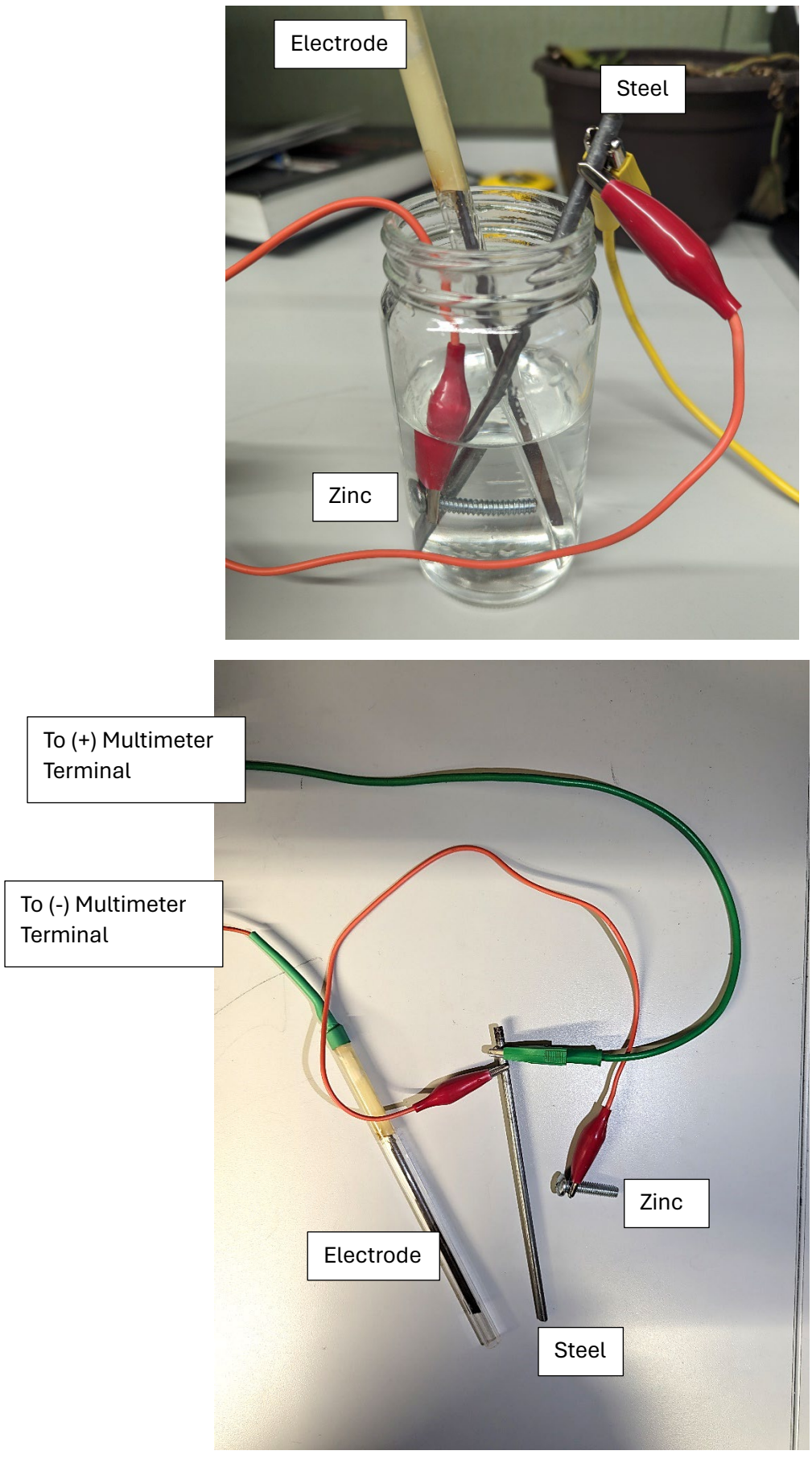

Figure 2: Calibration Configuration Shown with and without Beaker for Clarity

Appendix B

USCGC William Chadwick (WPC 1150) NILM Documentation

Appendix B includes the documentation submitted to the U.S. Coast Guard for approval to install two NILM AIO boxes on *USCGC William Chadwick* (WPC 1150). The documentation is modified from its original form for presentation and public release purposes. The Coast Guard granted approval for the installation on 20 April 2023 and the equipment was installed on July 11, 2023. This appendix is reproduced from [21].

B.1 MIT NILM Installation Plan for WILLIAM CHADWICK

B.1.1 Proposed Mounting

The proposed installation and mounting will be set up to be temporary. That is, no permanent modifications will be made with regard to the mounting hardware for the All-in-One (AIO) boxes. Instead, all hardware and bracketry will be installed using existing holes or brackets on the ship. Additional hardware, provided by the Massachusetts Institute of Technology Research Laboratory of Electronics (MIT RLE), will be custom-built and modified for the AIO boxes to be mounted securely without making permanent alterations to the cutter. Figure B.1 shows the AIO box installed on the USCGC STURGEON (WPB 87336) and the same style AIO box is to be installed on USCGC WILLIAM CHADWICK (WPC 1150) The brackets will be bolted and clamped to existing structures on the cutter, which will be explained in detail in this section. Notably, semi-circular pipe straps and circular hose straps will be used as anchor points to attach the new AIO box framing to the railings. Then, the AIO boxes will mount directly to the installed bracketry for a secure fit.

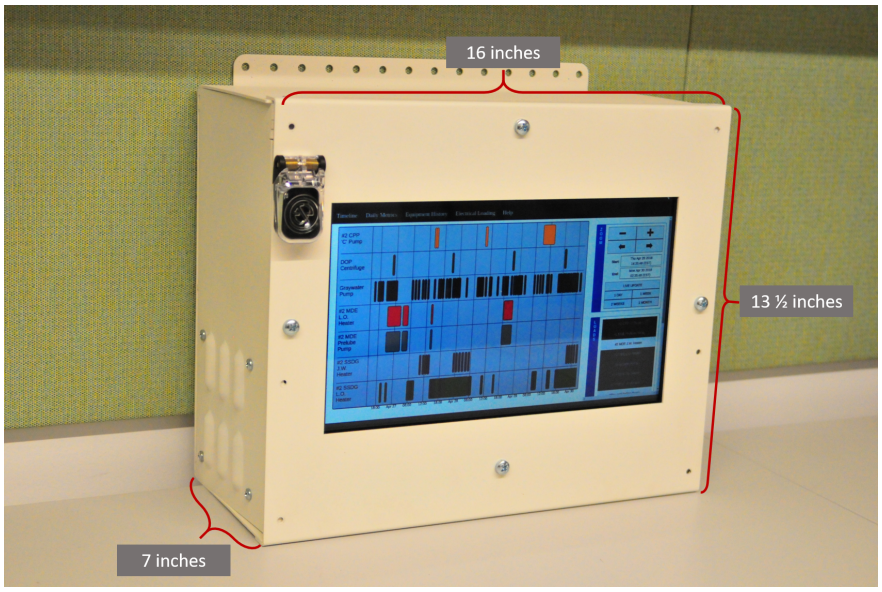

Figure B.1: Example AIO boxes installed on USCGC STURGEON (WPB 87336).

AIO Box 1 Anchor Points: Engine Room Catwalk STBD Railing

The AIO box framing will be anchored at 10 points using "pipe straps" and "hose straps". Pipe straps act as semi-circular railing brackets. Hose straps act as a fully circular railing bracket, and are used to maintain railing grab area and maximize safety. The location of the AIO box placement is shown in Figure B.2. Each pipe strap is fastened with 2 bolts which attach through the framing pieces. Three brackets are to be attached to the bottom railing. Each hose strap is fastened with 1 bolt which attaches through the framing. Three hose

straps are to be attached to the top railing, and two to each vertical railing. Three pieces of vertical framing will connect the top and bottom brackets, and two horizontal piece of framing will attach the side railings. The location and framing design is shown in Figures B.2 and B.3. Each pipe strap will have a thin piece of rubber underneath to reduce damage to the mounting system due to potential vibrations.

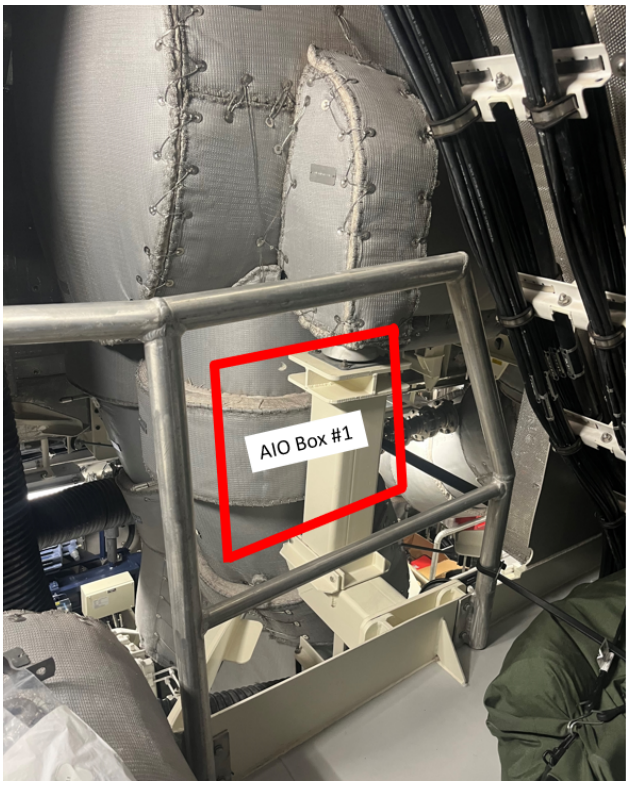

Figure B.2: Location to mount the STBD side AIO Box

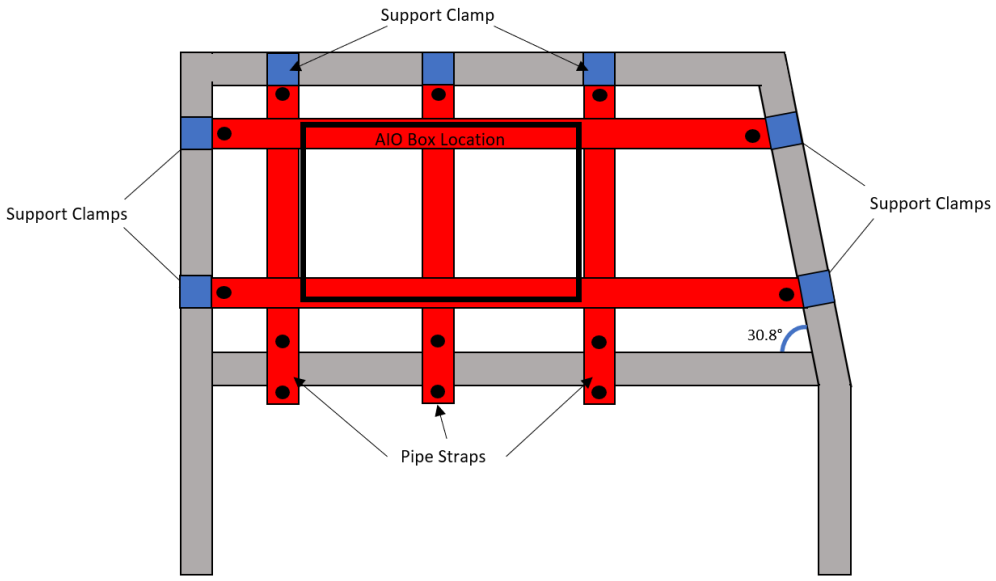

Figure B.3: Bracketry for AIO Box 1 and Box 2

AIO Box 2 Anchor Points: Engine Room Catwalk Port Railing

The AIO box framing will be anchored at 10 points using "pipe straps" and "hose straps". Pipe straps act as semi-circular railing brackets. Hose straps act as a fully circular railing bracket, and are used to maintain railing grab area and maximize safety. The location of the AIO box placement is shown in Figure B.2. Each pipe strap is fastened with 2 bolts which attach through the framing pieces. Three brackets are to be attached to the bottom railing. Each hose strap is fastened with 1 bolt which attaches through the framing. Three hose straps are to be attached to the top railing, and two to each vertical railing. Three pieces of vertical framing will connect the top and bottom brackets, and two horizontal piece of framing will attach the side railings. The location and framing design is shown in Figures B.2 and B.3. Each pipe strap will have a thin piece of rubber underneath to reduce damage to the mounting system due to potential vibrations.

Final Mount

The final mounting positions for the AIO Boxes are shown in Figure B.6. This shows that there is ample space for both boxes in the proposed arrangement. The two AIO boxes will be mounted in "landscape" orientation. That is, the long edge will be on the bottom while the short edge is on the side.

B.1.2 Cable Runs

Cables will come out the side of the mounted AIO Boxes. The 3 Conxall cables and the conduit containing voltage leads for each box will be joined together by zip-ties and run forward to the large vertical "L" stiffener on the outboard bulkhead. There, they can be secured to the holes in the stiffeners using bolts, lock-nuts, and zip-ties. The cables will then

Figure B.4: Location to mount the Port side AIO Box

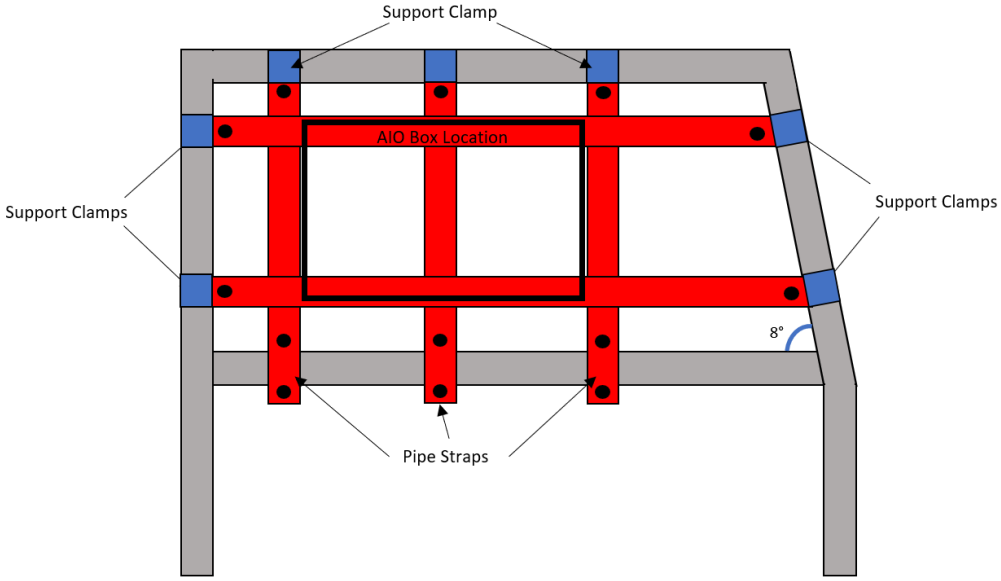

Figure B.5: Bracketry for AIO Box 2

run in the overhead cable runs to their respective panels, once again being secured along the way using zip-ties.

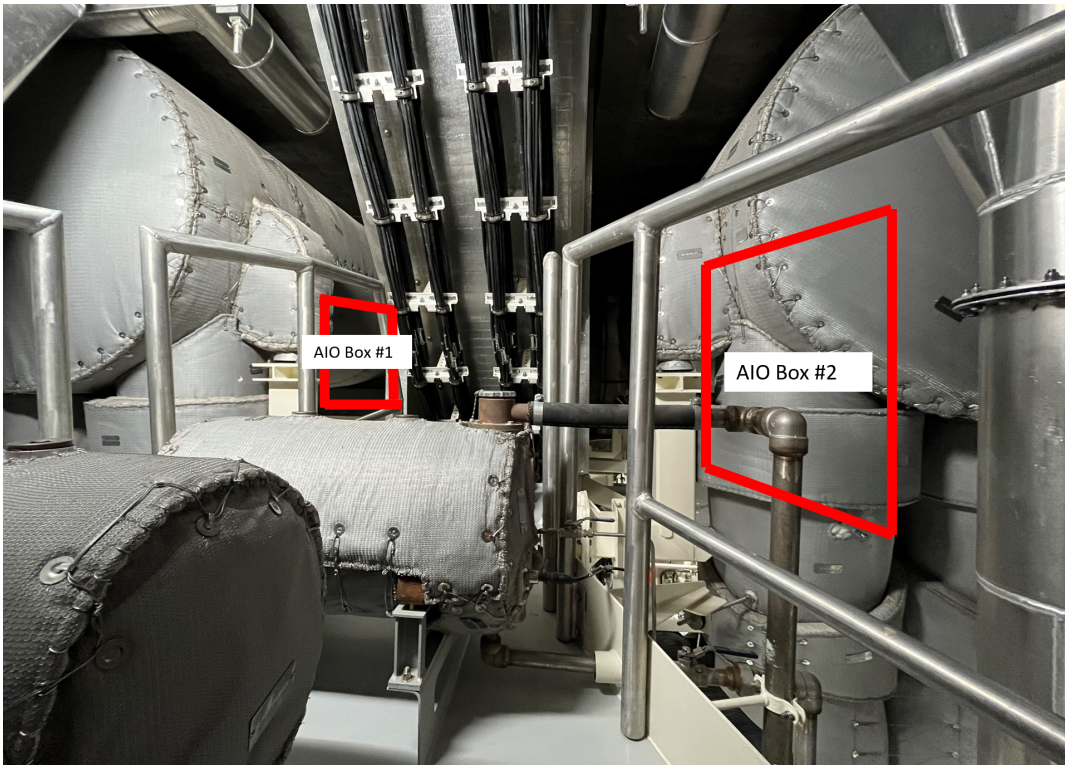

Figure B.6: Scale rendering of final location of AIO Boxes (proposed bracketry not pictured). AIO Boxes will be mounted in "Landscape" orientation.

The IEC Power Cords will run forward to the receptacle similar to the one shown in Figure B.7. Both receptacles will be utilized to provide power to Data Acquisition Unit (DAQ).

All cords will run along existing cableways and fittings that will allow them to be secured with zip-ties. They will not impede movement of personnel or equipment in any area.

B.1.3 Installation on Panel

This section will detail the plan for equipment installation on the electrical panel. This will include installation of the current transducers, their connection to the Conxall cables, and the wiring of the voltage leads to the spare breaker.

B.1.4 Cable Entry into Panel

Cables will enter into the panel via new holes that will be fitted with boot shrinks. **For the new holes to be drilled, assistance from a Ship's Force (SF) Electrician's Mate (EM) is necessary. The SF EM must Tag Out the panel being install on and verify that the power is secured in accordance with (IAW) all electrical tag out and safety procedures. Then, the SF EM may proceed to drill the necessary holes in the panel.** Use of an SF EM in this step is necessary for safety and quality

Figure B.7: Power outlet for IEC Cords.

assurance of work. MIT RLE graduate students are not certified electricians, therefore they should not conduct the work on the electrical panel.

For installation, two groups of cables will enter each panel: the three Conxall cables, and the voltage leads encased in conduit. The proposed method for both groups to enter the panel safely is to drill two 1.25" diameter holes in the top of the power panel. Then, the cables can enter into the panel via bootshrink fittings like those pictured in Figure B.8. These fittings are watertight and meet military specifications (MILSPEC) for running cables into power panels onboard ships and in engineering spaces. Later, following removal of equipment, these fittings will be fit with neoprene plugs IAW ASTM F1836M. The running of cables into the panel and installation of bootshrink fittings will be conducted by the MIT RLE graduate students. Other commonly used fittings include cord grips, which are shown in Figure B.8 as well.

3-27-1 STBD Machinery Panel

Figure B.9 shows the top of power panel 3-27-1. NILM Conxall cables and voltage leads in conduit will enter through two new holes in this section of the panel. As can be seen, many cords enter the panel, and cord grips are used as the watertight fittings.

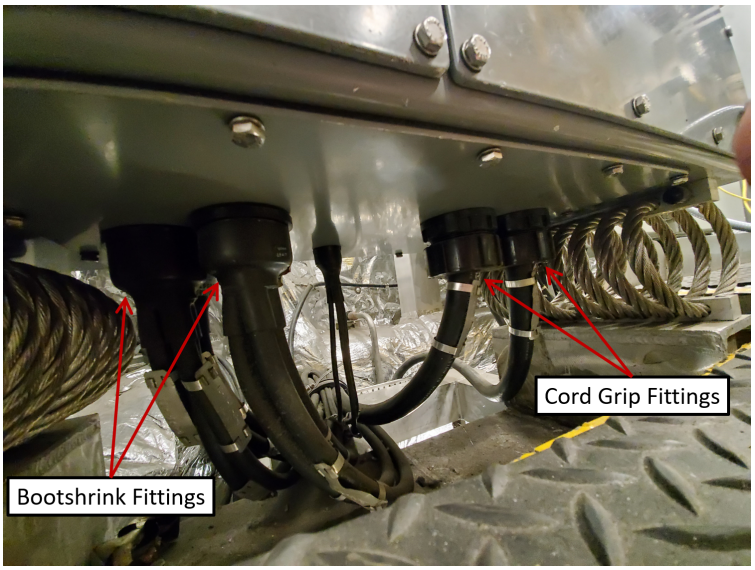

Figure B.8: Example of bootshrink and cord grip fittings feeding into power panel (from US Navy panel).

3-27-2 Port Machinery Panel

Figure B.10 shows the top of power panel 3-27-2. NILM Conxall cables and voltage leads in conduit will enter through two new holes in this section of the panel. As can be seen, many cords enter the panel, and cord grips are used as the watertight fittings.

B.1.5 Inside the Panel

This step will also require the assistance of the SF EM. **To begin, the SF EM will tag out the entire panel to be installed upon IAW the shipboard tag out and electrical safety procedures. The SF EM will then remove the front casing on the power panel, and ensure power is secured using a multi-meter IAW all shipboard electrical safety procedures.**

Current Transducer Installation

Once confirmed that power has been secured to the panel, the SF EM will remove the lugs on the power cables feeding the panel for each phase. This will allow the current transducers to be installed on each power cable by slipping them over the open lugs. Then, the SF EM will reinstall the power cable lugs.

Next, MIT RLE graduate students will secure the current transducers using zip ties and connect the Conxall cables to the current transducers. Figure B.11 shows the end result of the current transducers and Conxall cables inside the electrical panel on USCGC MARLIN (WPB 87304). As is shown, the current transducers and Conxall cables are neatly organized inside the panel and secured with zip ties. Figures 12 and 13 show the interior of the port machinery panel onboard USCGC WILLIAM CHADWICK (WPC 1150).

Figure B.9: Cable entries into the top of STBD Machinery Panel (3-27-1).

Voltage Lead Installation

The next step in the internal panel installation is to wire the voltage leads into the spare breaker. As is shown in Figure B.13, there are adequate spare breakers for installation on both panels. For the starboard panel, the MIT RLE team proposes using the (3-27-1)-4P-P spare breaker shown in the upper left corner of Figure B.14a. For the port panel, the MIT RLE team proposes using the (3-27-2)-4P-M breaker shown in the upper right corner of Figure B.14b.

This step requires assistance from the SF EM once again. The SF EM will need to wire the 3 voltage leads into the designated spare breaker. Each lead will wire into one power phase on the breaker. Additionally, there is a ground lead that will need to lead to an appropriate ground location as determined by the SF EM. In previous installs ground bolts inside the panels have been used. Figure B.15 shows a complete voltage lead install on a spare breaker from USCGC MARLIN (WPB 87304) and will appear nearly identically onboard USCGC WILLIAM CHADWICK.

Once the voltage leads are connected to the spare breaker, the current transducers are installed on the power cables, the Conxall cables are connected to the current transducers, the cables and wires from the NILM installation are neatly organized within the panel with zip ties, and bootshrink fittings are secured, the SF EM will close the panel and reenergize it IAW all electrical safety and tag out procedures.

B.1.6 Equipment Testing

Following all setup steps on the panels, the MIT RLE team will work to ensure the equipment is working correctly. This will include energizing all MIT equipment, as well as the downstream loads, to ensure proper operation of NILM sensors. In the event of poor or inept readings, the panels will need to be tagged out once again and hardware be adjusted

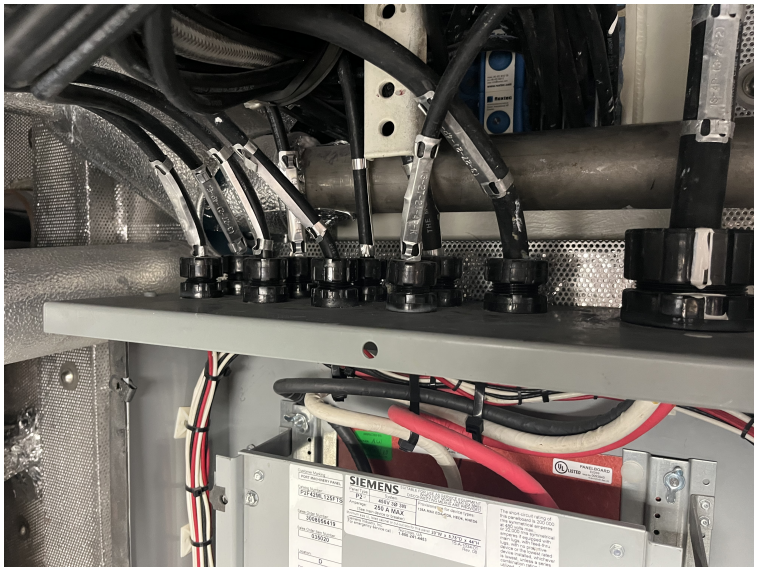

Figure B.10: Cable entries into the top of power panel 2DS-4P.

to ensure proper data capture.

Once data is capturing correctly, the MIT RLE would like to energize all downstream loads if possible. This will provide the MIT RLE team with "test data" for each piece of equipment, allowing for it to be classified individually for processing and further understanding. Acquiring this data early allows for NILM Dashboard software to be customized to work for the 154' Patrol Cutter as quickly as possible.

B.1.7 Equipment Removal

B.1.8 Electrical

This step will also require the assistance of the SF EM. To begin, the SF EM will tag out the entire panel which the NILM is being removed from IAW the shipboard tag out and electrical safety procedures. The SF EM will then remove the front casing on the power panel, and ensure power is secured using a multi-meter IAW all shipboard electrical safety procedures.

Current Transducer Removal

The first step in removing the NILM is securing power to the panels. Once confirmed that power has been secured to the panel, the SF EM will remove the lugs on the powercables feeding the panel for each phase. This will allow the current transducers to be removed from each powercable by slipping them over the open lugs. Then, the SF EM will reinstall the power cable lugs. MIT RLE Grad Students will take custody of the current transducers and remove conxall leads, zipties and any other equipment from inside the power panel. Next the SF EM will inspect the inside of the power panel to ensure it is clear of debris.

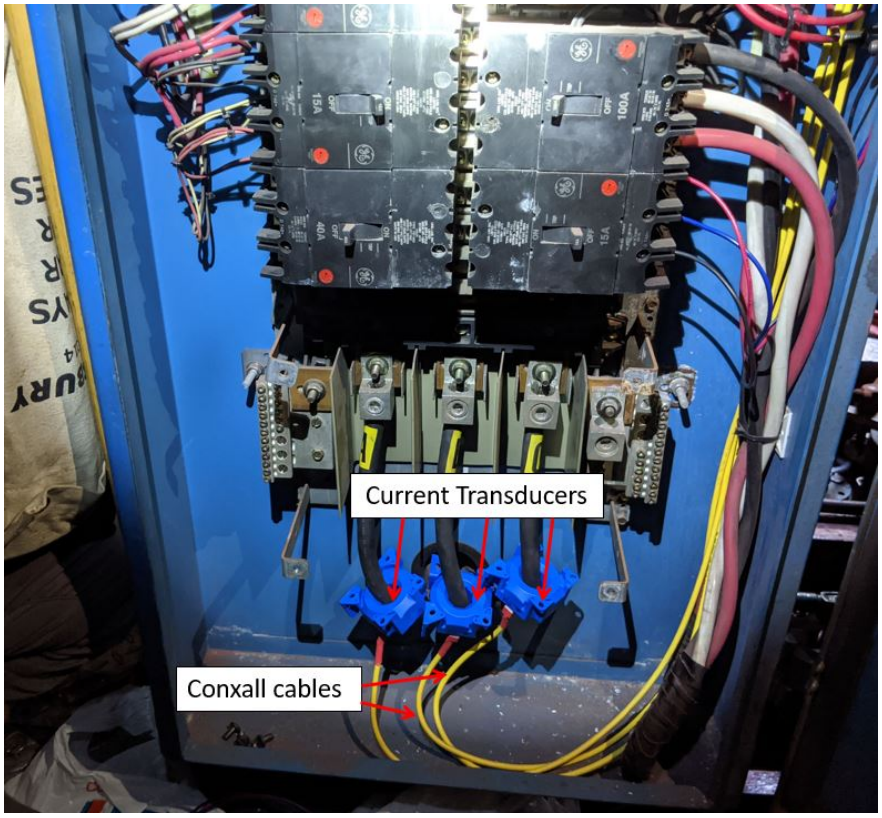

Figure B.11: Current transducers and Conxall cables installed on power cables feeding an electrical panel on USCGC MARLIN (WPB 87304).

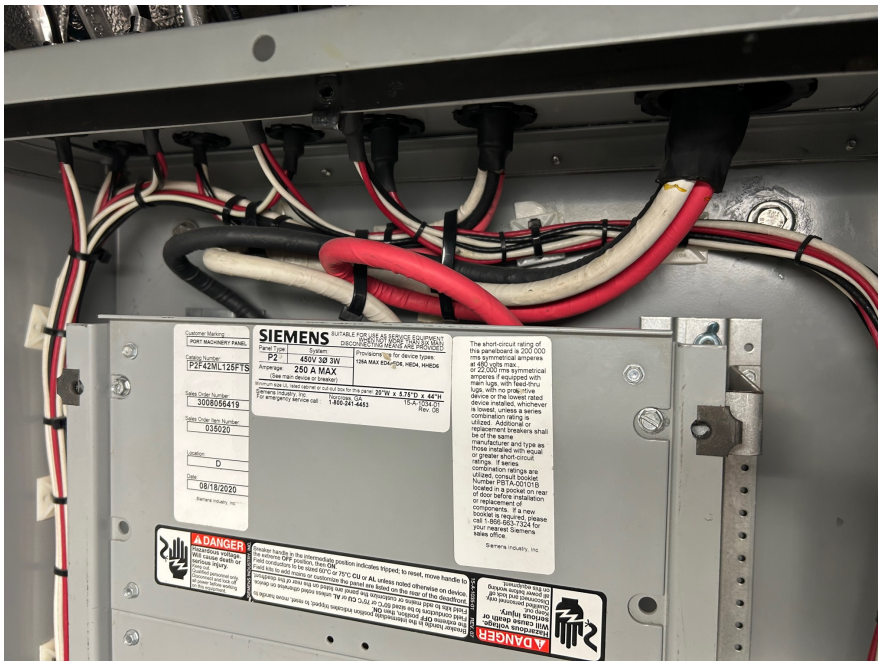

Figure B.12: USCGC WILLIAM CHADWICK (WPC 11050) Power Panel Interior

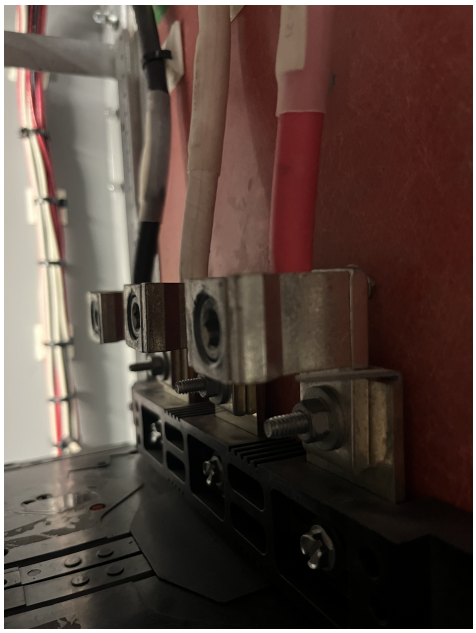

Figure B.13: USCGC WILLIAM CHADWICK (WPC 11050) Power Panel Interior

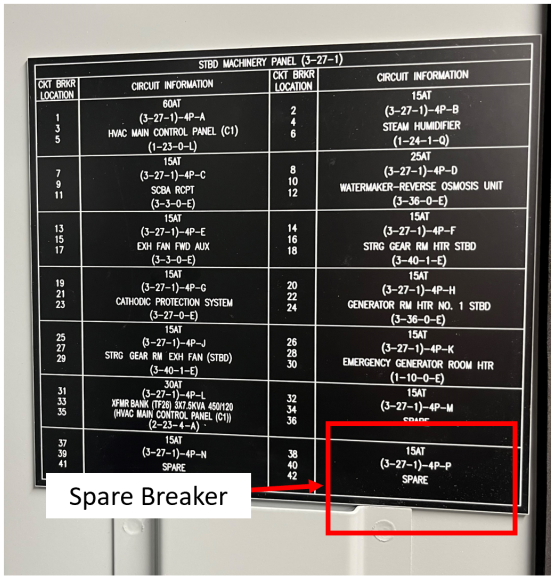

(a) STBD Machinery Panel (3-27-1)

(b) Port Machinery Panel (3-27-2)

Figure B.14: USCGC WILLIAM CHADWICK (WPC 11050) Power Panels

Voltage Lead Removal

The second step of the electrical uninstall is the removal of the voltage leads. This step requires assistance from the SF EM once again. The SF EM will need to unwire the 3 voltage leads from the designated spare breaker. Additionally the ground wire will need to be unwired. Once all voltage leads, current conxall cables, current transducers and zip ties are removed both MIT RLE Grad Students and SF EM will inspect the panel ensuring

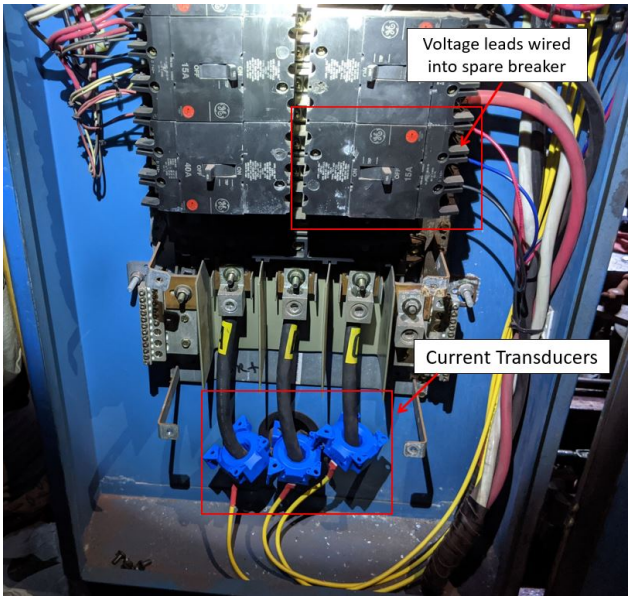

Figure B.15: Interior panel view for reference on USCGC MARLIN (WPB 87304) showing voltage leads wired into a spare breaker as well as current transducers installed on power feed cables.

equipment is removed and the panel is in good working order. Upon concurrence that the panel is restored to the original condition the SF EM will close the panel and reenergize it IAW all electrical safety and tag out procedures.

Cable Holes

The bootshrink fitted holes into the panels will be sealed with bootshrink caps. This provides adequate watertightness and prevents intrusion into the energized panel. MIT RLE students will provide the caps and install caps under SF supervision.

B.1.9 Hardware

Because the mechanical portion of the supporting bracketry is temporary there will be no permanent alterations to the physical structure of the vessel. MIT RLE students will remove all associated bolts, nuts, brackets and hardware mounting under the supervision of SF. All cable runs will be removed and NILM hardware and cabling will be removed by MIT RLE students after the electrical portion of the system has been removed.

B.1.10 Conclusion

This document summarizes the steps necessary for the MIT RLE NILM installation onboard USCGC WILLIAM CHADWICK (WPC 1150). Further information regarding the nature of this project can be found by contacting the US Coast Guard graduate students at MIT (listed below). The details of the project proposal can be found in the Research Proposal.

Further details regarding MIT and the Coast Guard's roles with regard to this situation can be found in the Memorandum of Agreement between MIT-RLE and SFLC-ESD.

B.2 MIT NILM Research Proposal for WILLIAM CHADWICK

The purpose of this proposal is to provide detailed information regarding the request for authorization for the Massachusetts Institute of Technology's (MIT) Research Laboratory of Electronics (RLE) to conduct research onboard United States Coast Guard Cutter (USCGC) WILLIAM CHADWICK (WPC 1150). This proposal comes from the above US Coast Guard Officers in the Electromechanical Systems Group (ESG) under the supervision of Professor Steven Leeb in the MIT Research Laboratory for Electronics (RLE).

Since 2004, a strong relationship has existed between United States Coast Guard (USCG) officers pursuing DCMS sponsored graduate level education and USCG assets located in the Boston area including USCGC ESCANABA (WMEC 907), USCGC SENECA (WMEC 906), USCGC SPENCER (WMEC 905), USCGC THUNDER BAY (WTGB 108), USCGC MARLIN (WPB 87304), and USCGC STURGEON (WPB 87336) . Students have researched vibration and electrical monitoring to improve fault detection, determine machinery health, extrapolate human activity, and provide energy scorekeeping to improve automation and machinery-monitoring technology. These research opportunities allow active duty officers to remain engaged with the fleet while pursuing higher education, simultaneously posing an opportunity for the USCG to remain at the forefront of maritime automation and monitoring research.

B.2.1 Research Focus

Current research is focused on Non-Intrusive Load Monitoring. A Non-Intrusive Load Monitor (NILM) takes electrical power readings from a centralized monitoring point, making it a low-cost, durable, and sustainable method of equipment monitoring. Applications of these readings include energy savings, load factor management, platform energy use optimization, activity monitoring, log generation, and machinery health monitoring. The NILM systems are low-cost and easier to install compared to equivalent systems comprised of individual sensors on each piece of equipment.

MIT RLE requests authorization to install two NILM boxes onboard USCGC WILLIAM CHADWICK (WPC 1150) in accordance with the Memorandum of Agreement between MIT-RLE and USCG Surface Forces Logistics Center (SFLC) Engineering Services Division (ESD). Details of the proposed installations will be provided in this document. Installation specifics will be outlined in a separate Installation Plan.

The proposed installation will last for one year, beginning on the installation date. At the end of that year, the MIT RLE will communicate with SFLC ESD to determine if the project will continue or not.

B.2.2 Background

Power system microgrids serve mission critical systems for naval platforms. System component degradation can often be observed as changes in demand on the power system. As

the performance of a critical component in a system degrades, automatic controllers often compensate to maintain commanded output levels. By design, feedback control works to mask the effect of "soft faults," variations and vagaries in internal component performance in a larger system that do not fully stop the system. Low refrigerant charge, slipping belts, fouled fans, vacuum leaks, and degraded hydraulic fluid are all examples of mechanical insults to a system with insidious effect: the system will continue to operate and provide apparently acceptable service and performance while an automatic controller forces more energy consumption and induced wear. Soft faults may elude even vigilant watchstanders. These situations can persist for expensively long periods before a "hard fault" finally stops the system, alerting operators but also creating a "casualty" that may cripple mission readiness.

The vast implementation of automatic controllers often masks soft faults by automatically altering run times and drawing excess power to maintain system operability. Enhanced vigilance in watchstanding can lead to soft fault detection, but it is at the expense of the watchstander. Further, such enhanced inspection leads to increased monitoring efforts and a greater watchstanding demand, as well as a dependence on a multitude of sensors which could introduce additional fault points in an already complex system. While this introduction of new sensors to a system can provide a more detailed view of individual component operation, it does not simplify system operation or watchstanding practices. Instead, it commonly adds to the burden of system maintenance by producing a raft of raw data that is often not presented in a useful way. The ability to parse useful data and present it in an easily-extractable manner is necessary to successfully identify soft faults and allow operators to address them prior to system failure.

B.2.3 NILM Technology

Non-intrusive electrical power monitoring has been applied for condition-based maintenance, energy scorekeeping, and activity tracking in marine environments for several decades. The nonintrusive load monitor can determine the operating schedule of individual loads and components by observing electrical transients in an aggregate electrical power stream. Figure B.16 illustrates a NILM installation at the feeder to an electrical panel that serves a collection of loads. Strictly from measurements made at this aggregate point, a NILM determines the operating schedule of the downstream loads through association of observed waveforms with specific loads. This technology can then develop a physics-based load model and determine the health of the loads. Then, by effectively detecting transient events, a NILM can automatically log operation of system components, producing a computer-generated log that rivals or exceeds human-made logs for accuracy and vastly reduces watchstander effort in documenting equipment operation. A NILM's ability to record the operation time and power consumption for individual loads creates a convenient, one-stop access point for energy scorekeeping.

Within a NILM, sensors record current and voltage from the electrical panel and analyze waveforms to compute real power, reactive power, apparent power, and higher harmonic content. This information directly corresponds to the physics that governs load behavior, producing distinct signatures in power data, to which the NILM is "trained" to recognize. Such load transients can be identified by developing fingerprint exemplars in the laboratory through testing of example loads, from previous shipboard equipment observation, or from

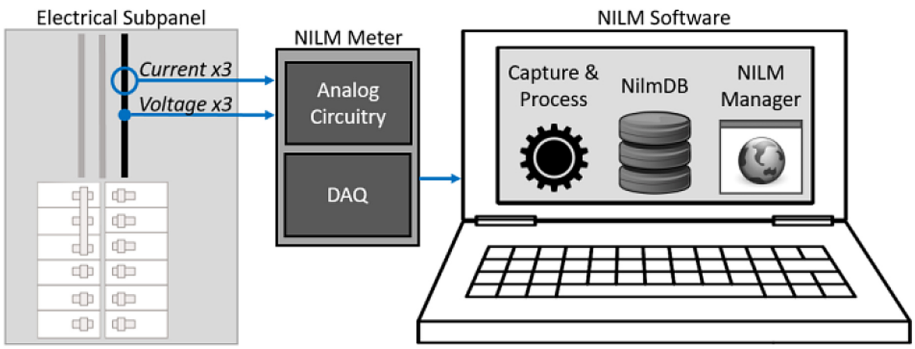

Figure B.16: Schematic overview of a typical installation of a NILM at the feeder to a power panel on a ship. The NILM Meter provides sensing for waveform measurement. The NILM Software runs on a Linux-based personal computer, laptop, or similar platform.

on-site observations of loads during a training period following installation. The monitor can also observe load behavior for a period of time and classify the loads using guided machine learning and clustering to produce a data set that is likely most useful after a facilities operator has reviewed and corrected the automatic load identifications as needed.

B.2.4 Past NILM Installations

Various configurations of nonintrusive monitoring equipment have been installed onboard USS Michael Murphy (DDG-112), USS Independence (LCS-2), USS Champion (MCM-4), the USNA YP (Yard Patrol) Fleet, USS Indianapolis (LCS-17), USCGC THUNDER BAY (WTGB 108), USCGC MARLIN (WPB-87304), USCGC STURGEON (WPB-87336), and the Famous-class US Coast Guard Cutters in Boston. The longest installations have provided observations from the three Famous-class Medium Endurance Cutters (MECs) SENECA, ESCANABA and SPENCER for over 10 years with various hardware setups. These 270 ft. (82 m) length overall vessels have a 440 V electrical power distribution system run by diesel power generation and distribution equipment required to support missions and sustain operations at sea.

On SPENCER, a readout for the crew displayed the NILM Dashboard. Figure B.17 shows front and side views of a touch screen installed that displayed graphical results from NILM Dashboard. The front view on the left shows the NILM Dashboard displaying a timeline of operation for three different service loads in the main engineering space, extracted from the power monitoring of the electrical panel feeding these loads. The side view on the right shows the screen displaying "meter"-style displays with green (normal), yellow (worrisome), and red (poor) operating zones for the different statistics concerning the monitored load of interest. This display allows the crew to quickly select and interpret visual indicators that draw awareness to unusual or unacceptable operating parameters, including too frequent or infrequent operation, excessive power demand, excessive or inadequate duration of operation, and other unacceptable operating states. With such a tool available to the crew, watchstanders have the ability to identify soft faults in their engineering systems prior to their failure as highlighted by the NILM.

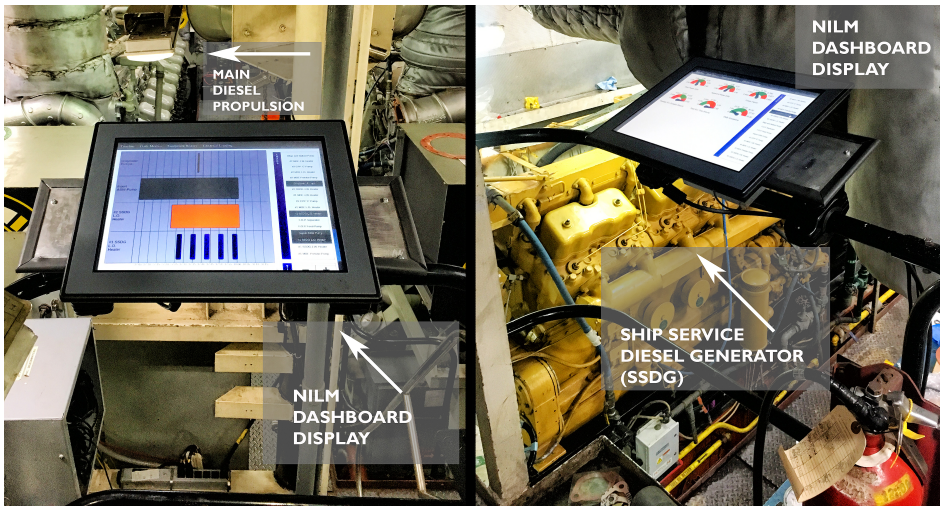

Figure B.17: The NILM Dashboard display on USCGC SPENCER (WMEC 905).

B.3 Installation Requirements

This section will denote the details regarding the proposed NILM installation for USCGC STURGEON (WPB 87336). It will begin outlining the equipment required for the installation, then detail the proposed locations for installation onboard the WPB. Each proposed NILM installation will include the following components:

- All-in-One (AIO) NILM Box (1)
- Current transducers (3, one per phase)
- Conxall cables (3, one per phase)
- Voltage leads (encased in single conduit)
- IEC power cord (1)
- Mechanical mounting hardware

B.3.1 All-in-One (AIO) NILM Box

The All-in-One (AIO) NILM Box combines several aspects of NILM technology into a single, robust, easily-installed box designed for shipboard installation. This configuration minimizes space requirements by combining the sensor hardware, computer, and backup power supply necessary to collect data and display it in a useful manner into a single enclosure that is reasonably-sized with respect to the limited space within shipboard engineering spaces. Figure B.18 shows an example of an AIO NILM Box install. As shown, this single box includes a touch-screen computer display on the outside, while also encasing the majority of the NILM sensor hardware. Figure B.18 also showcases much of the additional hardware required for installation, including the IEC power cord, voltage leads encased in conduit, and Conxall cables. The box dimensions are 16 in x 7 in x 13.5 in.

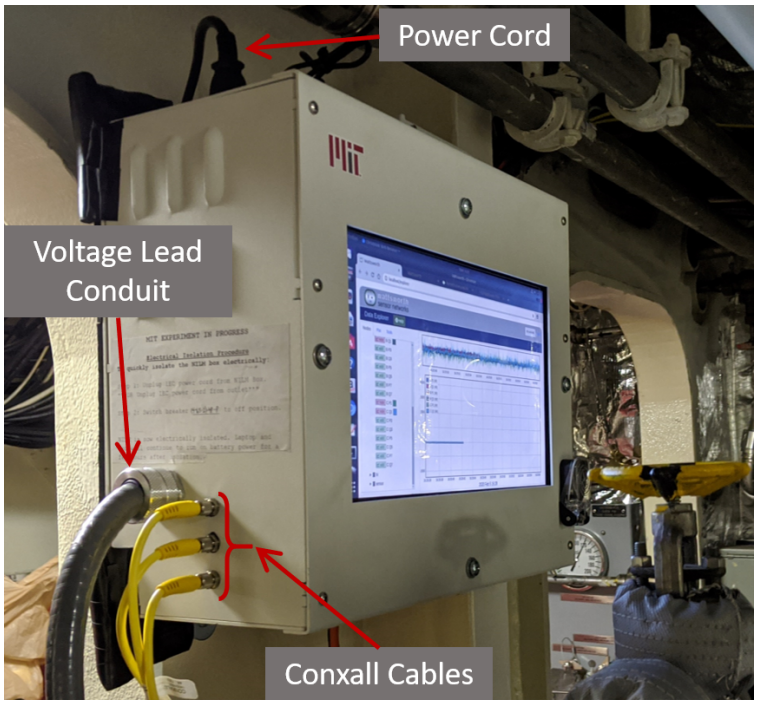

Figure B.18: AIO NILM Box install.

B.3.2 Other Installation Hardware

The current transducers, shown in Figures B.19a and B.19b (blue), are installed onto each phase of the power cables feeding the panel. These sensors connect to the yellow Conxall cables, (also depicted in Figure B.19a), which then feed current readings to the All-in-One Box as shown in Figure B.18. Figure B.19b also shows the voltage lead installation onto the spare breaker within the power panel. Once these wires exit the power panel, they are encased in conduit that runs to the AIO box, which is shown in Figure B.18. The final piece of hardware to install is a IEC Power Cord that connects the AIO Box to a 120V power supply. This IEC cord will plug into the nearest power outlet and run through neighboring cable runs to provide power to the AIO Box. All mounting hardware is specific to each ship and each install, and will be addressed in greater detail in the Installation Plan.

B.4 Proposed Installation & Mounting

The MIT NILM team proposes that NILM devices be installed on the starboard and port machinery power panels. Each device will include all the items listed previously (AIO Box, current transducers, Conxall cables, etc.). Each AIO box would monitor one of the designated panels. Figure B.20 shows a modified schematic of the electrical generation and distribution plant onboard USCGC WILLIAM CHADWICK (WPC 1150), highlighting the power panels that will be monitored using NILM sensors.

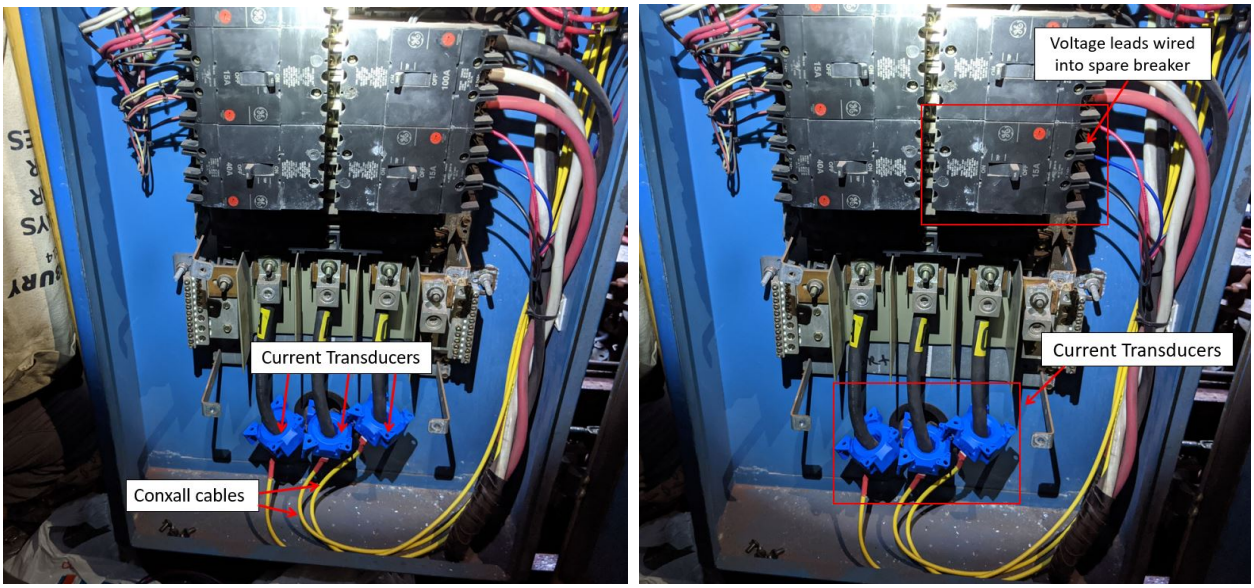

(a) Close-up view of installed current transducers (blue). Conxall cables connect to each current transducer.

(b) Open power panel with NILM hardware installed. Current transducers are shown at the bottom installed on the 3-Phase power cables leading into the panel. Voltage leads are shown wired into a spare breaker on the panel (red, white, & blue wires leading into breaker.)

Figure B.19: Current and voltage sensor installation on USCGC MARLIN (WPB 87304).

B.4.1 Hardware Mounting Location

The proposed installation locations for the boxes can be found in Figures B.21. The AIO boxes for panels 3-27-1 and 3-27-2 will be mounted on the center catwalk located above and in between the two MDEs. The NILM boxes will be attached to the railings using additional framing and this location provides ample space for the AIO boxes to be mounted on temporary brackets, to be installed by the MIT-RLE team. Further, because of the close proximity to the Power Panels, the length required for the Conxall Cables and Voltage Leads will be minimized.

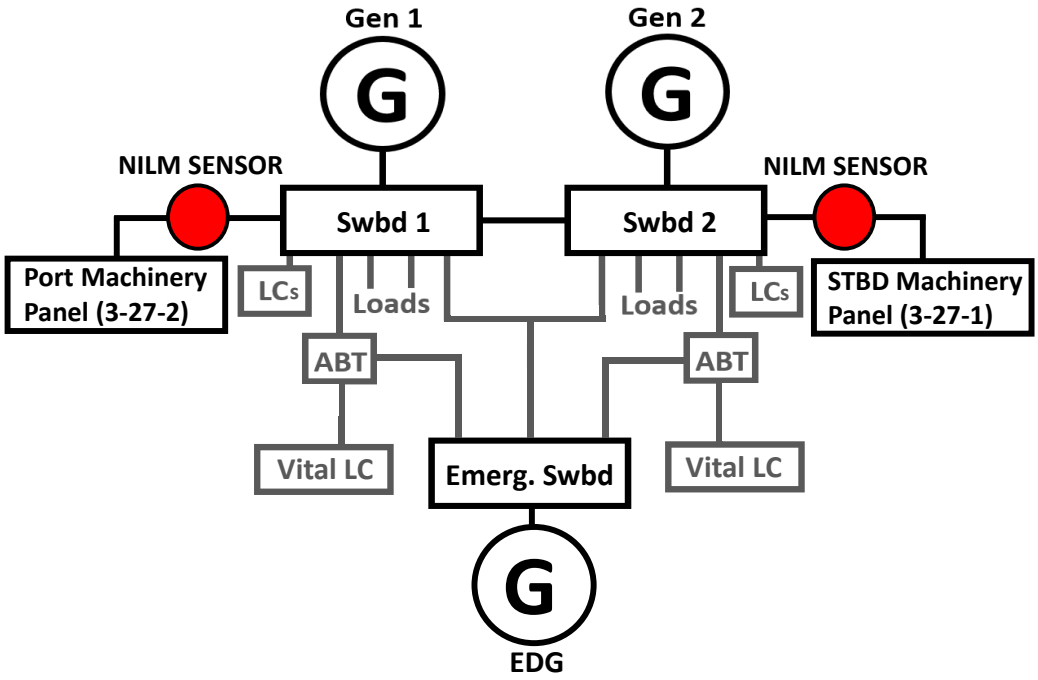

Figure B.20: USCGC WILLIAM CHADWICK (WPB 1150) electrical diagram with NILM sensor installation points identified (red circles).

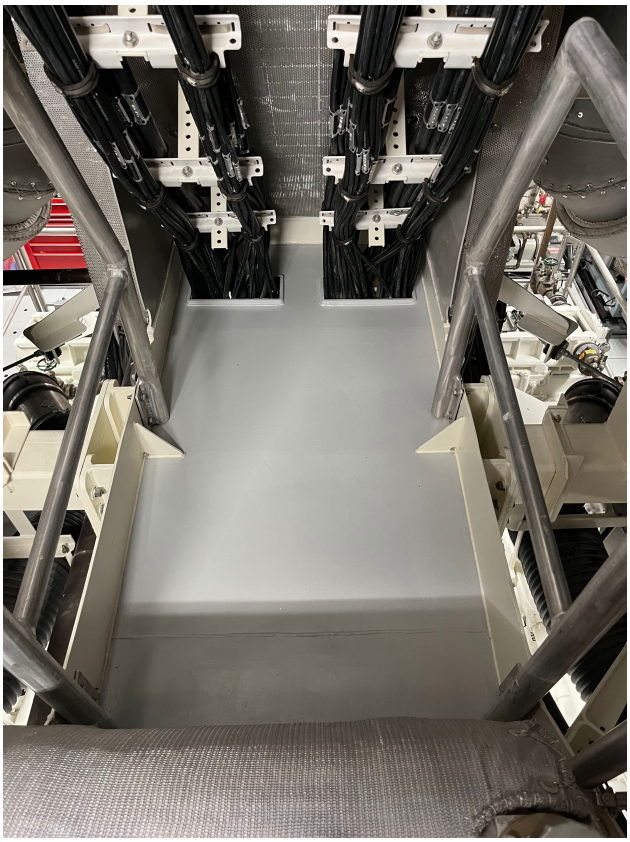

Figure B.21: Proposed installation location of USCGC WILLIAM CHADWICK AIO boxes

Appendix C

Custom Reference Electrode Documentation

C.1 Electrode Construction

These instructions describe how to make the screw-type electrodes used in the experiment on *USCGC Margaret Norvell* (WPC 1105) on March 14, 2023. They can be made in any machine shop equipped with a lathe, drill press, and other miscellaneous tools. The stick-type electrodes have no strict requirements for form factor and can be made in any convenient way, but they follow the same procedure for the formation of the silver chloride coating.

Order the following materials or suitable equivalents:

- $\frac{3}{8}$-16 threaded rod, 3" long, polyoxymethylene (McMaster p.n. 93665A634)
- $\frac{3}{8}$-inch round stock, polyoxymethylene (McMaster p.n. 8572K53)
- 1-inch round stock, polyoxymethylene (McMaster p.n. 8572K61)
- 99.9% (or higher purity) silver bezel strip, 0.06 inches wide, 0.005 inches thick (Amazon link[1])
- Silver bearing solder (Kester 1670500062 or equivalent)
- Weatherproof barrel jack connector (DCCONN-AB from JacobsParts[2])
- 3M DP110 epoxy (McMaster p.n. 7467A22)

Follow these steps to assemble the electrode. See Figure C.1 for an idea of how the different parts interact with each other.

1. Cut the threaded rod to $3\frac{7}{16}$ inches long and chuck it in the lathe. Use a no. 4 drill bit to bore a hole through the length of the rod. This is the *threaded section*.

[1] https://www.amazon.com/gp/product/B005G05UG8/ref=ppx_yo_dt_b_search_asin_title?ie=UTF8&psc=1

[2] https://www.jacobsparts.com/items/DCCONN-AB

2. Now chuck the 1-inch polyoxymethylene rod in the lathe. Face off the end of the rod, then drill an axial hole with a $\frac{5}{16}$-inch drill bit at least two inches deep.

3. Taper the end of the rod to match the countersink profile of the screw hole on the stern tube inspection cover, i.e. 41° as measured from perpendicular.

4. Cut off the part $\frac{3}{4}$-inch from where the taper ends on the outside of the cylinder. This is the *screw head*.

5. Use a $\frac{3}{8}$-16 tap to thread the inside of the screw head.

6. Insert the threaded section into the screw head *from the tapered side* until the end of the end of the threaded section is flush with the flat side of the screw head.

7. Drill a $\frac{3}{8}$-inch hole through the side of the screw head, perpendicular to the long axis of the assembly. The center of the hole should be in the middle between the flat side of the screw head and the start of the taper.

8. Cut a 3-inch long section of the $\frac{3}{8}$-inch dowel rod. This is the *cross bar*. Tap it through the hole in the side of the screw head until its center aligns with the middle of the assembly. The axial hole through the assembly should now be blocked by the cross bar.

9. Use the no. 4 drill bit to drill back through the axial hole in the screw assembly through the cross bar. The axial hole should now be continuous again.

10. Drill a $\frac{1}{8}$-inch hole in the screw head perpendicular to the long axis of the assembly and the cross bar up to the center of the assembly. Drill another hole in the threaded section about $\frac{3}{4}$-inch from the end of the taper all the way through the threaded section.

11. Cut a 2-inch section of the silver strip. Use silver bearing solder to attach both wires from the weatherproof barrel jack connector to the end of the silver strip. Sand the surface of the strip lightly with fine-grit sandpaper to remove oxidation, then degrease it with acetone or another suitable degreaser. From here on, do not let any oil come into contact with the silver.

12. Insert the silver strip into the screw assembly *from the head side* so that the insulation from the cable on the barrel jack connector tucks into the end of the axial hole. If it does not fit, enlarge the hole slightly to a depth of about $\frac{1}{4}$-inch and try again. Ensure the silver strip reaches to about $\frac{1}{4}$-inch from the end of the threaded section. If it does not, remove some of the outer insulation on the barrel jack connector's cable and fit it again.

13. Inject two-part epoxy through the hole in the side of the screw head until it reaches but does not block the crosswise hole in the threaded section. Let it fully cure.

14. Rinse the electrode assembly once more with alcohol, acetone, or another suitable degreaser to remove organic contamination. It is now ready for silver chloride formation.

C.2 Silver Chloride Formation Process

Conversion of silver to silver chloride was achieved by two methods: immersion in ferric chloride (hydrated iron(III) chloride) or electrochemical oxidation of silver in a chloride solution. Either approach will achieve a similar result, but the electrochemical process is substantially faster.

C.2.1 Ferric Chloride Immersion

Place the electrode in MG Chemicals 415 Ferric Chloride or equivalent solution, ensuring that there are no bubbles inside the electrode and that the solution contacts all exposed silver surface area. Cover the solution with parafilm to prevent evaporation. Either leave the immersed electrode in a dark space or cover the container in aluminum foil; silver chloride is light-sensitive, and prolonged exposure may cause it to deteriorate. Leave the electrode immersed for 24-48 hours, then rinse it with water, dry it, and store it in a dark environment. Staining of plastics and epoxies to a rusty color is expected with the use of ferric chloride, but will not affect function.

C.2.2 Electrochemical Silver Chloride Formation

After assembly, place the electrode in 0.1 M nitric acid (HNO_3) for 10 seconds, then rinse with deionized water. The nitric acid wash removes remaining surface contaminants or oxides. Place the electrode in 0.1 M hydrochloric acid (HCl) and connect to an appropriate current source. Ensure that there are no bubbles inside the electrode and that the solution contacts all exposed silver surface.

The current source may be constructed from a simple op-amp. It is also possible to use a voltage source, high-value resistor, and current meter (with supervision) since the current does not require tight control. The silver must be connected as the anode, so current will flow into the electrode through the wire, and then into the electrolyte.

A counter electrode will be necessary, and should be resistant to hydrochloric acid. Here, a platinum-coated titanium electrode was used. The counter electrode must be connected to the current source as the cathode.

Drive the current source to achieve 0.4-1 mA/cm^2 current density for the exposed silver surface. Run the current source for at least 10 minutes, or 30 minutes for best results and longer electrode lifespan. Light exposure during this process will affect the color of the final coating, but the reaction does not need to be shielded from light.

Disconnect the electrode and rinse it with deionized water, dry it, and store it in a dark place. The electroplating process only requires a chloride environment, so saltwater may be used in place of hydrochloric acid. However, additional ions present in saltwater may cause contamination of the AgCl, so this is not preferred. The nitric acid wash is also not strictly necessary, but will give better results.

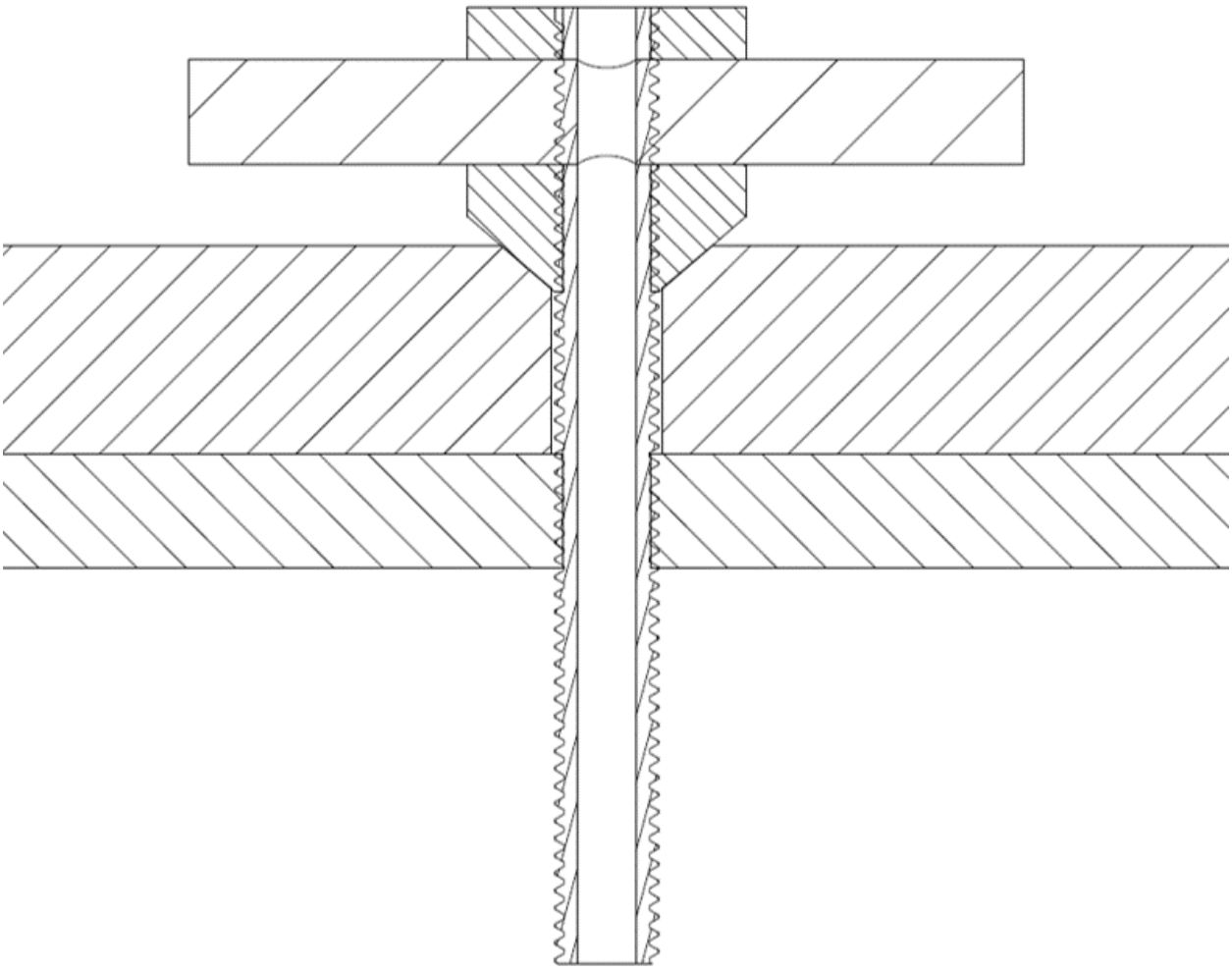

Figure C.1: Section view of a screw-type electrode inserted in the stern tube. Silver strip and cable not shown.

C.3 Magnetic Electrode Holder

This holder is designed to temporarily attach a reference electrode to the steel hull using a magnet. It can hold both the stick-type and screw-type electrodes and should be made of polyoxymethylene or another inert material. Once the top and bottom sections are made, set the magnet inside the bottom section and screw it to the top section with the countersunk screws. A screw can then be inserted in the hole on top to clamp down on the electrode (only the bottom half of the hole is tapped - the top is a clearance fit to accommodate the clamping action).

Buy the following parts to make the holder:

- $1\frac{1}{4}$"x1" polyoxymethylene bar stock (McMaster p.n. 8739K56)
- $\frac{1}{4}$-20 nylon screw, $\frac{3}{4}$-inch long (McMaster p.n. 94735A765)
- $\frac{1}{4}$-20 nylon screw, countersunk, $\frac{1}{2}$-inch long (McMaster p.n. 92929A219)
- Neodymium magnet, 1"x2"x$\frac{1}{8}$" (Internet link[3])

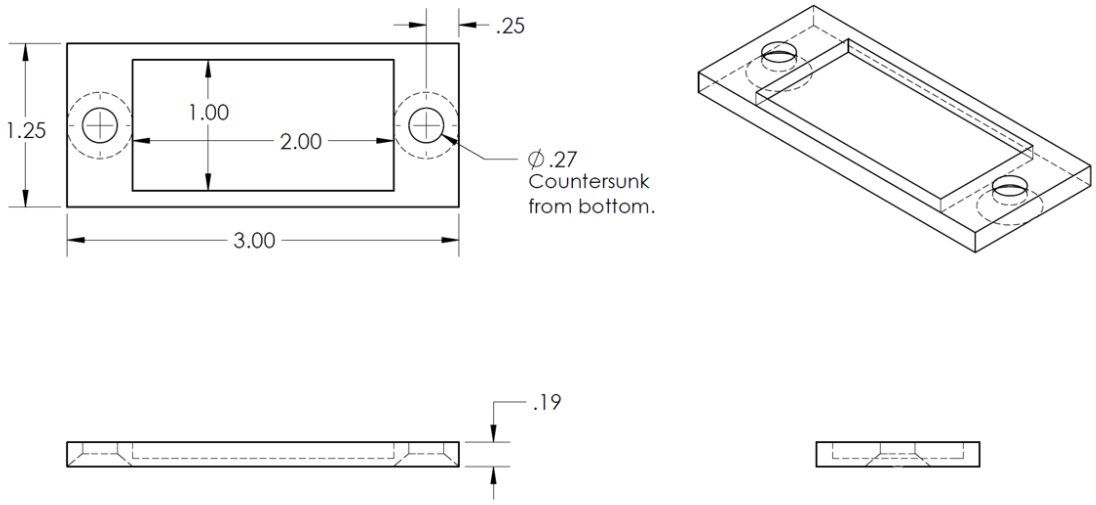

Figure C.2: Bottom section of the magnetic electrode holder.

[3]https://totalelement.com/products/2-x-1-x-1-8-inch-large-neodymium-rare-earth-block-magnets-n42-5-pack?variant=43139300982962

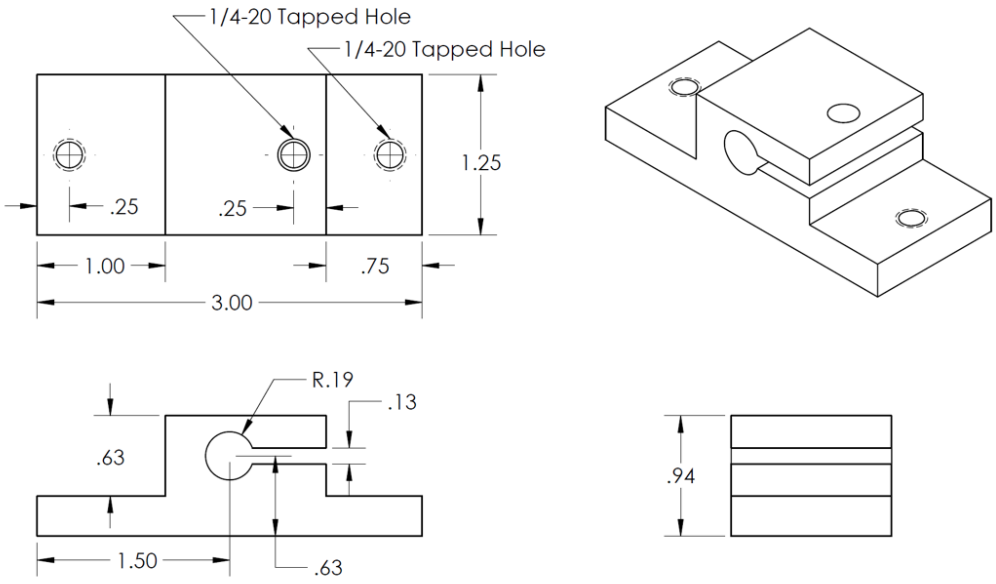

Figure C.3: Top section of the magnetic electrode holder.

References

[1] R. Randall, *Vibration-Based Condition Monitoring*, 2nd ed. Hoboken, NJ: Wiley, 2021.

[2] K. Barrion, "The elephant in the engine room," *U.S. Naval Institute Proceedings Magazine*, vol. 149, no. 8, pp. 18–21, Aug. 2023.

[3] G. Hart, "Nonintrusive appliance load monitoring," *Proceedings of the IEEE*, vol. 80, no. 12, pp. 1870–1891, Dec. 1992.

[4] J. Nation, "Nonintrusive monitoring for shipboard fault detection," *IEEE Sensors Applications Symposium*, pp. 1–5, 2017.

[5] A. W. Moeller, "Extracting electromechanical signals for icebreaker insights," SM thesis, Massachusetts Institute of Technology, Cambridge, MA, 2022.

[6] J. S. Donnal, "Wattsworth: An open-source platform for decentralized sensor networks," *IEEE Internet of Things Journal*, vol. 7, no. 1, Jan. 2020.

[7] D. G. et al., "Nilm dashboard: Actionable feedback for condition-based maintenance," *IEEE Instrumentation and Measurement Magazine*, vol. 23, no. 5, pp. 3–10, Aug. 2019.

[8] D. Chandler, "Energy monitor can find electrical failures before they happen," *MIT News Office*, 2019.

[9] Z. Ahmad, *Principles of Corrosion Engineering and Corrosion Control*, 1st ed. Burlington, MA: Elsevier, 2006.

[10] A. Peabody, *Peabody's Control of Pipeline Corrosion*, 3rd ed. Houston, TX: NACE International, 2018.

[11] V. G. DeGiorgi, "Evaluation of perfect paint assumptions in modeling of cathodic protection systems," *Engineering Analysis with Boundary Elements*, vol. 26, no. 5, pp. 435–445, May 2002.

[12] E. V. W. et al., "Determination of adhesion loss of marine epoxy coatings by impedance measurement," in *Progress in the Understanding and Prevention of Corrosion*, J. Costa and A. Mercer, Eds., vol. 2, London, UK: The Institute of Materials, 1993, pp. 1–51. DOI: 10.1016/S0065-2156(08)70370-3.

[13] J. Pearson, "Electrical examination of coatings on buried pipelines," *The Petroleum Engineer*, Jun. 1941.

[14] P. R. Roberge, *Handbook of Corrosion Engineering*, 3rd ed. New York, NY: McGraw Hill, 2019.

[15] R. Singh, *Corrosion Control for Offshore Structures: Cathodic Protection and High-Efficiency Coating*, 1st ed. Waltham, MA: Elsevier, 2014.

[16] V. Cox, "Boat anodes: A practical guide for sailors," *Practical Boat Owner*, 2024. URL: https://www.pbo.co.uk/expert-advice/boat-anodes-a-practical-guide-for-sailors-85933.

[17] C. Biesecker, "Doj sues bollanger over failed coast guard cutter conversion program," *Defense Daily*, 2011.

[18] "Sentinel class," *Naval Technology*, 2019. URL: https://www.naval-technology.com/projects/sentinel-class/?cf-view&cf-closed.

[19] "Fifth fast response cutter delivered to u.s. coast guard," *GCaptain*, 2013. URL: https://gcaptain.com/fifth-fast-response-cutter-delivered-to-us-coast-guard/.

[20] U.S. Coast Guard, "154-WPC-161-310 Stern Tube Drawing," *Department of Homeland Security*, Sep. 2012.

[21] M. J. Bishop, "Preventing stern tube corrosion through shipboard cathodic protection," SM thesis, Massachusetts Institute of Technology, Cambridge, MA, 2023.

[22] I. C. Patnode, "Protecting our investment: Solving fast response cutter corrosion," SM thesis, Massachusetts Institute of Technology, Cambridge, MA, 2023.

[23] U.S. Coast Guard Surface Forces Logistics Center, "CGC RICHARD DIXON (1113) Stern Tube Inspection," *Department of Homeland Security*, 2022, Slides for internal presentation June 10, 2022.

[24] U.S. Coast Guard Surface Forces Logistics Center, "CGC CHARLES MOULTHROPE (1141) Stern Tube Inspection," *Department of Homeland Security*, 2023, Slides for internal presentation November 2, 2023.

[25] Bollanger Shipyards, "154-WPC-361-301 Rev. B: FRC Paint and Preservation Schedule," *Department of Homeland Security*, 2017, June 22, 2017.

[26] M. Schumacher, *Seawater Corrosion Handbook*, 1st ed. Park Ridge, NJ: Noyes Data Corporation, 1979.

[27] *Cathodic Protection of Ships*. Spring, TX: American Bureau of Shipping, Dec. 2017.

[28] *Coverings for Waterborne Main Propulsion Shafting on U.S. Naval Surface Ships and Submarines*. Washington, DC: Department of Defense, Jul. 2010.

[29] U.S. Coast Guard, "Cathodic Protection System - Model CA44227," *Department of Homeland Security*, Sep. 2018.

[30] O. T. et al., "Hydrogen uptake end embrittlement suceptibility of ferrite-pearlite pipeline steels," *Materials Performance in Hydrogen Environments*, 2018, Proceedings of the 2016 International Hydrogen Conference, Jackson Lake Lodge, Wyoming, USA, 11–14 September 2016. ASME Press; New York, NY, USA: 2017. pp. 487–494.

[31] M. F. et al., "The effect rust and over-protectioin voltage of impressed current cathodic protection toward lr grade a steel disbondment," *Applied Mechanics and Materials*, vol. 842, pp. 92–98, 2016.

[32] T. D. et al., "Biofaouling and corrosion rate of welded nickel aluminum bronze in natural and simulated seawater," *Taylor & Francis Online*, Mar. 2024.

[33] L. D. et al., "Biofouling protection for marine environmental sensors," *Ocean Science*, vol. 6, pp. 503–511, 2010.

[34] T. Huber and Y. Wang, "Effect of propeller coating on cathodic protection current demand: Sea trial and modeling studies," *Corrosion*, vol. 68, no. 5, pp. 441–448, 2012.

[35] E. Santana-Diaz and R. Adey, "Predicting the coating condition on ships using iccp system data," *International Journal for Numerical Methods in Engineering*, Nov. 2004.

[36] *Corrosion Module User's Guide, Version 6.2*. Burlington, MA: COMSOL, 2023.

[37] V. G. DeGiorgi and S. Wimmer, "Geometric details and modeling accuracy requirements for shipboard impressed current cathodic protection system modeling," *Engineering Analysis with Boundary Elements*, vol. 29, no. 1, pp. 15–28, Jan. 2005.